2016

Improving Recovery of Liquids from Shales Through Gas Injection

Fragoso Amaya, Alfonso Rafael

UNIVERSITY OF CALGARY

Improving Recovery of Liquids from Shales Through Gas Injection

by

Alfonso Rafael Fragoso Amaya

A THESIS

SUBMITTED TO THE FACULTY OF GRADUATE STUDIES

IN PARTIAL FULFILMENT OF THE REQUIREMENTS FOR THE

DEGREE OF MASTER OF SCIENCE

GRADUATE PROGRAM IN CHEMICAL AND PETROLEUM ENGINEERING

CALGARY, ALBERTA

SEPTEMBER, 2016

Abstract

This thesis investigates the use of gas injection for improving liquids recoveries from oil and condensate containers in shale reservoirs. The objective is accomplished by building simulation models of a shale reservoir that contains gas, condensate and oil. In these shales, the gas container is at the bottom, the condensate container in the middle, and the oil container at the top of the structure.

Results show that liquids recoveries can be increased by injecting dry gas from the lower part of the structure and recycling gas from the condensate container. The reservoir model is coupled with wells and surface facilities models. This study demonstrates that the proper design of wellbore and surface installations is critical as they can also lead to significant improvements in liquid recoveries.

The effect of refracturing horizontal wells is also investigated. It is found that refracturing can yield the same incremental production obtained by infill drilling.

Acknowledgements

I would like to express my sincere gratitude to my supervisor Dr. Roberto Aguilera, for accepting me as part of the GFREE research group in the Department of Chemical and Petroleum Engineering at the University of Calgary. Thanks for his teaching, guidance, patience, and motivation throughout my MSc studies.

I want to thank CNOOC Limited, NEXEN for providing the financial resources that made this thesis possible.

My gratitude to my colleagues of the GEFREE team for their continuous collaboration and support.

Thanks to Schlumberger for providing the well and surface facilities simulator FORGAS.

It is also acknowledged the donation of the CMG simulation software to the University of Calgary.

I am thankful to Mona Trick for her invaluable help and her guidance on the use of FORGAS.

Special thanks to Varun Pathak for his assistance in the use of GEM.

Dedication

A mis dos amores: Gissela y Tomás.

A mi hermosa familia: Mami, Papi y La Barbie.

Table of Contents

List of Tables

List of Figures and Illustrations

List of Symbols, Abbreviations and Nomenclature

If you do not have any symbols, abbreviations, or specific nomenclature in your thesis, you do not need to fill out this table. To add another row to the table, with your cursor in the bottom right cell, press the TAB key (beside the letter Q on your keyboard).

Acronyms	**Definition**
GFREE	(F), reservoir drilling, completion and stimulation (R), reservoir engineering (E), economics and externalities (EE)
NPV	Net present value
TOC	Total organic carbon, % weight

Nomenclature	**Definition**
A	area of cross section normal to the bedding plane, ft^2
A_0	total initial investment costs
a_1	fitting factor for parameter *D*
a_2	fitting factor for parameter *D*
b_i	inverse of the Langmuir pressure for component "*i*", 1/psi
b_1	sub-parameter for α exponent
b_2	sub-parameter for α exponent
C_f	natural fracture compressibility, 1/psia
C_i	net cash flow during the period *i*
C_m	matrix compressibility, 1/psia
C_w	water compressibility, 1/psia
D	parameter *D* in Eq. 6-1
D_R	formation top, ft
f_g	fraction of flowing stream that is gas
h	reservoir thickness, ft
k	permeability, darcies
$k_{hf}*w_{hf}$	flow capacity of hydraulic fractures, md-ft
k_m	matrix permeability. md
k_{ro}	relative permeability to oil, fraction
k_{rg}	relative permeability to gas, fraction
k_2	natural fracture permeability, md
L	length, ft
M	mobility ratio
q_T	total flow rate through area *A* , res ft^3/D
S_g	gas saturation, fraction

P_i	initial reservoir pressure, psi
P_L	Langmuir pressure, psia
P_k	net confining pressure, psi
P_{wf}	bottomhole flowing pressure, psi
r	discount rate
S	skin factor, dimensionless
t	time, days
V_i	adsorbed volume of component "*i*", scf/ton
V_L	Langmuir volume, scf/ton
x_{hf}	hydraulic fracture half-length, ft

Greek Symbols	**Definition**
α	empirical exponent in Eq. 6-1
β	angle of dip, positive downdip, degrees,
Δ	difference operator/delta
μ_o	viscosity of oil, cp
μ_g	viscosity of gas, cp
ρ	density, lbm/ft^3
ϕ	porosity, fraction.
ϕ_m	matrix porosity, fraction
ϕ_2	natural fractures porosity, fraction

Chapter One: **Introduction**

In recent years, shale reservoirs have become a very important source of hydrocarbons, mainly in the US and Canada. Shale oil in the US changed the slope depicted by production rates during the last few years from negative to positive making it a huge success and corroborating at the same time the creativity, innovation and resilience of the petroleum industry. These results are significant as the endowment of oil, gas and condensate in shales throughout the world is quite gigantic. The success of shale reservoirs exploitation in the US and Canada has awakened the interest of all countries around the world where these resources are available.

The current technique to produce shale oil and gas consists of drilling horizontal wells and stimulating them with multistage hydraulic fracturing treatments. This approach has proven successful. However, recoveries as a percent of original hydrocarbons-in-place are very low (typically less than 10%) compared with conventional reservoirs, leaving thus a huge volume of hydrocarbons that remain in the shale rocks after primary recovery.

In practice, some shale reservoirs such as the Eagle Ford in the US and the Duvernay in Canada present the challenge of unconventional fluids distribution: shallower in the structure, there is black oil, deeper is condensate and even deeper is dry gas. So the fluids distribution is exactly the opposite of what occurs in conventional reservoirs. Ramirez and Aguilera (2016) have shown that fluids in shale reservoirs have remained with approximately the same original distribution over geologic time.

This thesis focuses on the possibility of injecting dry gas present in the lower part of the shale's structure into the oil and condensate reservoir containers, in order to increase liquid recoveries. This dry gas injection process is complemented with the reinjection of the gas stripped from the condensate. A container is defined as "a reservoir system subdivision, consisting of a pore system,

made up of one or more flow units, which respond as a unit when fluid is withdrawn" (Hartmann and Beaumont, 1999; Aguilera and Aguilera, 2002). This geologic characteristic allows the 'upside-down' vertical containment of oil, dry gas and condensate in shale reservoirs. A flow unit is defined as a "stratigraphically continuous reservoir subdivision characterized by a similar pore type" (Hartmann and Beaumont, 1999, p. 9-7; Aguilera and Aguilera, 2002).

1.1 Research Objectives

The main goal of this work is to propose a method to increase liquid recoveries from shales where three reservoir fluids are present: oil, condensate and dry gas. To accomplish this goal, the following research objectives are defined:

1. Develop a numerical simulation model of a shale reservoir that stores gas, condensate and oil in separate geologic containers. Published data from the Eagle Ford Shale are used for this purpose.
2. Integrate the reservoir simulation model with well and production facilities models.
3. Compare results of liquids recoveries obtained by primary recovery, continuous gas injections and huff and puff gas injection.
4. Evaluate the potential of hydraulic refracturing to improve production rates and ultimate recoveries from shale reservoirs.
5. Compare economic results from the above projects.

1.2 Thesis Organization

This thesis is divided into seven chapters, a brief description of them is presented below:

1. Chapter 1 (this chapter) provides an introduction to this thesis, the objectives of this research and the technical publications derived from this study.

2. Chapter 2 presents a literature review where the concepts of primary, secondary and tertiary recovery are defined. It also discusses immiscible gas injection in conventional reservoirs and briefly explains the huff and puff injection technique. Finally, the chapter presents some geological aspects of the Eagle Ford shale and summarizes previous studies related to improved oil recovery from shales.
3. Chapter 3 focuses on the use of gas injection to increase oil recoveries from a shale oil reservoir container. Single porosity, dual porosity and dual permeability simulation models are built. Different injection gas compositions are considered. Two injection techniques are investigated: continuous and huff and puff injection.
4. Chapter 4 presents a holistic model of the Eagle Ford shale. Reservoir simulation is used to investigate the use of the dry gas stored in the bottom of the structure and the gas stripped from the condensate to improve liquid recoveries in the oil and condensate containers. Economic comparisons of continuous, and huff and puff gas injections are included in this chapter.
5. In chapter 5, the model developed in chapter 4 is coupled with well and surface process models, with a view to investigate the effect of these systems on the performance of the gas injection projects.
6. Chapter 6 concentrates on refracturing. The case where the refracturing job creates new fractures is compared with the case where the previous fractures are reopened. Finally, the recovery and economic benefits of refracturing are contrasted with those of infill drilling.
7. Chapter 7 states the conclusions and recommendations derived from this thesis.

1.3 Technical Publications

Part of the research developed in this thesis has been presented at the following SPE conferences:

- ✓ Fragoso, A., Wang, Y., Jing, G. and Aguilera, R., 2015. Improving Recovery of Liquids from Shales through Gas Recycling and Dry Gas Injection. SPE paper 177278 presented at the Latin America and Caribbean Petroleum Engineering Conference (LACPEC) held in Quito, Ecuador, 18-20 November 2015.
- ✓ Urban, E., Orozco, D., Fragoso, A., Selvan, K. and Aguilera, R., 2016. Refracturing vs. Infill Drilling – A Cost Effective Approach to Enhancing Recovery in Shale Reservoirs. SPE paper 2461604 presented at the Unconventional Resources Technology Conference held in San Antonio, Texas, USA, 1-3 August 2016.

Chapter Two: **Literature Review**

The Schlumberger Oilfield Glossary defines shale as “A fine-grained, fissile, detrital sedimentary rock formed by consolidation of clay- and silt-sized particles into thin, relatively impermeable layers”. Shale, which is the most abundant sedimentary rock, has been recognized as source rock and “cap rock” due to its low permeability. Developments in horizontal drilling and hydraulic fracturing technology have changed the way the industry and the world “see” the shales, as they have allowed to take advantage of the huge volume of hydrocarbon stored in these rocks.

Shale reservoirs are different from conventional reservoirs in several aspects. In conventional reservoirs, hydrocarbons are generated mostly in shales, migrate short or long distances and eventually are trapped and stored in different types of rocks, particularly in sandstone and carbonate reservoirs. In shale reservoirs, hydrocarbons are generated and stored in the shale rock and there is not fluid migration to other reservoirs. Storage mechanisms are also different in conventional and shale reservoirs. In conventional reservoirs, hydrocarbons are stored in a free state within pores and natural fractures. In shale reservoirs, in addition to the previous storage mechanisms, there is also gas adsorbed on the internal surface of the organic pores (and in some cases in the inorganic pores) and gas dissolved in the kerogen material.

Another important aspect of shale reservoirs of the type considered in this thesis is that dry gas, condensate and oil are stored ‘upside-down’ within the same structure in separate containers with gas at the bottom, condensate in the middle and oil at the top (Fragoso et al., 2015). The same vertical containment and distribution of fluids has remained in these shales though geologic time (Ramirez and Aguilera, 2016).

2.1 Improved Oil Recovery

Primary recovery factors from conventional oil reservoirs are in general very low, “the actual range is very wide, but the average recovery is around 15%” (Maini, 2015). When dealing with unconventional reservoirs, which are characterized by very low permeabilities, recoveries are even smaller.

Many efforts have been done to increase these recoveries including multilateral horizontal wells, hydraulic fracturing, gas and water injection, miscible processes, chemical flooding and thermal processes. The idea is to reduce the oil that is left in the reservoir after its production life.

2.1.1 Primary Recovery

Hydrocarbon production is generally categorized in three stages: primary recovery, secondary recovery and tertiary recovery.

“Primary recovery results from the use of natural energy present in a reservoir as the main source of energy for the displacement of oil to producing wells. These natural energy sources are solution-gas drive, gas-cap drive, natural water drive, fluid and rock expansion and gravity drainage. The particular mechanism of lifting oil to the surface, once it is in the wellbore, is not a factor in the classification scheme.” (Green and Willhite, 1998)

2.1.2 Secondary Recovery

In most reservoirs, the natural driving mechanisms do not provide enough energy to achieve the desired hydrocarbon recovery. The most basic methods to introduce some form of artificial drive are gas and water injection (Ahmed, 2001). “Gas could be injected either, into a gas cap for pressure maintenance or either into oil column wells to displace oil immiscibly. An immiscible gas displacement is not as efficient as a waterflood and is used infrequently as a secondary recovery process today” (Green and Willhite, 1998).

2.1.3 Tertiary Recovery

Tertiary recovery [also generally known as Enhanced Oil Recovery (EOR)], as opposed to secondary recovery, which uses simple methods, employs sophisticated techniques that modify the original properties of the oil. Its purpose is not only to restore reservoir pressure, but to create favorable conditions for oil displacement. Many EOR methods have been developed, but the most important can be included in three main categories: chemical flooding, miscible displacement and thermal recovery (Schlumberger, 2016).

2.2 Immiscible Gas Injection in Oil Reservoirs

Although today the expression secondary recovery is today used in most cases as synonym of waterflooding, many immiscible gas injection projects have been undertaken, first as a pressure maintenance method and then to increase recovery by immiscible displacement. These projects are in general conducted when a source of gas is available. It could be generally produced from the same reservoir or from a close gas field.

In addition to the aforementioned mechanisms of pressure maintenance and oil displacement, gas injection also may help increasing recoveries by vaporizing liquid components in a gas condensate reservoir if retrograde condensation has occurred and by swelling the oil if the reservoir is very undersaturated.

2.2.1 Gas/Oil Linear Displacement Efficiency

The Buckley-Leverett (1942) fractional flow equation for any gas saturation is (Warner et al., 2006):

$$f_g = \frac{1+\left(0.044kk_{ro}\Delta\rho A\sin\beta \Big/ q_t\mu_o\right)}{1+1/M} \qquad \textbf{Eq. 2-1}$$

Where M is the mobility ratio:

$$M = \left(\frac{k_{rg}}{k_{ro}}\right)\left(\frac{\mu_o}{\mu_g}\right) \qquad \textbf{Eq. 2-2}$$

And $\Delta\rho$ is the difference between the densities of oil and injected gas.

When the gravity effects are ignored, the equation is reduced to:

$$f_g = \frac{1}{1+1/M} \qquad \textbf{Eq. 2-3}$$

Figure 2-1 presents the gas fractional flow curves calculated using **Eq. 2-1** and **Eq. 2-3** based on data from the Hawkins field. It shows the importance of the gravity effects on recovery.

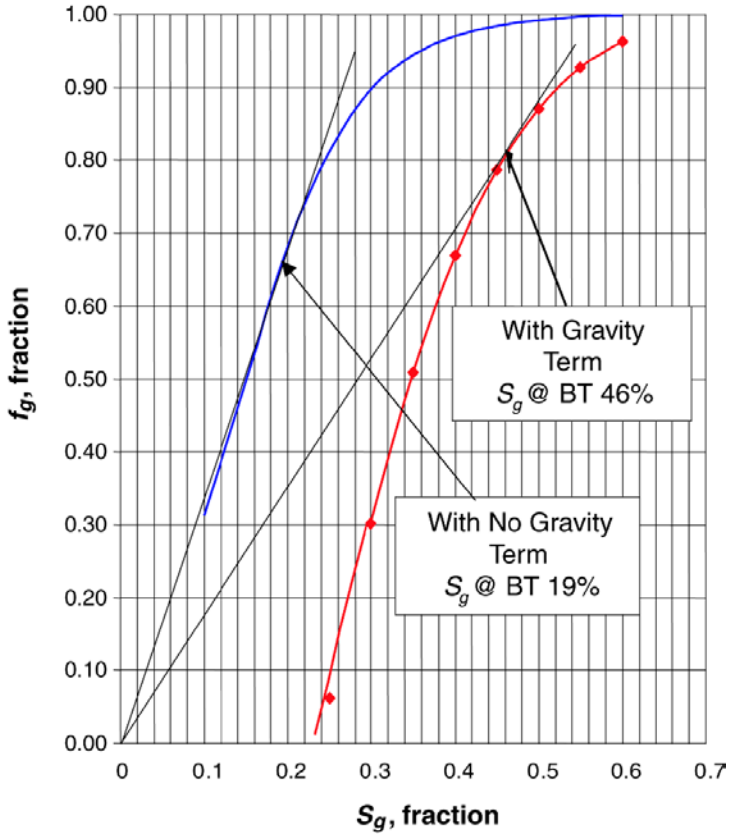

Figure 2-1. Buckley-Leverett fractional gas flow plot (Warner, et al., 2006)

The fraction of gas flowing can be related to time by using the equation developed by Buckley and Leverett (1942):

$$L = \frac{q_T t}{\phi A}\left(\frac{df_g}{dS_g}\right) \qquad \textbf{Eq. 2-4}$$

The derivative df_g/dS_g may be determined as the slope of the curve f_g vs S_g at a given gas saturation. **Figure 2-2** presents the gas saturation distributions calculated with and without gravitational effects. "The gas/oil displacement efficiency, the percent of the oil volume that has been recovered, can be calculated for any period of gas injection by integrating the volume of the gas-invaded zone as a function of gas saturation" (Warner et al., 2006).

The gas/oil displacement efficiency is affected by several factors including initial saturation conditions, fluid viscosity ratios, relative permeability ratios, formation dip, capillary pressure, permeability, density difference, rate of injection, and cross section open to flow.

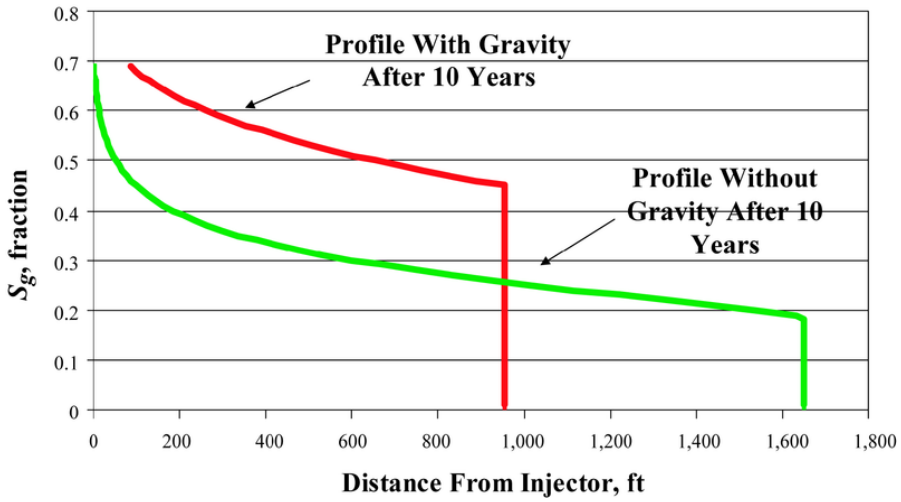

Figure 2-2. Typical Buckley-Leverett saturation profiles (Warner, et al., 2006).

In gas/oil injection projects, mobility ratios are very unfavorable. This makes the displacements unstable and cause viscous fingering, especially if it is occurring horizontally. When the

displacement occurs vertically, gravity helps to stabilize the flood front. However, if the flow rate is too high, instabilities can still occur. In general, reservoir simulators do not accurately represent the effects of viscous fingering. This may affect to some extent the results of this study.

2.2.2 Gas/Oil Compositional Effects During Immiscible Gas Displacement

In an immiscible gas injection project, the injected gas/oil composition interactions can help to increase oil recoveries. These interactions can be classified as swelling effects and stripping effects.

2.2.2.1 Swelling Compositional Effects

This phenomenon occurs when the oil is not saturated at reservoir pressure or if the gas injection increases the reservoir pressure. Under these circumstances, the amount of gas dissolved in the oil will increase until it is saturated. As a result, the oil formation volume factor will also increase. If the reservoir pressure is very high compared to the bubble point pressure, the swelling effect will play a very important role in the displacement process.

2.2.2.2 Stripping Compositional Effects

Generally, the injected gas is very lean and when it is in contact with oil in the reservoir, it vaporizes some of its intermediate components until the gas and the oil phases reach compositional equilibrium. Nonhydrocarbon injected gases can also vaporize intermediate components of the oil. Carbon dioxide, has a phase behavior similar to propane, therefore it is able to vaporize an important amount of hydrocarbon components from the oil. On the other hand, Nitrogen is less efficient than methane in this process. The impact of this phenomenon is more pronounced in light oils as a bigger percentage of hydrocarbon components is vaporized by the injected gas compared to heavier oils.

2.2.3 Immiscible Gas/Oil Displacement Techniques

Gas injection operations are usually classified into two different types depending on where the gas is injected.

2.2.3.1 Crestal Gas Injection

It is also called external or gas-cap injection. The injection wells are located in the structurally higher positions of the reservoirs, usually in the gas cap. This kind of injection is applied to take advantage of gravity drainage in reservoirs with significant structural relief or thick oil columns with good vertical permeability. Due to the gravity drainage benefits, crestal injection is generally considered superior to pattern gas injection.

2.2.3.2 Pattern Gas Injection

It is also called dispersed or internal gas injection. An arrangement of injection wells is done to distribute the gas throughout the reservoir. Pattern gas injection is applied to reservoirs with low structural relief, relatively homogeneous reservoirs with low permeabilities, and reservoirs with low vertical permeability. The main advantage of this type of injection is the rapid pressure and production response. Low areal sweep efficiency, high installation cost and little benefits from gravity drainage are among the limitations. (Warner et al., 2006).

2.3 Huff and Puff (Cyclic) Injection

Cyclic steam simulation is a thermal recovery method that has been successfully applied in heavy oil reservoirs in the last five decades. In this technique, the same well is used as a producer and as an injector. Steam is injected for periods of two to four weeks. Then, the well is shut in during a soak period and finally the well is allowed to produce (**Figure 2-3**). Initial oil rates are

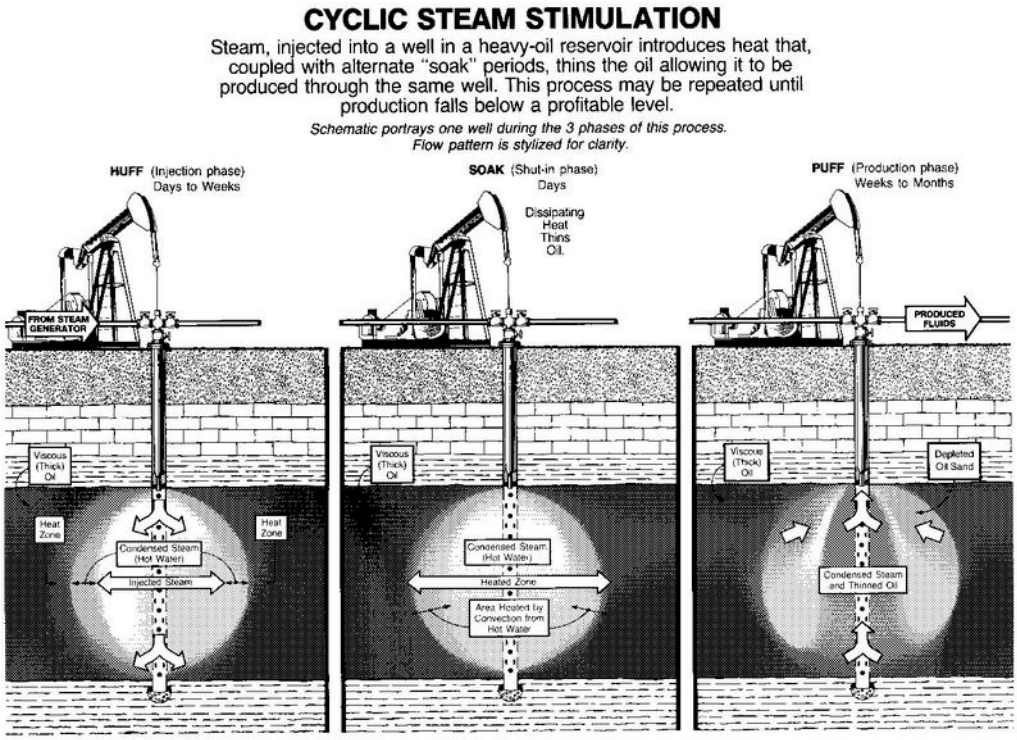

Figure 2-3. Cyclic steam stimulation process (Green and Willhite, 1998).

high due to the reduction in oil viscosity caused by the increased temperature and due to the increment in reservoir pressure near the wellbore. With time, oil rates decline as heat is removed with the produced fluids and is lost by conduction to adjacent formations. A new cycle begins when production falls below a determined value (Green and Willhite, 1998).

Recently, several authors have considered the possibility to extend this method to shale reservoirs. Instead of steam, a lean gas or non-hydrocarbon gases such as CO_2 or N_2 would be injected to increase oil recovery. The possible use of the huff and puff gas injection technique for shale petroleum reservoirs is investigated in this thesis.

2.4 The Eagle Ford Shale

The Eagle Ford is one of the most important shale plays in the US. According to the Railroad commission of Texas "The shale play trends across Texas from the Mexican border up into East

Texas, roughly 50 miles wide and 400 miles long with an average thickness of 250 feet. It is Cretaceous in age, resting between the Austin Chalk and the Buda Lime at a depth of approximately 4,000 to 12,000 feet." Different range of depths have been reported by some authors. For example, Pathak (2014) published depths ranging from 1500ft to 14000ft. The Eagle Ford is the source rock for the Austin Chalk and the giant East Texas Field. The first well in the Eagle Ford shale was drilled by Petrohawk in 2008. It was a 3200 ft horizontal well stimulated with 10 hydraulic fracturing stages (Railroad commission of Texas, 2016).

"The Eagle Ford Shale consists of two intervals generically classified as lower and upper. The lower consists of a transgressive marine interval dominated by dark, well-laminated organically rich shales. The upper Eagle Ford Shale is the beginning of a regressive cycle characterized by a high stand system tract in which near-shore sediments were deposited. The regressive section consists of interstratified calcareous shales, bentonites, limestones, and quartzose siltstones" (Martin, 2011).

The fluids distribution in the Eagle Ford shale is exactly the opposite of what occurs in conventional reservoirs (**Figure 2-4**), where the fluids distribution is governed by gravity/density segregation. Ramirez and Aguilera (2016) have shown that fluids in shale reservoirs have remained with approximately the same original distribution (i.e. approximately the same dry gas-condensate contact and approximately the same condensate-oil contact) over geologic time.

Matrix porosities in the Eagle Ford range between 5% and 14%, matrix permeabilities range from 40nd to 1300nd, and total organic carbon (TOC) ranges from 0.7% to 9.2% (Wang and Liu, 2011). Due to the low and ultra-low permeabilities of shales, horizontal drilling combined with multistage hydraulic fracturing, is applied in almost all the wells.

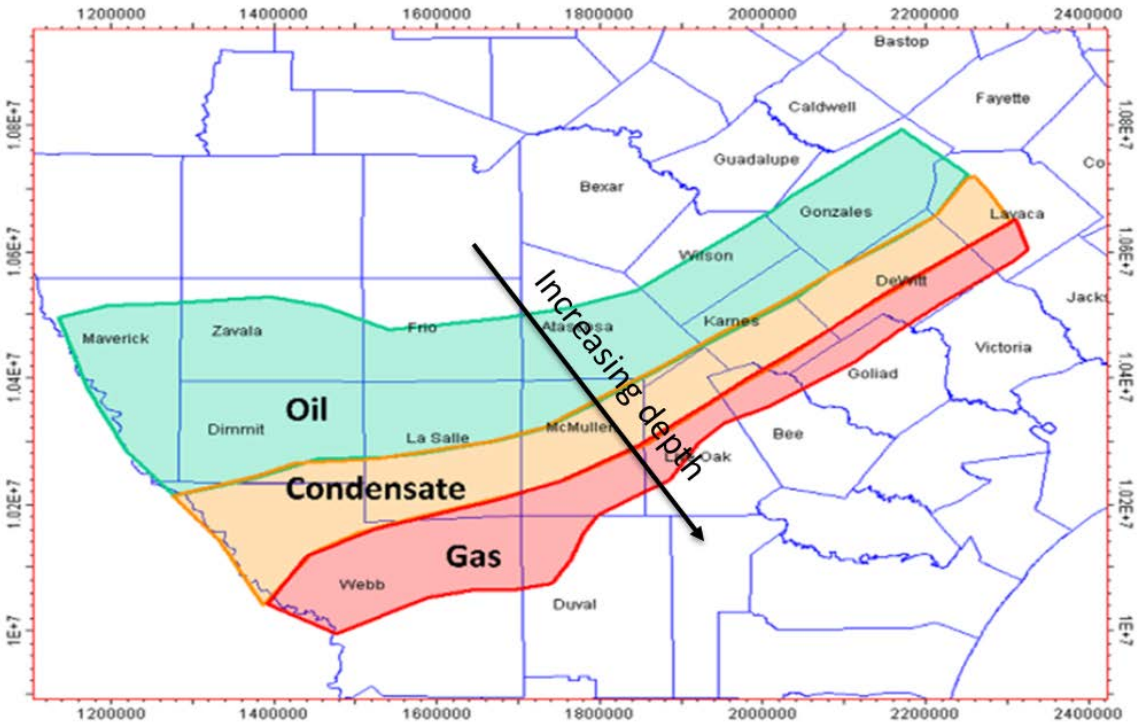

Figure 2-4. Map showing the maturation windows of the Eagle Ford (adapted from Fan et al., 2011).

In the early stages of the Eagle Ford development, production was focused on gas rich areas. In recent years, however, the focus has changed and the activity is located now almost entirely in liquid rich areas.

2.5 Previous Studies

Various authors have investigated the possibilities of enhanced oil recovery (EOR) in shales. Miscible CO2 flooding has been considered as an adequate method to enhance oil recovery in shale reservoirs.

Kovscek et al. (2008) conducted laboratory experiments to study the possibility of CO_2 injection in siliceous shales. Their experiments were carried out in core samples of low permeability (0.02md - 1.3 md) and large porosity (30%-40%). The samples were initially saturated with either depleted live oil or dead oil. CO_2 was injected at pressures varying from immiscible conditions to

near miscible conditions. Two injection modes were used: countercurrent flow and co-current injection. Their results showed that by immiscible CO_2 injection, oil recovery can be incremented up to 10% for countercurrent flow mode and from 18% to 25% for co-current flow mode, whereas for near miscible conditions, the increments were 25% for countercurrent flow and 10% for co-current flow mode.

Wan el al. (2013a), evaluated the possibility of cyclic natural gas injection in a shale oil reservoir using a single porosity black oil simulator. They considered different degrees of miscibility and determined the incremental oil recovery obtained for each case. In the case of total miscibility, the incremental recovery was a very significant 20.9%. Wan et al. (2013b), conducted a similar study, but using a dual permeability model. Again, they obtained a considerable increase in oil recovery. In addition, they determined the impact of some hydraulic fracture properties. More recently, Wan et al. (2015) evaluated the effect of diffusion on continuous gas injection in a shale oil reservoir using a dual permeability compositional simulator. They concluded that diffusion plays an important role in the gas flooding process in shales. Reservoir properties used by Wan et al. are based on published data for the Eagle Ford Shale.

Fragoso et al. (2016) evaluated the possible use of continuous gas injection as well as huff and puff gas injection in the oil and condensate containers of the Eagle Ford shale. The utilized single porosity, dual porosity and dual permeability numerical simulation for their purpose. In addition, they investigated the effect on recovery of bottomhole pressure (BHP), natural fracture permeability and spacing, hydraulic fracture length and spacing, and distance between parallel wells. They concluded that liquid recovery in shale condensate and shale oil reservoirs could be improved by means of dry gas injection.

Wang et al. (2016a) investigated the use of surfactant imbibition to increase oil recovery in shales. They used cores from the Bakken Formation in North Dakota saturated with crude oil from the same formation. A number of surfactant formulations and brine were used for imbibition studies. They concluded that if the shale can be properly contacted by the surfactant, oil recovery can be significantly increased. With optimized surfactant formulations, they observed recoveries up to 20% over brine imbibition. Optimization of water chemistry to improve oil recovery from the Middle Bakken has been discussed by Wang et al. (2016b).

Hoffman et al. (2016) have discussed a number of pilot tests for both water and gas injection in the Bakken shale conducted during the last 8 years. The authors indicated that results showed, in general, early breakthrough times and poor reservoir sweep efficiencies. Additional oil recovery in offset wells was insignificant, but the authors emphasized that the pilots were limited in scope and duration.

Shuler et al. (2016) have described a conventional surfactant ‘huff-n-puff' treatment to investigate the relationship between increased oil production and the surfactant soaking period. Surfactant chemistry is considered as a possible IOR solution. The authors indicated that if properly selected and designed, the surfactant additives in stimulation/fracturing fluids could have multi-functions towards improving both IP and the longer-term oil production.

Akinluyi et al. (2016) evaluated EOR potential for lean gas reinjection in zipper fracs in liquid-rich basin. In zipper frac,”two or more parallel wells are drilled and then perforated at alternate intervals along the wellbores and fractured at the perforations. This creates a high-density network of fractures between the wells that increases production in both wells.”(Gilleland, 2011). Akinluyi et al. used new analytical solutions to the diffusivity equation for analyzing the time for inter-fracture communication development. This includes interference, and productivity index for both

classical bi-wing fractures in a zipper configuration and complex fracture networks. The authors discussed whether spacing currently considered for primary production is sufficient for direct implementation of EOR or if changes to current practices are required.

The oil industry has also recognized the potential of EOR in shale reservoirs. Recently, EOG Energy announced successful results for gas injection pilots developed in the Eagle Ford by this company (Addison, 2016). According to EOG executives, improved oil recoveries by gas injection produces returns similar to those obtained by premium drilling programs but higher net present values.

Chapter Three: **Oil Container**

The upper part of the Eagle Ford structure considered in this study stores oil. Production from this container to date has been relatively small as efforts have concentrated on production of condensate. Recovery factors from the oil container are also very small. This part of the investigation analyzes the oil container separately, in order to evaluate the possible use of gas injection in a shale oil reservoir. A holistic representation of the Eagle Ford is described later in Chapter 4.

3.1 Simulation model

A model of a shale oil reservoir container is built using a compositional simulator (GEM, CMG). Data is gathered from the Eagle Ford shale literature. The oil composition is simplified to pseudo-components in order to reduce simulation times (**Table 3-1**). The simulation model (**Figure 3-1**) utilizes a Cartesian grid with an area of 153 acres divided into 65x41 grid cells. The shale oil container thickness is 200 ft divided into 5 layers of 40 ft each.

Several test cases are run for determining the optimum grid sizes. When using smaller blocks, there are significant increments in simulation times with no appreciable changes in simulation results.

Single porosity, dual porosity and dual permeability models are used and compared in this study. The matrix permeability is 250 nd and the matrix porosity is 8%; the reservoir has a dip angle of 2º. In the dual porosity and the dual permeability models, the fracture permeability is 0.04 md and the fracture spacing is 10 ft. All these properties are taken as constant throughout the simulation model (in this sense the reservoir properties are homogeneous). **Table 3-2** summarizes the reservoir properties.

Relative permeability curves for the matrix system are built using data published by Honarpour et al. (2012) for calcite rich regions in shale reservoirs. For the fracture system, straight line relative permeabilities are adopted. **Figure 3-2** shows the relative permeability curves.

The study takes into account molecular diffusion as a mass transport mechanism. Sigmund (1976) correlation is used to calculate gas phase and oil phase diffusion coefficients.

Table 3-1. Fluid composition for the oil container

Component	***Molar Fraction***
CO_2	0.0091
N_2	0.0016
C_1	0.3647
C_2	0.0967
C_3	0.0695
C_4 to C_6	0.1255
C_{7+1}	0.20
C_{7+2}	0.10
C_{7+3}	0.0329

Two horizontal wells, one injector and one producer, are drilled in the third layer of the model; the injector is updip of the producer. The horizontal length of the wells is 3250 ft. Multistage hydraulic fracturing stimulation is applied to both wells, the number of stages is 13, the hydraulic fractures half-length is 500 ft in the producer and 450 ft in the injector, the fracture width is 0.01 ft and the hydraulic fracture permeability is 1000 md in both wells. In the production well, the minimum allowed bottom hole pressure is set at 2000 psi, while in the injection well the bottom hole pressure is restricted to a maximum of 5000 psi.

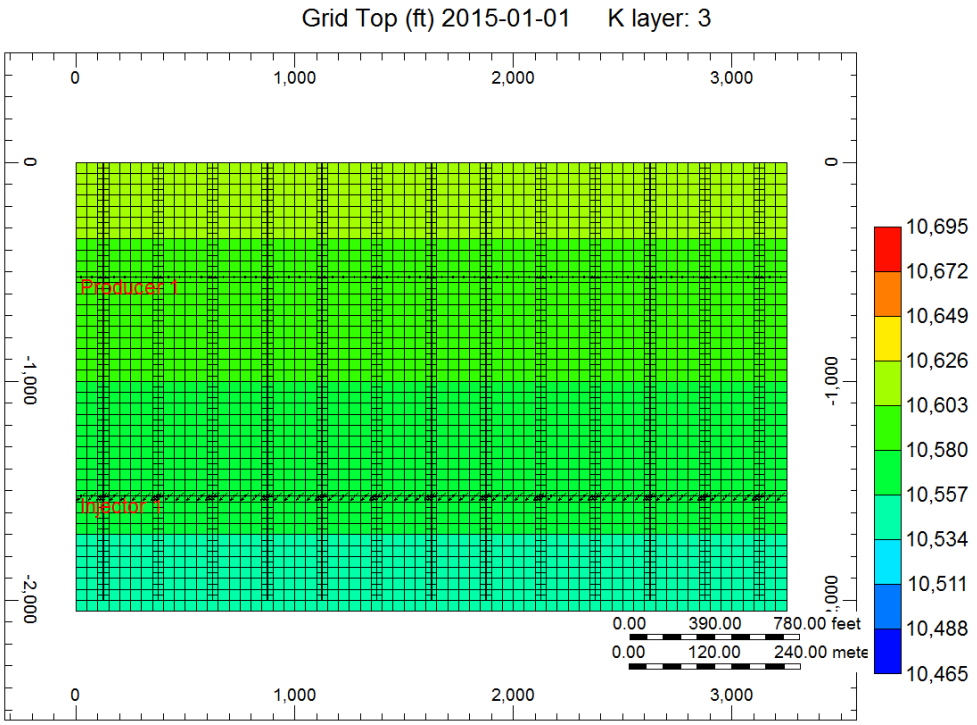

Figure 3-1. Reservoir grid for the oil container

Table 3-2. Reservoir and wellbore parameters for the simulation model

Parameter	*Symbol*	*Value*	*Units*
Initial reservoir pressure	P_i	6,000	psi
Reservoir temperature	T	158	°F
Water compressibility	C_w	3.00E-06	1/psia
Matrix compressibility	C_m	1.00E-6	1/psia
Natural fracture compressibility	C_f	1.00E-5	1/psia
Formation Top	D_R	10,500	ft
Dip Angle		2	°
Matrix porosity	ϕ_m	0.080	Fraction
Natural fractures Porosity	ϕ_2	0.0008	Fraction
Matrix Permeability	k_m	0.00025	md
Natural Fracture Permeability	k_2	0.04	md
Natural Fracture Spacing		10	ft
Reservoir thickness	h	200	ft
Well drainage area	A	153	Acres
Hydraulic fracture half-length	x_{hf}	450	ft
Hydraulic Fracture Spacing		250	ft
Length of the horizontal well	L	3,250	ft
Skin factor	S	0	-
Initial flow capacity of hydraulic fractures	$k_{hf}*w_{hf}$	10	md-ft
Bottomhole flowing pressure	P_{wf}	2,000	psi

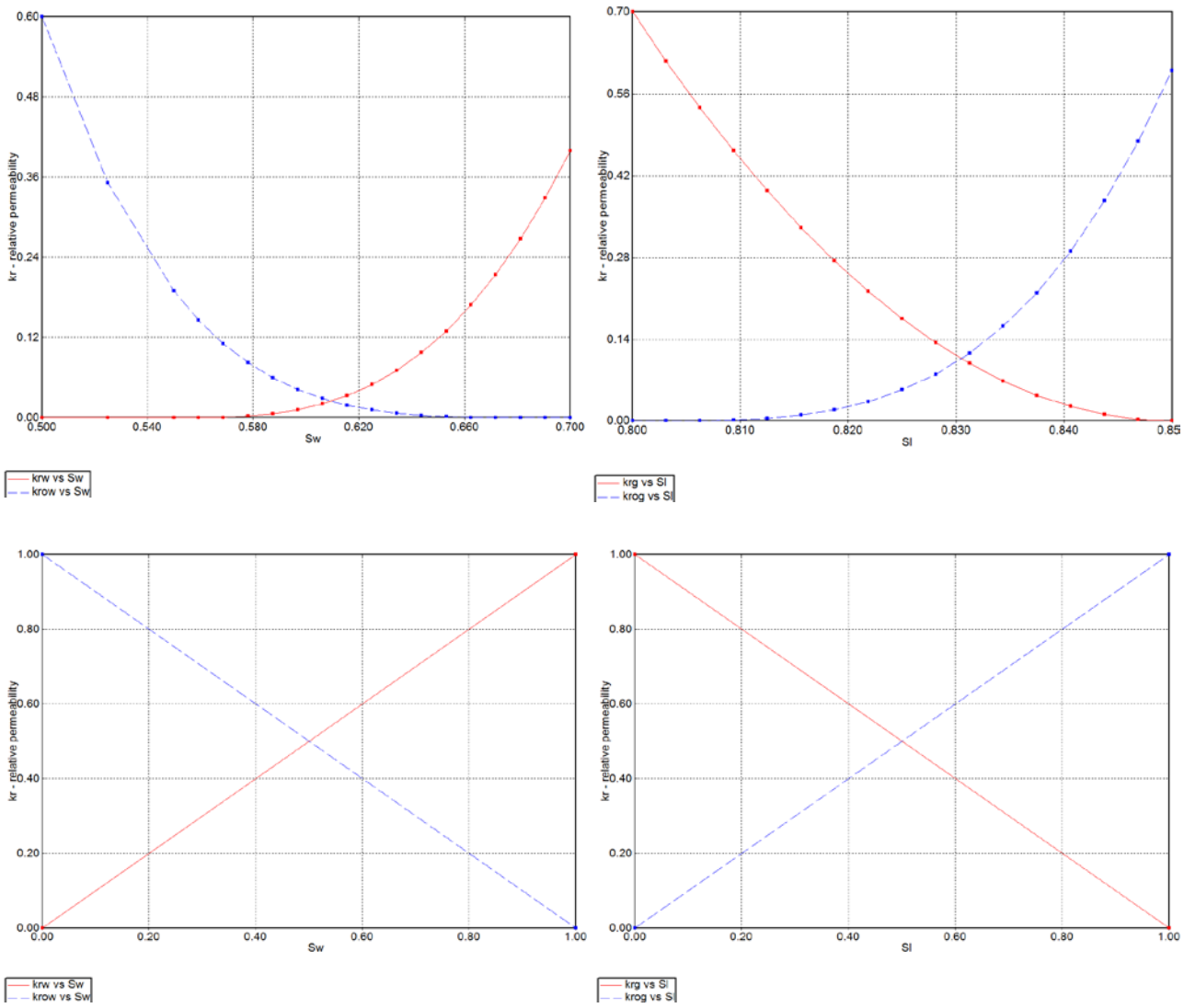

Figure 3-2. Relative Permeability Curves for the Matrix System (Top) and the Fracture System (Bottom).

In order to reduce simulation times, a submodel of 5x41x5 grid cells with only one hydraulic fracture is constructed. **Figure 3-3** presents the submodel.

Two injection techniques are considered: continuous gas injection and huff and puff gas injection. The cyclic huff and puff process is an improved thermal oil recovery method applied in heavy oil reservoirs in which a horizontal well is used for both injection and production. The possibility of

extending this method to gas injection in shale reservoirs has been proposed by Wan et al. (2013a). In this work, cyclic huff and puff gas injection is studied for the Eagle Ford Shale. Each cycle consists of 100 days of injection followed by 100 days of production.

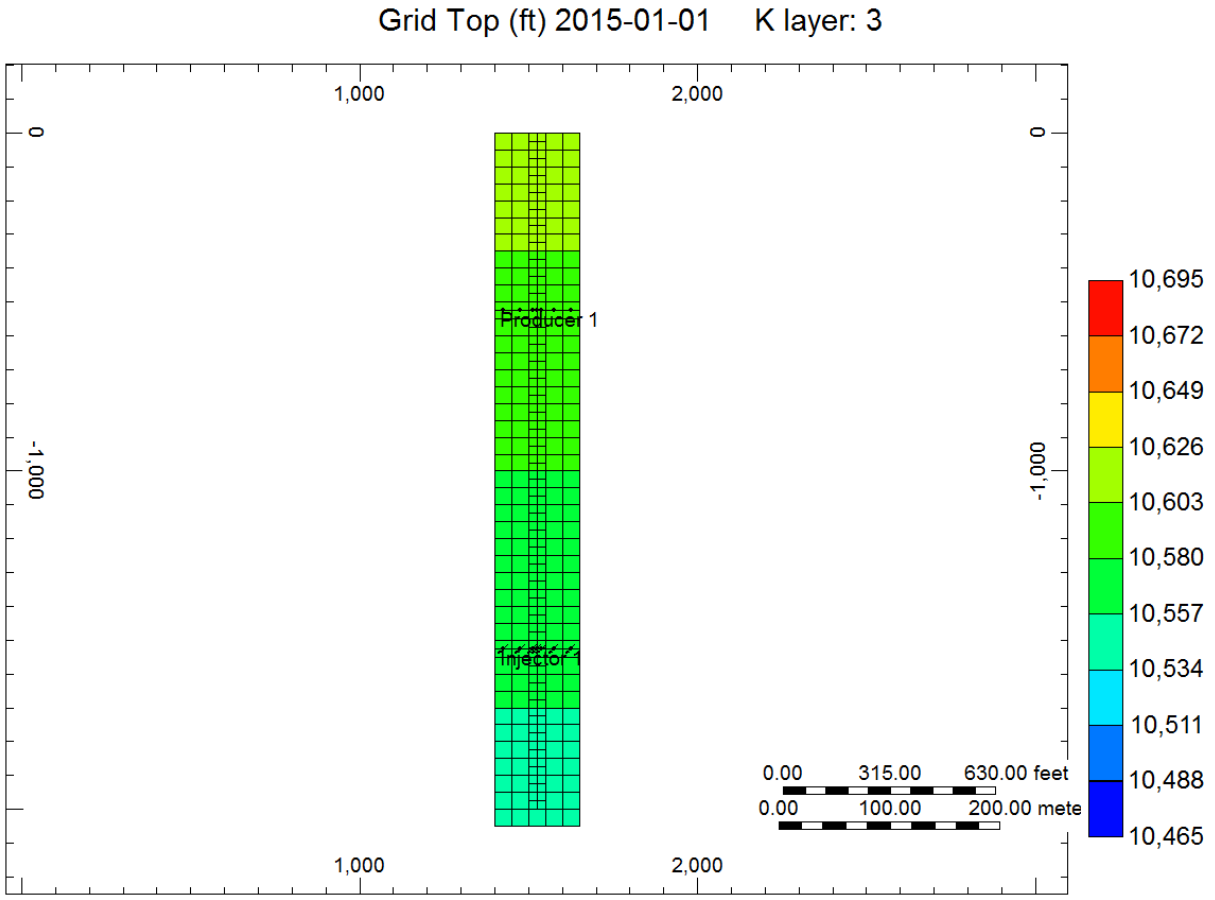

Figure 3-3. Reservoir grid submodel.

3.2 Single Porosity Model

The sweet spots of the Eagle Ford shale are known to be naturally fractured. However, a single porosity simulation model is built as a starting point to get an idea with respect to the possibilities of gas injection in those areas where only matrix porosity might be present. A sensitivity analysis to the matrix permeability is performed with a view to evaluate the effect of this property on gas injection performance. Four cases with different values of permeability are simulated: 250 nd,

0.001 md, 0.005 md and 0.01 md. Two injection fluids are considered; the first fluid composition is 100% methane and the second is 70 % C1, 20% C3 and 10% C6. This composition was suggested by Wan et al. (2015).

Injection starts after 5 years of production. **Table 3-3** summarizes the results of the sensitivity analysis. It shows that for a matrix permeability of 250 nd, oil recovery is not improved with injection of any of the two fluids, as the injected gas can barely penetrate the matrix due to the very low permeability. A slightly better result is obtained when the matrix permeability is 0.001 md. However, the increment in oil recovery by gas injection is not significant in this case.

Table 3-3. Oil recovery factors obtained with the single porosity model for different matrix permeabilities. Continuous gas injection starts after 5 years of primary production.

Matrix Permeability	Primary Recovery (%)	Recovery by CH_4 injection (%)	Recovery by (70% C1 + 20%C3+ 10%C6) injection (%)
250 nd	5.25	5.25	5.25
0.001 md	7.04	7.28	7.72
0.005 md	8.94	10.72	13.55
0.01 md	9.39	13.21	16.80

A matrix permeability of 0.005 md allows the injected gas (70 % C1+ 20% C3 + 10% C6) to flow into the matrix and increase oil recovery. For methane injection, the increment becomes important only when the matrix permeability is 0.01 md. Subsequent single porosity simulations use a 0.01 md matrix permeability. It is found that the shale oil reservoir performance under gas injection is strongly affected by matrix permeability when using single porosity models. However, the permeability values that allow increasing oil recoveries in these cases depend on the reservoir fluids composition, the injected fluid composition, the injection pressure and the injection rate. Therefore the threshold permeability must be determined for each particular injection project.

Figure 3-4 compares oil recovery for the primary production and methane injection cases. **Figure 3-5** presents the oil production rate, gas injection rate and reservoir pressure throughout 20 years for the methane injection case. During the five years of primary production, reservoir pressure decreases very quickly. When methane injection starts, pressure increases and is maintained approximately constant due to the gas injection. The oil rate also presents an abrupt decline during the five years of primary production. When methane injection starts, it helps to maintain production rates for a longer time. **Figure 3-6** presents oil recoveries for the injection case with 70% C1 + 20 % C3 + 10% C6.

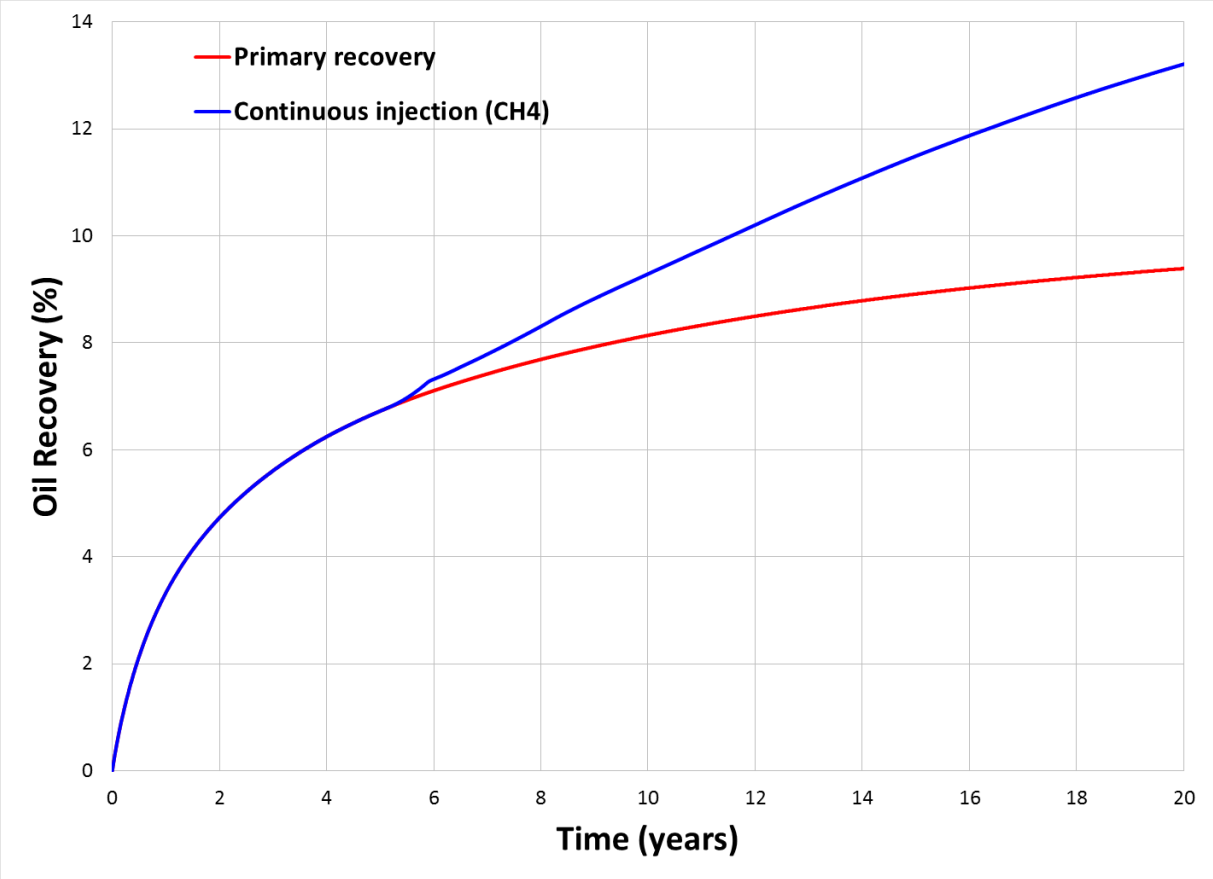

Figure 3-4. Oil recovery for the single porosity model (k = 0.01 md). The red line corresponds to primary production and the blue line corresponds to methane injection starting after five years of primary production.

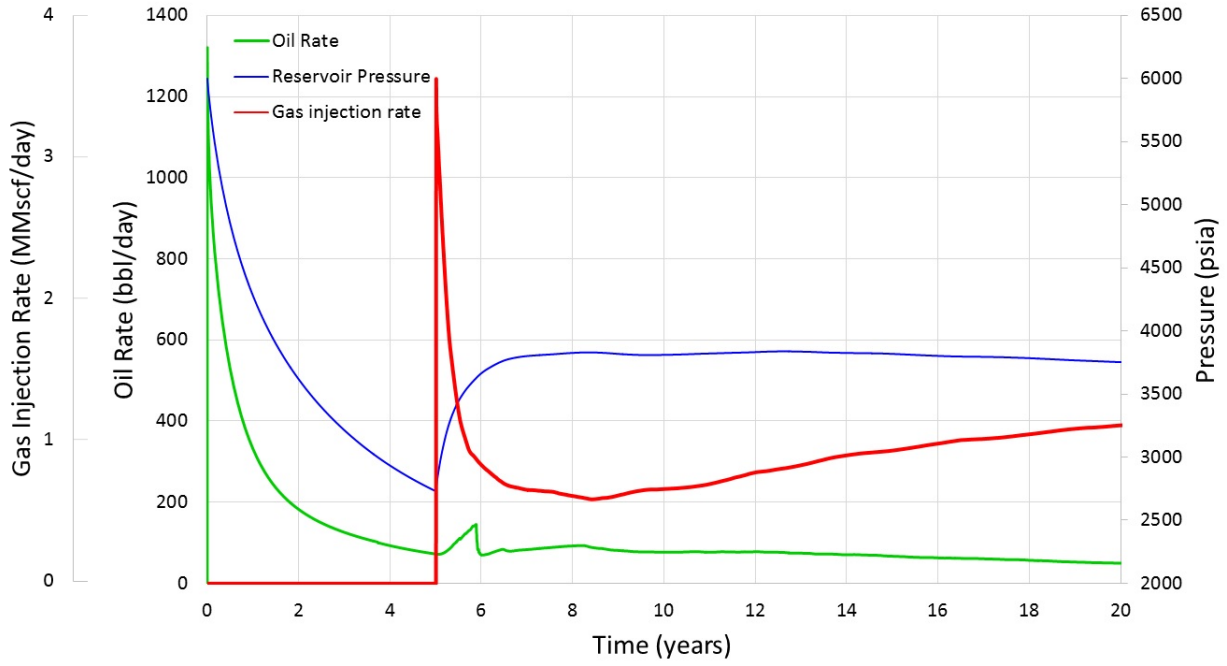

Figure 3-5. Oil production rate (green line), gas injection rate (red line) and reservoir pressure (blue line) for the methane injection case in a single porosity model (k =0.01 md). Rates have been multiplied by 13 to include all the stages.

An important issue in an injection project is the time when the injection should start. Two starting times are compared in this study for the case of continuous gas injection: (1) injection starts at the beginning of production and (2) injection starts after five years of production. For huff and puff, gas injection starting after two years of production is also evaluated. The injected fluid is methane in all these cases.

It is found that starting injection earlier in the production life of the well does not improve oil recoveries in the single porosity model. The best results for both continuous and huff and puff gas injection are obtained when injection starts after five years of production as shown in **Figure 3-7** and **Figure 3-8**, respectively.

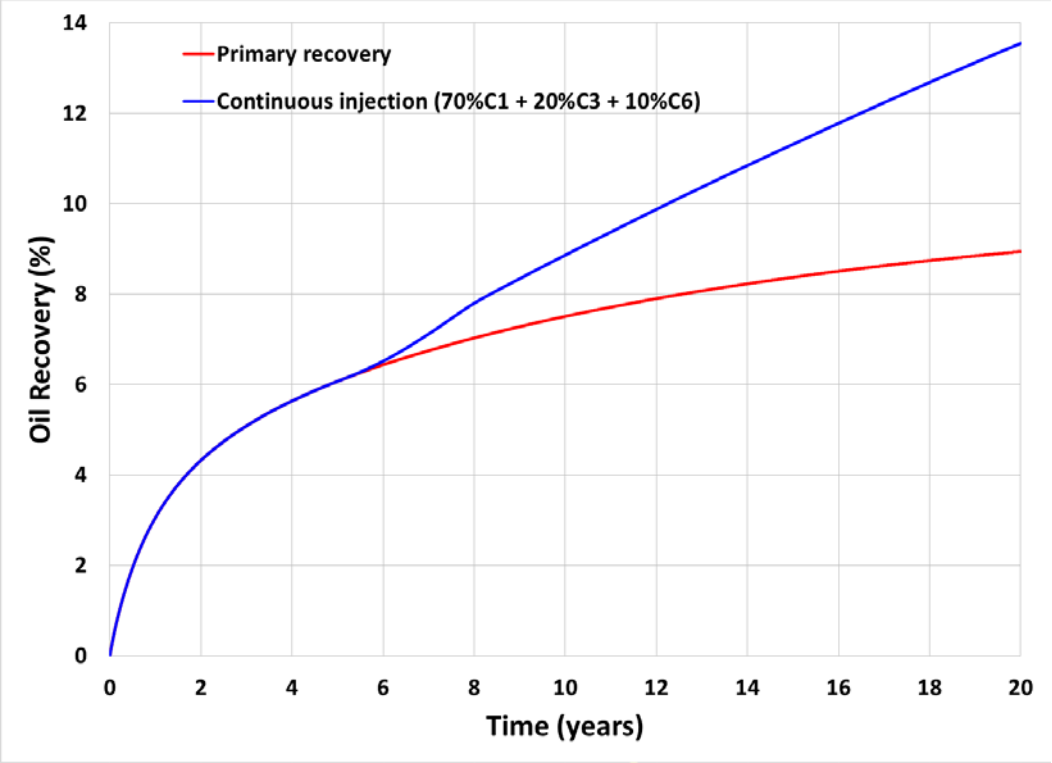

Figure 3-6. Oil recovery for the single porosity model (k = 0.005 md). The red line corresponds to primary production and the blue line corresponds to 70% C1 + 20 % C3 + 10%C6 gas injection starting after five years of primary production.

The effect of four injected gas compositions is contemplated in this study for different models. **Table 3-4** compares the oil recovery obtained after 20 years when injection starts after 5 years of primary production. It also compares performance with the two gas injection techniques.

Table 3-4 shows that continuous gas injection gives slightly better results than huff and puff injection when dealing with a single porosity model, regardless the injected fluid composition. However, in all probability this small increment in oil recovery does not justify the cost of an additional well and the higher volume of gas needed in continuous gas injection. The table also

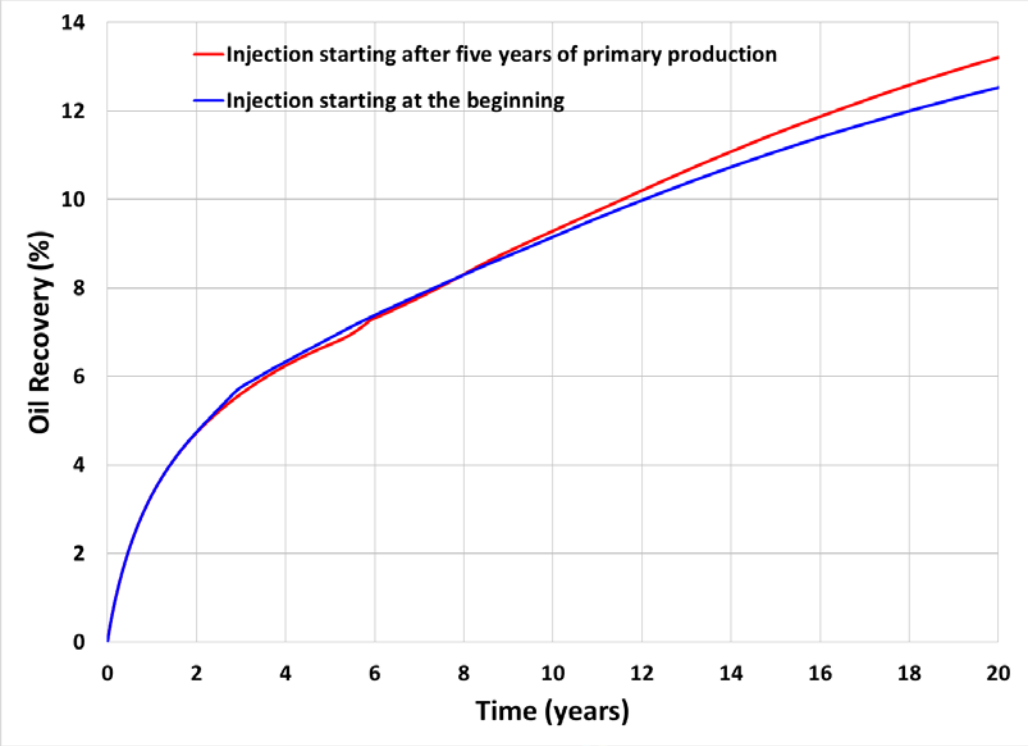

Figure 3-7. Different starting times for continuous gas injection in the single porosity model.

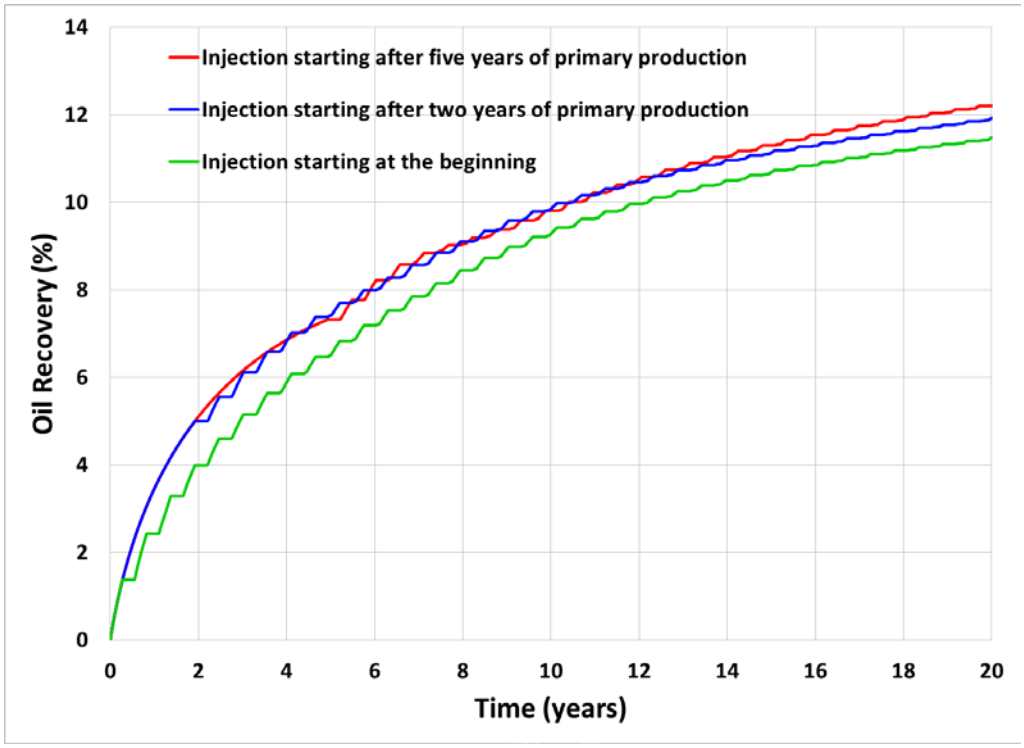

Figure 3-8. Different starting times for huff and puff gas injection in the single porosity model.

shows that small amounts of C2 added to the injected gas do not improve significantly the oil recovery compared to the 100 % methane case.

Only when the injected fluid is 70 % C1 + 20 % C3 + 10% C6, considerable recovery increments are obtained in the single porosity model. Some grade of miscibility with the reservoir oil might be achieved in this case increasing thus the oil recovery. However, the cost and availability of this gas may be an issue.

Table 3-4. Oil recovery factors after 20 years of production. Gas injection starts after 5 years of primary production. Matrix permeability for the single porosity case is equal to 0.01 md, whereas for both dual porosity and dual permeability it is 2.5x10-4 md.

Model	***Primary Recovery***	***Gas Injection***		
		Injected Fluid	***Continuous Gas Injection***	***Huff and Puff***
Single Porosity	9.39	Methane	13.21	12.82
		95% C1 + 5% C2	13.43	12.76
		80% C1 + 20% C2	14.26	12.79
		70 % C1 + 20 % C3 + 10% C6	16.80	15.42
Dual Porosity	10.62	Methane	15.83	26.29
		95% C1 + 5% C2	16.08	26.47
		80% C1 + 20% C2	17.26	27.08
		70 % C1 + 20 % C3 + 10% C6	40.63	32.55
Dual Permeability	10.03	Methane	18.22	19.66
		95% C1 + 5% C2	18.85	19.88
		80% C1 + 20% C2	20.52	20.54
		70 % C1 + 20 % C3 + 10% C6	32.83	20.96

3.3 Dual Porosity Model

The Eagle Ford shale is considered to be a naturally fractured reservoir in many areas. Therefore, dual porosity or dual permeability models are the most suitable to represent the Eagle Ford. **Figure 3-9** illustrates oil recovery for a dual porosity model when injection starts after five years of primary production. Continuous and huff and puff methane injection cases are included in the

figure. The plot shows that when the reservoir is naturally fractured, gas injection can help to improve recoveries in the oil container of the Eagle Ford shale.

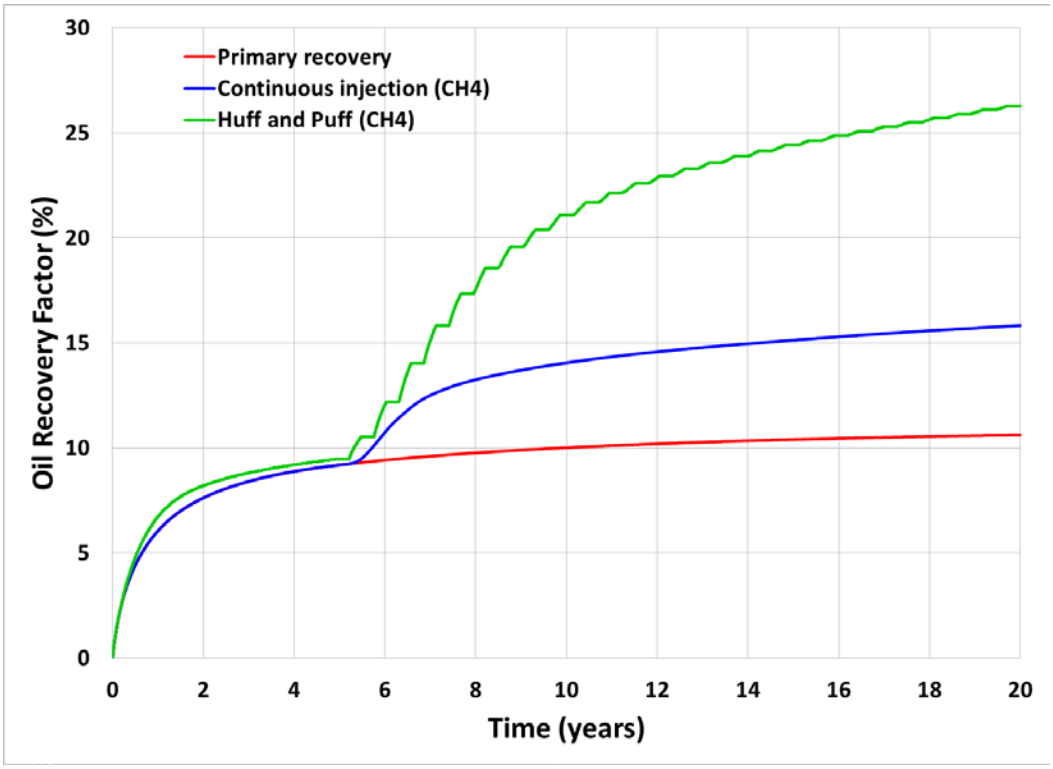

Figure 3-9. Oil recovery from the dual porosity model. Methane injection starts after 5 years of primary production. The red line corresponds to primary recovery, the blue line corresponds to continuous gas injection and the green line corresponds to huff and puff gas injection. The small differences between the huff and puff and continuous injection curves during the five years of primary recovery are due to different production well locations (it is centered in the huff and puff case).

Table 3-4 summarizes the results for different cases using a dual porosity model. The analysis allows to conclude that, in general, huff and puff immiscible gas injection generates considerably greater recoveries that continuous immiscible gas injection when a double porosity model is used (this is also illustrated in **Figure 3-9**). As in the single porosity model, adding C2 to the injected gas does not produce substantial improvements in oil production neither for continuous gas injection nor for huff and puff gas injection. Only the injected gas with composition 70 % C1 + 20

% C3 + 10% C6, which may achieve some grade of miscibility, produces significant better results than methane. In fact, the recovery obtained with this gas composition is almost 25 % more than the recovery using only methane.

Different injection starting times are also evaluated with this model. **Figure 3-10** shows that for continuous gas injection, the final recovery is higher when injection starts after five years of primary production. However, starting injection at the beginning of production life, gives higher early recoveries which may lead to better economic results. From **Figure 3-11**, it can be concluded that the best time to start the huff and puff gas injection is after two years of production. This time not only gives the highest final oil recovery, but also permits to obtain high early recoveries.

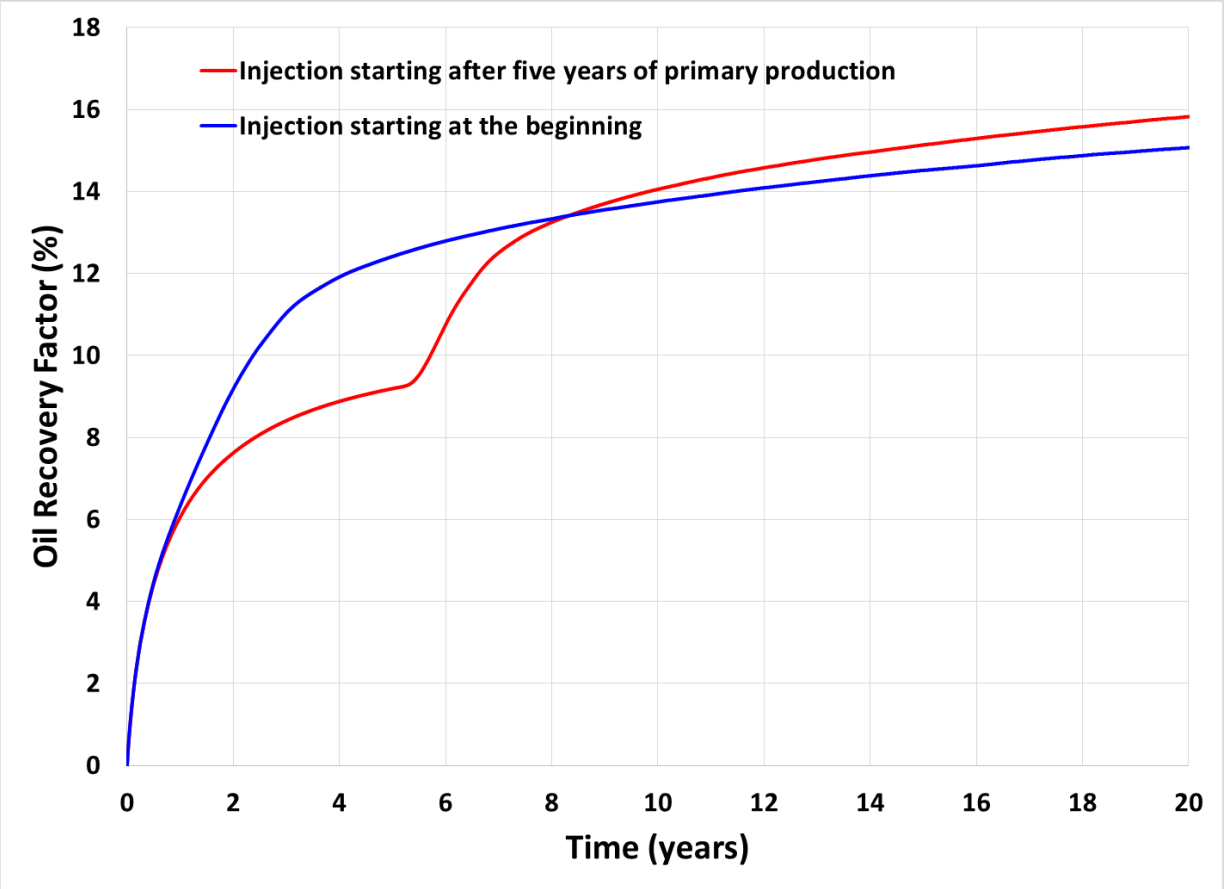

Figure 3-10. Different starting times for continuous gas injection in the dual porosity model.

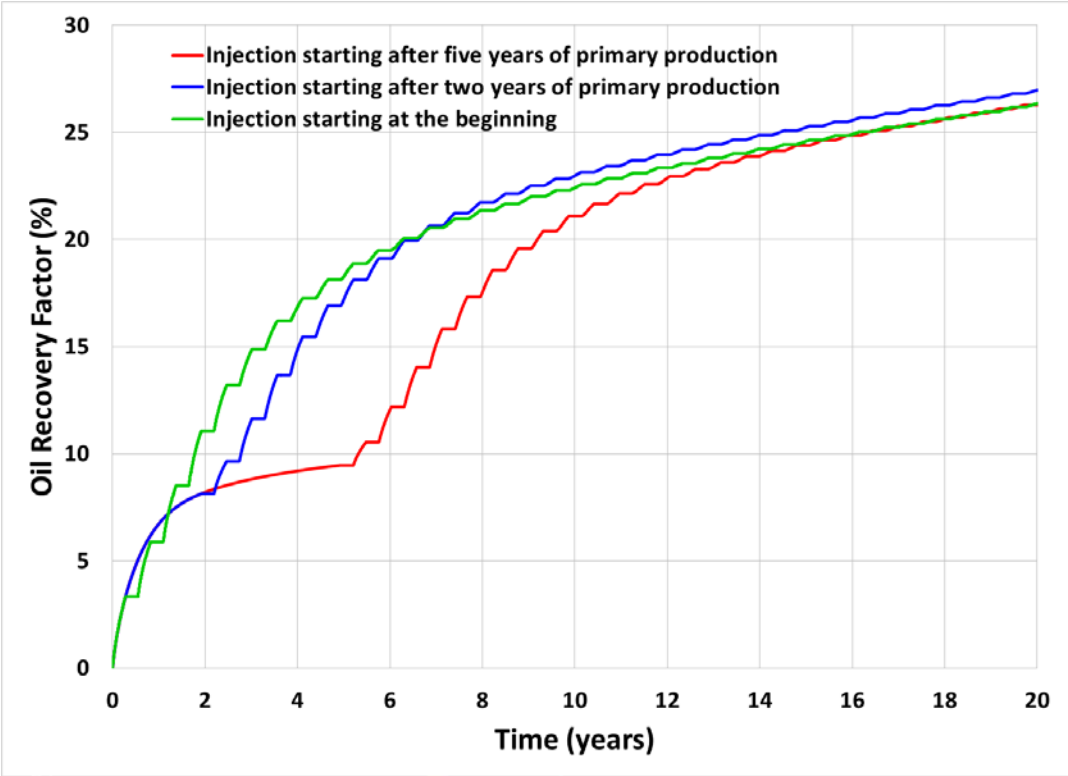

Figure 3-11. Different starting times for huff and puff gas injection in the dual porosity model.

3.4 Dual Permeability

A dual permeability model is also built in order to study gas injection in the naturally fractured Eagle Ford oil container. Input data in both the dual porosity (described above) and dual permeability models are identical. **Figure 3-12** is a plot of oil recovery vs time for the dual permeability model. It shows that, as in the case of the dual porosity model, huff and puff gas injection provides higher recoveries that continuous gas injection when the injection gas is methane.

From **Table 3-4**, it is concluded that when dealing with a dual permeability model, the effect of fluid composition is important in the continuous gas injection case. The use of a gas that can achieve miscibility (70 % C1 + 20 % C3 + 10% C6) improves greatly the performance compared to the use of only methane. On the other hand, fluid composition variations do not have an

important effect on the final recovery obtained by huff and puff gas injection in this model. **Table 3-4** also shows that unlike the dual porosity model, the differences between continuous and huff and puff gas injection results are not pronounced when the injected gas is methane or methane + C2 in the dual permeability model.

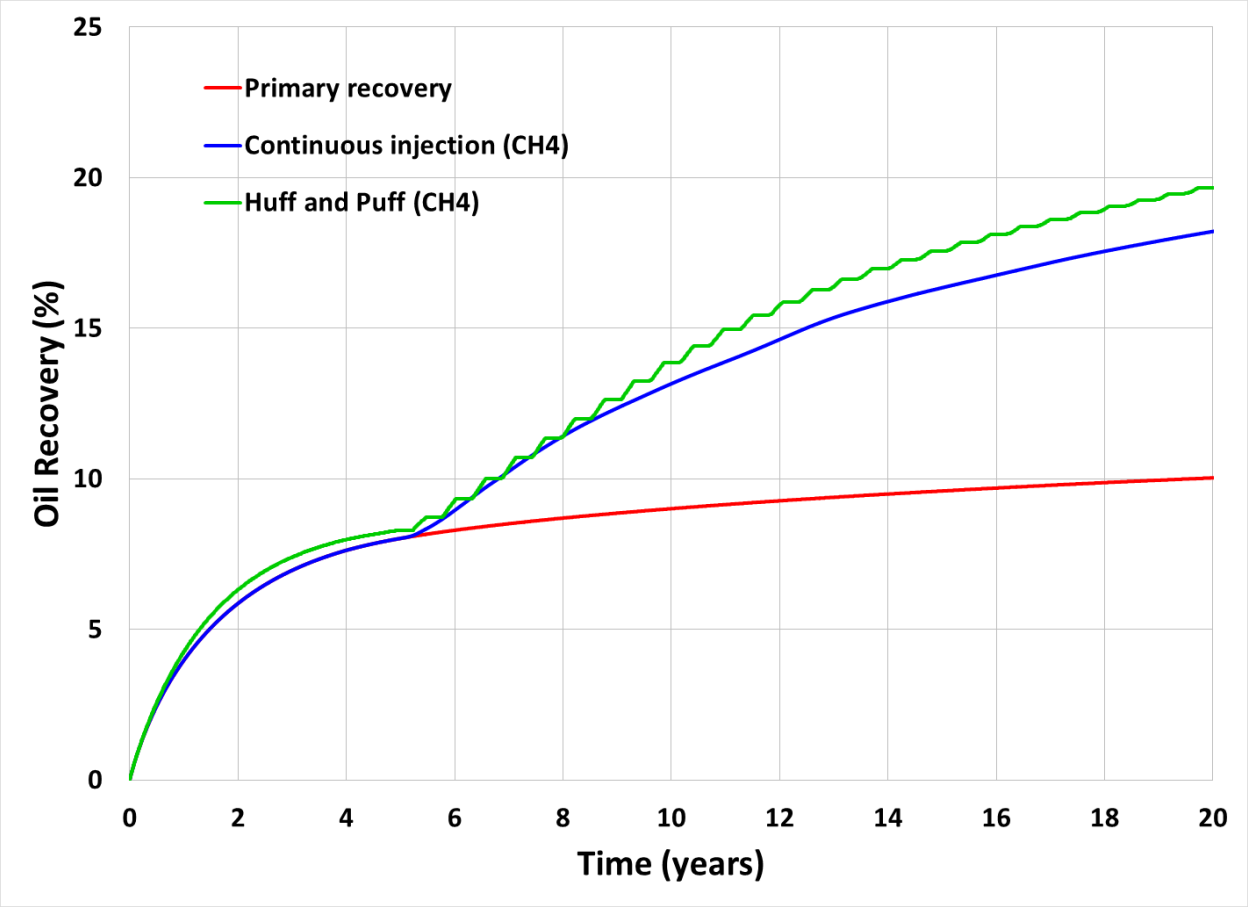

Figure 3-12. Oil recovery from the dual permeability model. Methane injection starts after 5 years of primary production. The red line corresponds to primary recovery, the blue line corresponds to continuous gas injection and the green line corresponds to huff and puff gas injection. The small differences between the huff and puff and continuous injection curves during the five years of primary recovery are due to different production well locations (it is centered in the huff and puff case).

3.5 Effect of Diffusion

So far, all simulations presented in this chapter have considered the effects of molecular diffusion. In order to determine the relevance of this phenomenon in the performance of a continuous gas injection project in a shale oil reservoir, additional simulations are done neglecting diffusion effects. **Table 3-5** summarizes the simulations results. In the single porosity model, diffusion does not play an important role in oil recovery by gas injection; increment in oil recovery is almost the same when diffusion occurs and when it is neglected. On the contrary, when the shale is naturally fractured (dual permeability and dual porosity models), which applies in the cases we are familiar with in the Eagle Ford, diffusion has a significant impact on oil recovery. When diffusion is neglected, the injected gas flows directly to the production well through natural fractures instead of penetrating the matrix. This can even affect negatively oil production as shown in **Table 3-5**. When diffusion occurs, oil recovery is increased due to transfer of solute from the fractures to the matrix emanating from a concentration gradient. Gas injection can improve oil recovery in fractured shale reservoirs in the absence of diffusion effects when there is miscibility as shown previously by Wan et al. (2015).

Table 3-5. Effect of diffusion on oil recovery by continuous CH4 injection.

Model	Without molecular diffusion			Molecular diffusion		
	Primary Recovery	Continuous CH4 Injection	RF Increment	Primary Recovery	Continuous CH4 Injection	RF Increment
Single Porosity	9.39	12.99	3.6	9.39	13.21	3.82
Dual Porosity	11.06	9.54	-1.52	10.62	15.83	5.21
Dual Permeability	10.14	8.89	-1.25	10.03	18.22	8.19

Chapter Four: **Eagle Ford Shale**

4.1 Conceptual Model

The conceptual model proposed in this study is holistic and shows how the production of liquids can be increased under favorable conditions with the use of gas injection. The addition of heavier ends to the injection stream increases even more the recovery of liquids. The basic idea is explained with the use of the schematic presented in **Figure 4-1**, which includes all the fluids considered in this investigation. Fluids are produced from the condensate container (C) in the middle of the structure, the oil container (O) in the upper part of the structure and the dry gas container (G) in the lower part of the structure. Liquids are stripped from the condensate and the left-over dry gas is re-injected into container C. Thus, this would be equivalent to a gas condensate re-cycling project. A portion of the dry gas produced from container G is injected jointly with re-cycled gas into container C with the ultimate goal of maintaining the pressure above the dew point. The other portion of the produced dry gas is injected into container O.

4.2 Simulation Model

To represent the previously presented conceptual model, a compositional simulation model is built in GEM, CMG. As the sweet spots in the Eagle Ford are known to be naturally fractured, a dual permeability approach is selected. The grid consists of three boxes that represent containers (O), (C) and (G) as shown in **Figure 4-2.** Each box has an area of 127 acres and a thickness of 200 ft. Reservoir fluid compositions published by Ramirez and Aguilera (2016) are used in the study (**Table 4-1**).

The production behavior of any reservoir is largely determined by relative permeabilities. Unfortunately this property is not fully understood yet in shale reservoirs. However, some authors have published shales relative permeability data. For example, Daigle et al. (2015) presented gas-

water permeability curves for Woodford and Green River shales as well as the Cretaceous Cameo Coal. Suhrer et at. (2013) used digital rock physic methods to calculate gas-water and oil-water relative permeabilities of samples from a shale formation in Colombia. Agboada et al. (2013) published relative permeability data obtained from history matching of two wells in the Eagle Ford shale. In this work, relative permeability curves are built using the end points and Corey exponents published by Honarpour et al. (2012) (**Table 4-2**).

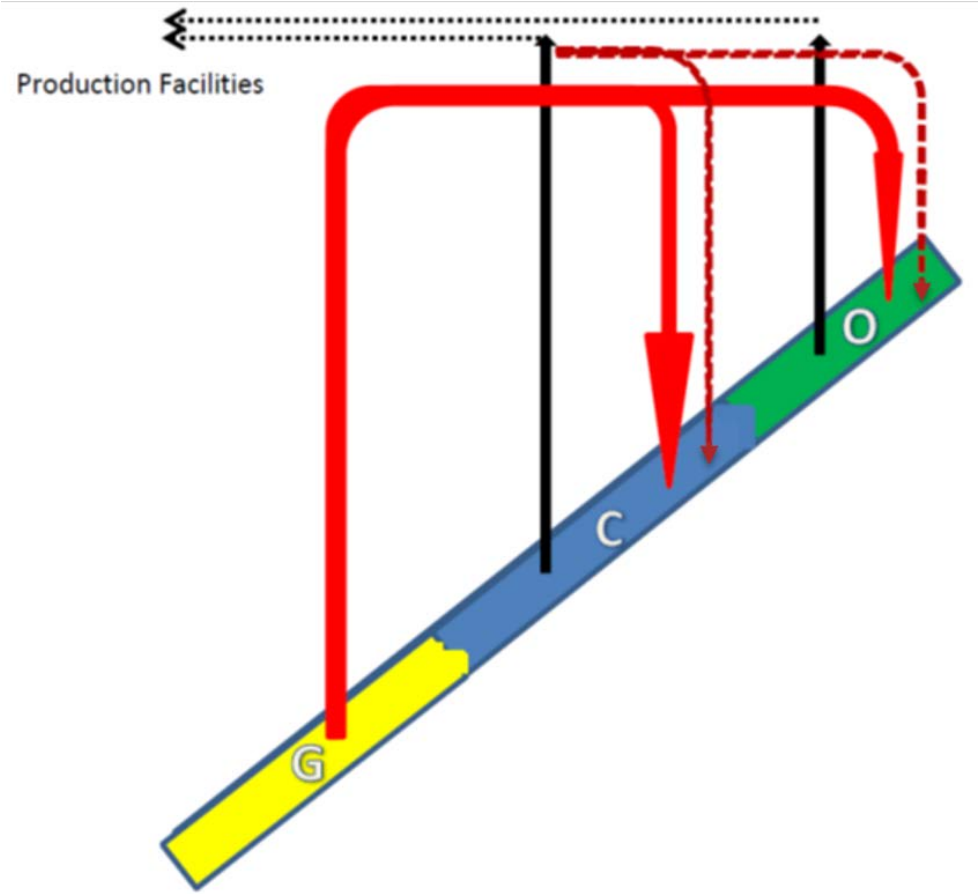

Figure 4-1. Conceptual model for gas injection in shale oil (O) and condensate (C) containers (not to scale). Thick red arrows show gas injection (essentially dry gas) produced from bottom of the structure (container G). Thin red dashed lines show injection in O and C of gas stripped from C.

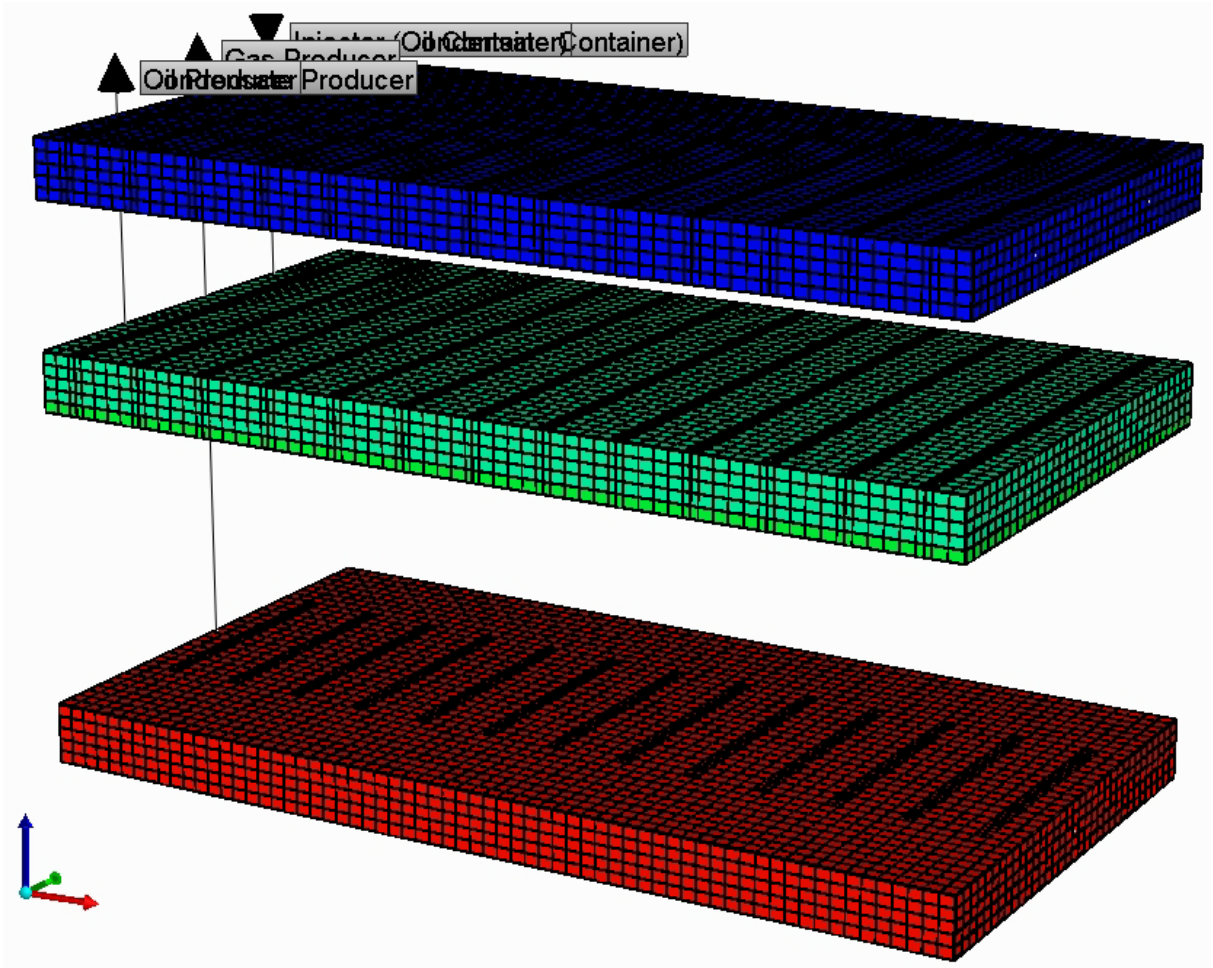

Figure 4-2. Simulation model for gas (red), condensate (green) and oil (blue) containers. Gas is injected in the shale oil and condensate containers, which correspond to letters O and C in Figure 4-1. Depths are not to scale.

Table 4-1. Fluid composition for the three containers defined in the model

	Molar Fraction		
Component	***Oil Container***	***Condensate Container***	***Dry Gas Container***
CO_2	0.0091	0.0121	0.0
N_2	0.0016	0.0194	0.0
C_1	0.3647	0.6599	0.9468
C_2	0.0967	0.0869	0.0527
C_3	0.0695	0.0591	0.0005
C_{4-6}	0.1255	0.0967	0.0
C_{7+1}	0.20	0.047448	0.0
C_{7+2}	0.10	0.015157	0.0
C_{7+3}	0.0329	0.003295	0.0

Honarpour et al. (2012) published data for the primary drainage process in the Eagle Ford calcite rich region, the organic rich region and the natural fractures. “The models were developed based on measurement conducted on cores and flow simulation by Lattice Boltzmann model using a 3D digital pore network” (Honarpour et al., 2012).

The Eagle Ford is divided into two intervals. The upper region, where an oil maturation window is present, is calcite rich. The lower region, where a gas maturation window is present, is rich in organic material. Data for the calcite rich region is used to build the relative permeability curves for the oil container. Data for the organic rich region is used to build the curves for the condensate and dry gas containers. **Figure 4-3** presents the relative permeability curves.

Due to the importance of relative permeabilities in the performance of oil and gas reservoirs, a sensitivity analysis to the end points and hysteresis must be carried out in order to analyze different scenarios (favorable and unfavorable) that can occur in practice when conducting gas injection projects. Other published curves or models for relative permeabilities in shales may also be used. This sensibility is not included in this thesis and is recommended for future research.

A producer horizontal well with multistage hydraulic fracturing (13 stages) is drilled in each container. Additionally, for the continuous injection case, injection wells are drilled in the oil and condensate containers. These are also horizontal wells with the same type of multistage hydraulic fractures. For the huff and puff injection, there is no need to drill injection wells as the producers are also used to inject gas in the condensate and oil containers. **Table 4-3** summarizes the reservoir properties and the wellbore parameters for the three containers in the model. Multicomponent adsorption is included using the extended Langmuir isotherm (Arri et.al, 1992):

$$V_i = \frac{(V_L)_i b_i P_i}{1 + \sum_j b_j P_j} \qquad \textbf{Eq. 4-1}$$

Table 4-2.Relative permeability models for fractures and matrix (organic and calcite rich). Honarpour et al. (2012).

	Gas Phase			*Oil Phase*			*Water Phase*	
TOC-rich			**Sensitivity**			**Sensitivity**		
	S_{gc}	0.2	0.18-0.22	**S_{org}**	0.5		**S_{wmin}**	0.25
	Corey Gas	3	2-7.5	**Corey O/W**	5		**S_{wcr}**	0.25
	K_{rg} at S_{wmin}	0.5		**Corey O/G**	4.5	3-6		
	K_{rg} at S_{org}	0.01		**K_{ro} at S_{omax}**	4			
Calcite-rich	*Gas Phase*			*Oil Phase*			*Water Phase*	
			Sensitivity			**Sensitivity**		
	S_{gc}	0.15	0.13-0.17	**S_{org}**	0.3		**S_{wmin}**	0.5
	Corey Gas	2	1-7.5	**Corey O/W**	4		**S_{wcr}**	0.55
	K_{rg} at S_{wmin}	0.7		**Corey O/G**	3.5	2-5		
	K_{rg} at S_{org}	0.01		**K_{ro} at S_{omax}**	0.6			
Fracture	*Gas Phase*			*Oil Phase*			*Water Phase*	
			Sensitivity			**Sensitivity**		
	S_{gc}	0.05	0.0-0.1	**S_{org}**	0.1		**S_{wmin}**	0.1
	Corey Gas	1.2	1-1.4	**Corey O/W**	2.5		**S_{wcr}**	0.1
	K_{rg} at S_{wmin}	0.9		**Corey O/G**	1.5	1-2		
	K_{rg} at S_{org}	0.05-0.5		**K_{ro} at S_{omax}**	0.7			

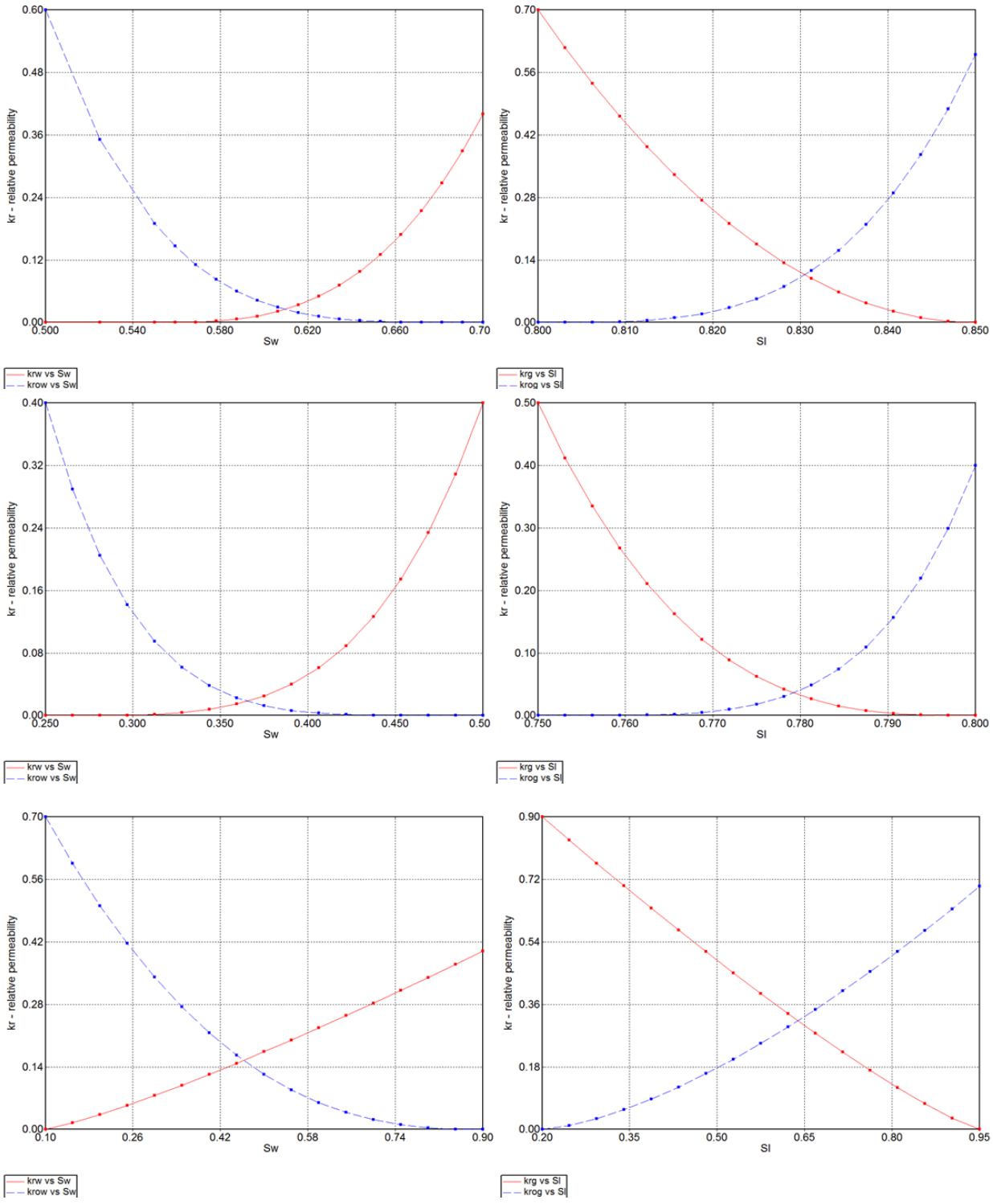

Figure 4-3. Relative permeability curves for the calcite rich zone (top graph), organic rich zone (middle) and fractures (bottom).

Table 4-3. Reservoir and wellbore geometry parameters for the Simulation Model

Parameter	Symbol	Oil Container	Condensate Container	Dry Gas Container	Units
Initial reservoir pressure	P_i	4,000	4,800	8500	psi
Water compressibility	C_w	3.00E-06	3.00E-06	3.00E-06	1/psia
Matrix compressibility	C_m	1.00E-6	1.00E-6	1.00E-6	1/psia
Natural fracture compressibility	C_f	1.00E-5	1.00E-5	1.00E-5	1/psia
Formation Top	D_R	6,000	8,000	14,000	ft
Matrix porosity	ϕ_m	0.055	0.066	0.077	Fraction
Natural fractures Porosity	ϕ_2	0.00055	0.00055	0.00066	Fraction
Matrix Permeability	k_m	0.0001	0.0001	0.0002	md
Natural Fracture Permeability	k_2	0.02	0.02	0.04	md
Natural Fracture Spacing		10	10	10	ft
Total Organic Carbon	TOC	-	2	2	% weight
Reservoir thickness	h	200	200	200	ft
Hydraulic fracture half-length	x_{hf}	400	400	400	ft
Hydraulic Fracture Spacing		250	250	250	ft
Length of the horizontal well	L	3,250	3,250	3,250	ft
Skin factor	S	0	0	0	-
Flow capacity of hydraulic fractures	$k_{hf}*w_{hf}$	50	50	50	md-ft
Bottomhole flowing pressure	P_{wf}	2,000	1,000	500	psi

Where V_i is the adsorbed volume of component "*i*" in scf/ton, $(V_L)_i$ is the Langmuir volume of component "*i*" in scf/ton, b_i is the inverse of the Langmuir pressure for component "*i*" and P_i is the partial pressure of component "*i*". The values of the Langmuir isotherm parameters are taken from Cao et al, 2015. They calculated Langmuir volumes for different TOCs. This thesis uses Langmuir volumes for a TOC of 2% (**Table 4-4**).

Table 4-4. Adsorption isotherm parameters

	N_2	CO_2	C_1	C_2	C_3	C_{4-6}	C_{7+1}	C_{7+2}	C_{7+3}
V_L (scf/ton)	0	78	34	51	95	121	121	121	121
P_L (psia)	0	836	1562	811	844	355	355	355	355

The presence of molecular diffusion as a mass transport mechanism is considered in this thesis except where noted. Sigmund correlation is used to calculate gas phase and oil phase diffusion coefficients.

4.3 Base case

The actual method for exploiting shale reservoirs consists of drilling horizontal wells and carrying out multistage hydraulic fracturing treatments to create flow channels that make possible the economic production of oil and gas from these ultratight rocks. To determine the benefits of a gas injection project, a base case that represents the performance of a shale reservoir under current exploitation practices is evaluated in the first place. In the base case, the simulation model is run for 20 years of primary production.

4.3.1 Oil Container

Figure 4-4 presents the oil rates and average reservoir pressures in the oil container for the base case. The initial oil rate is 1000 stb/day. This rate is maintained during the first two months and

then starts to drop very quickly. After five years, the oil rate is 16 bbl/day, and after 20 years it is only 3 bbls/day. This fast depletion is usually observed in shale reservoirs and illustrates the

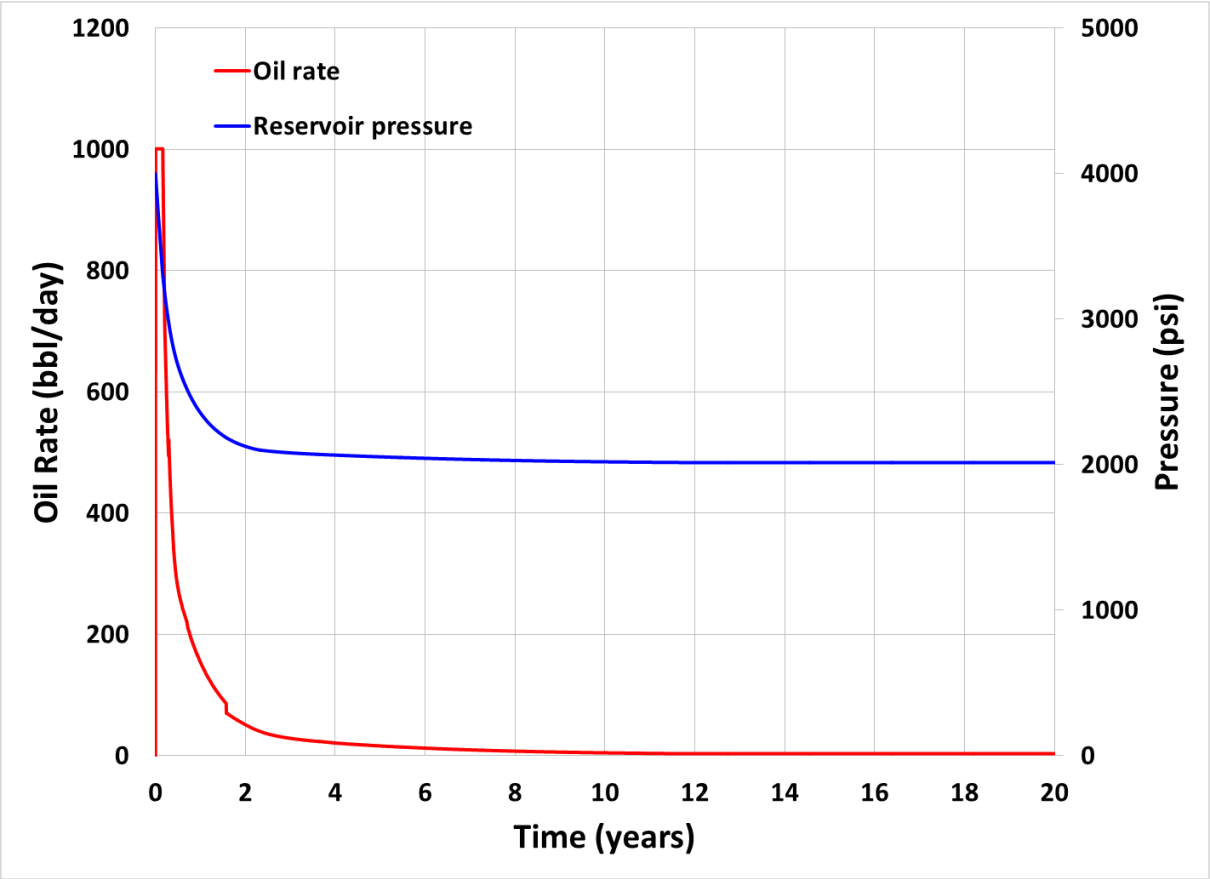

Figure 4-4. Oil production rate and average reservoir pressure in the oil container for the base case

necessity of implementing techniques to boost oil production and improve recoveries. The initial reservoir pressure in the oil container is 4000 psi, and it drops to 2015 psi after 20 years of primary production.

Figure 4-5 is a plot of oil recovery vs time for the base case. It shows that most of the oil in place remains in the reservoir container after 20 years of primary production. For this case, only 6.9% of the oil originally in place in this container is recovered.

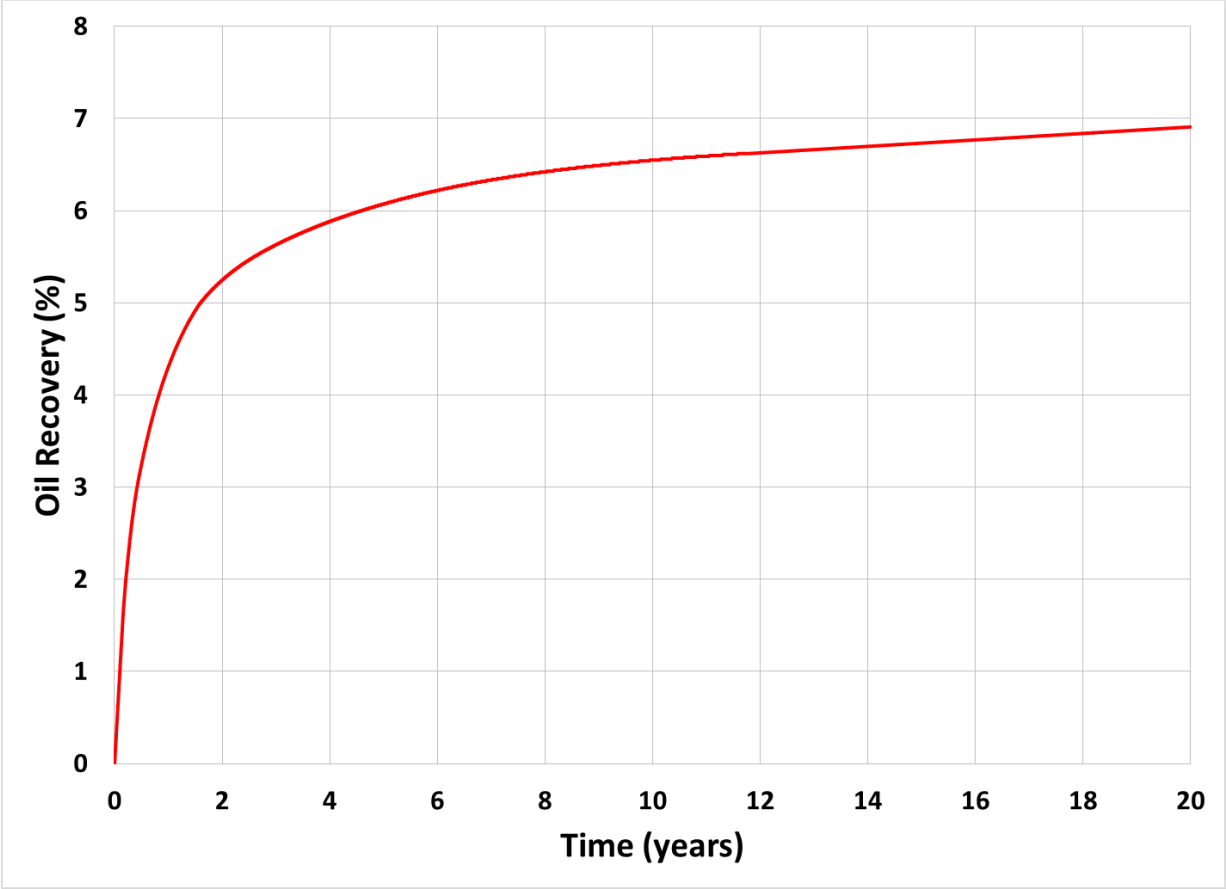

Figure 4-5. Oil recovery factor in the oil container for the base case

4.3.2 Condensate Container

Oil production in the condensate container also declines very fast during the early years of primary production as shown in **Figure 4-6.** On the other hand, although reservoir pressure decreases strongly during primary production, the reduction is more gradual in the condensate container as compared to the oil container.

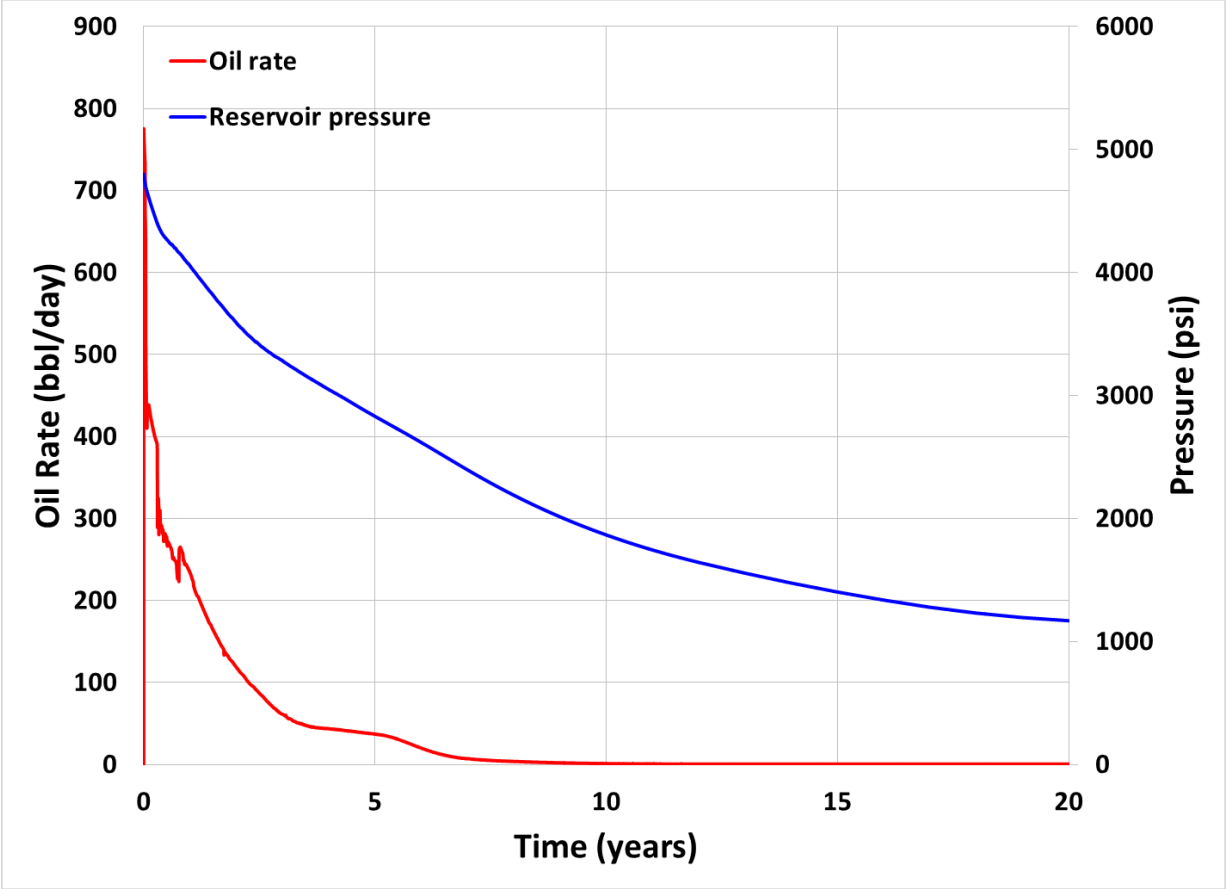

Figure 4-6. Oil production rate and average reservoir pressure in the condensate container for the base case

Figure 4-7 shows that oil recoveries are also very low in the condensate container. This low recoveries are not only due to the very low matrix permeabilities, but also to the formation of condensate banking around the wellbore as the pressure falls below the dew point.

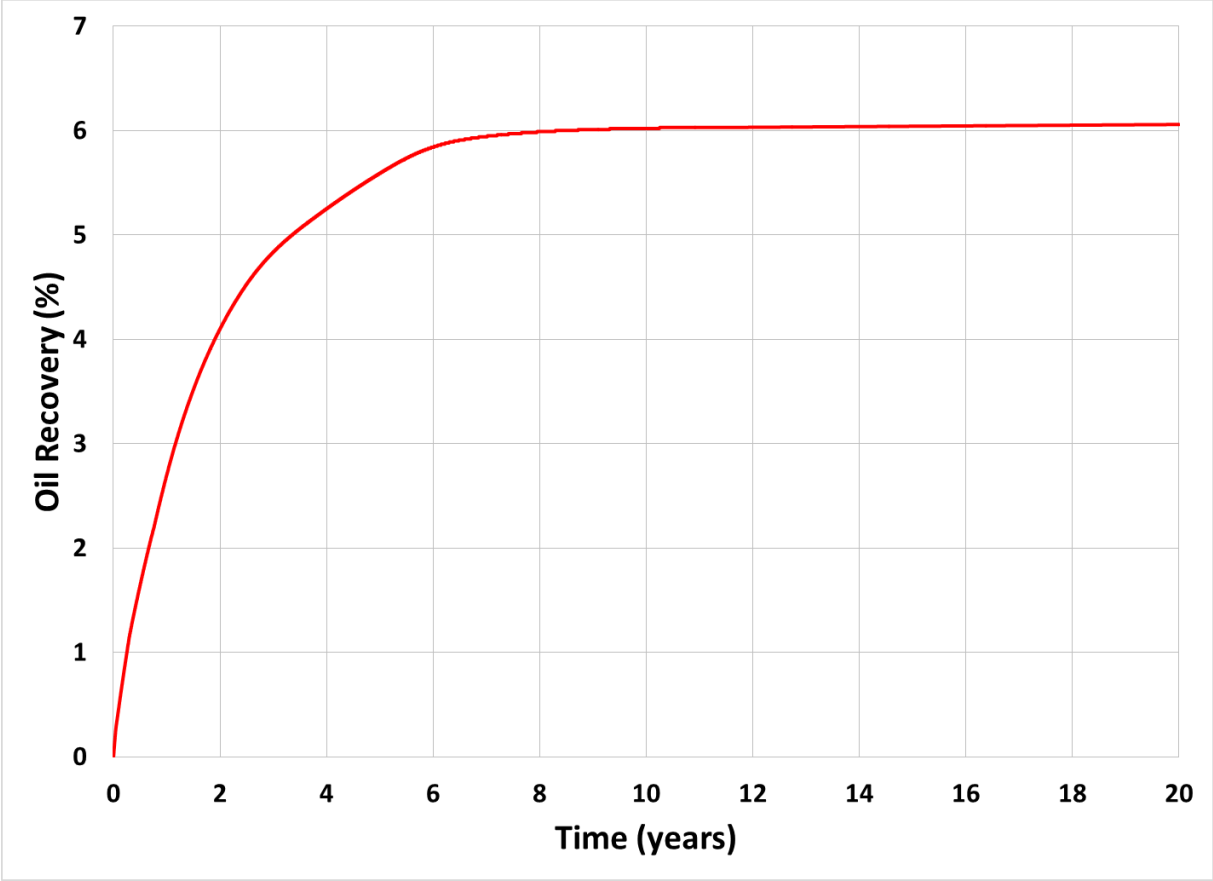

Figure 4-7. Oil recovery factor in the condensate container for the base case.

4.4 Continuous Gas Injection

The gigantic volume of dry gas stored in the deepest part of the structure in some shales such as the Eagle Ford in the United States and the Duvernay in Canada can be used to increase liquid recoveries in the condensate and oil containers of these reservoirs by implementing gas injection projects. Due to market conditions this dry gas is not being produced at this time. The gas injection can be complemented by the reinjection of the gas stripped from the condensate.

To simulate the methodology proposed in the conceptual model discussed in **section 4.1**, the production wells in the condensate and dry gas containers are defined as “CYCLPROD” in GEM. The injected fluid in the injection wells is defined as “CYCLING”. In addition, the molar recycling

is restricted to a maximum of 50 % in each injection well. In this way, the fluid injected is the gas produced from the dry gas container and the gas stripped from the condensate. The injection pressure is constrained to a maximum of 6500 psi and the injection is started after five years of production.

4.4.1 Oil Container

The low oil recoveries from the oil container can be increased by means of continuous dry gas injection. **Figure 4-8** illustrates the dramatic improvement in oil recovery. Recovery after 20 years goes from 6.9% by primary production to 20.6% by continuous gas injection.

This improved oil recovery is the results of both, an increase in reservoir pressure and the presence of molecular diffusion, which allows fluid flow from the fractures to the ultra tight matrix as well as fluid flow within the matrix due to differences in concentration. Results are also presented as oil recoveries vs injected pore volumes at reservoir conditions as shown in **Figure 4-9**. After 15 years of gas injection, 1.45 pore volumes of gas at reservoir conditions have been injected.

Oil rate in the oil container decreases from 1000 to 16.25 bbl/day after 5 years of primary production. Upon initiation of gas injection, the oil rate grows gradually until it reaches a maximum of 215 bbl/day. Then it decreases gradually and eventually stabilizes at approximately 70 bbl/day (**Figure 4-10).** Gas injection restores the reservoir pressure, which is significantly reduced during primary recovery. Gas injection rate remains constant at 5.2 MMscf/day during the continuous injection.

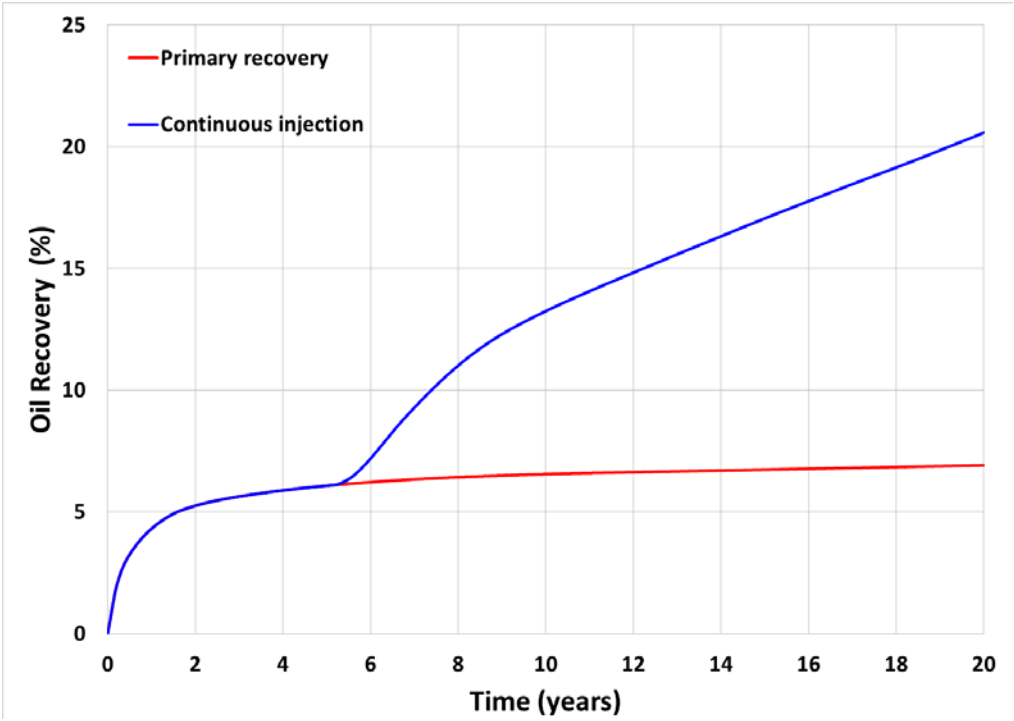

Figure 4-8. Oil recovery factor in the oil container by continuous gas injection starting after five years of production

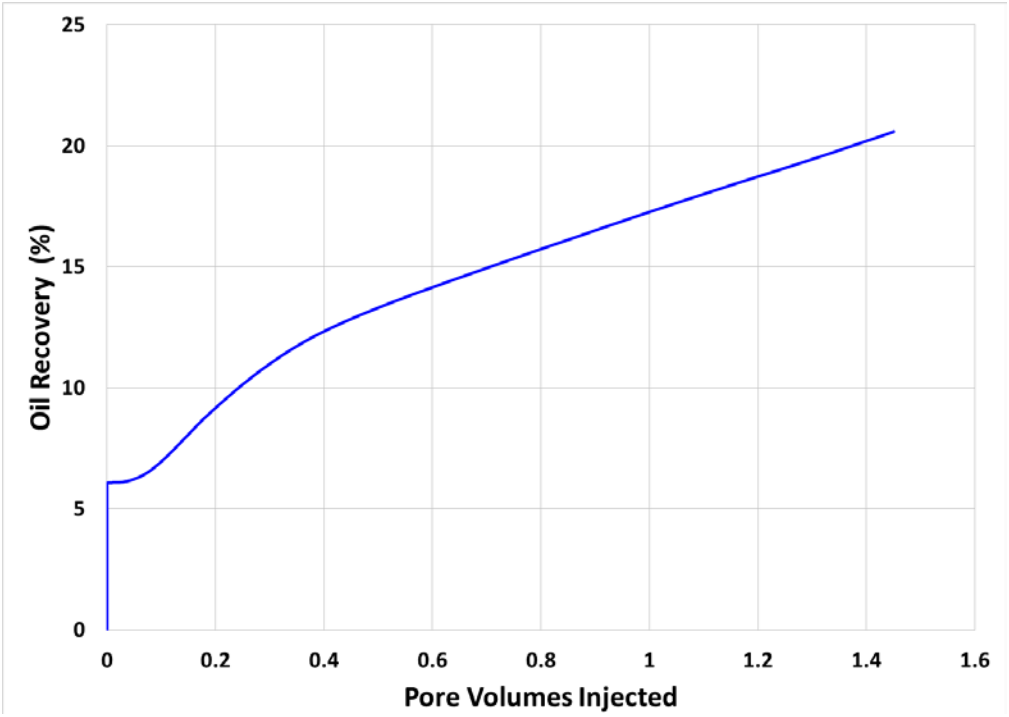

Figure 4-9. Oil recovery factor in the oil container by continuous gas injection vs pore volumes injected

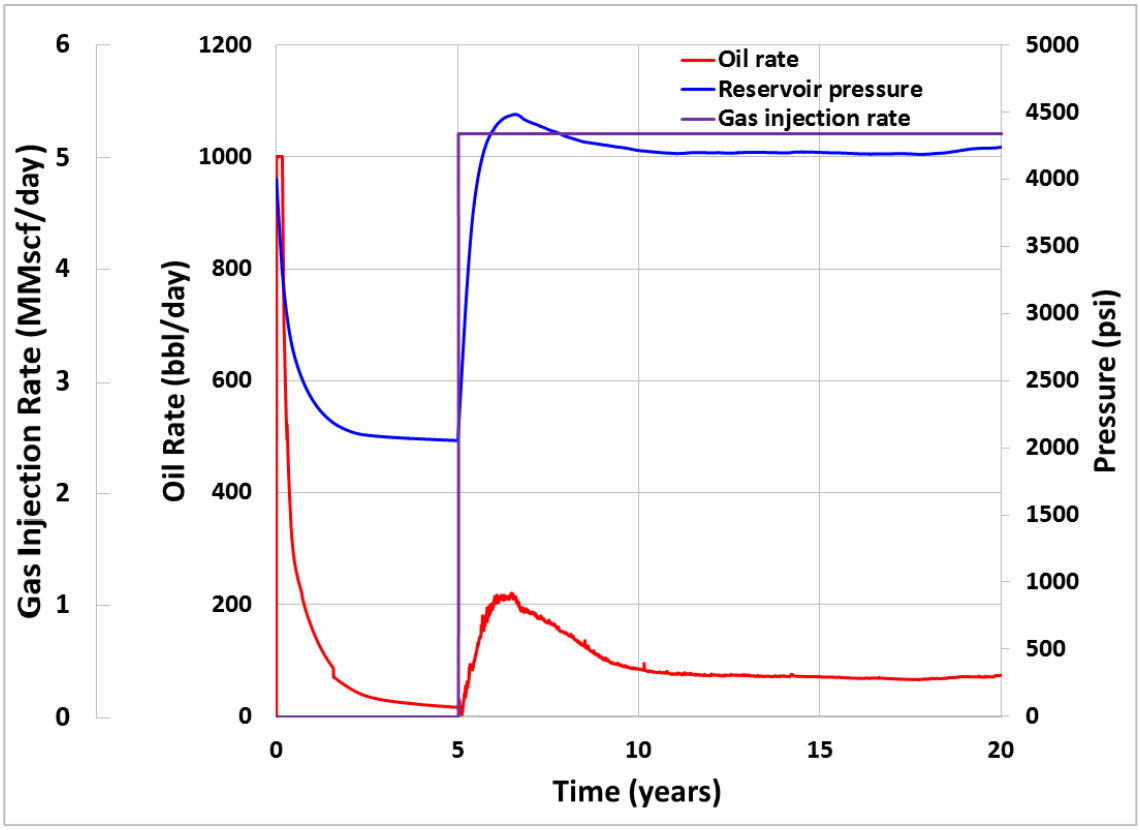

Figure 4-10. Oil production rate, gas injection rate and average reservoir pressure in the oil container for the continuous gas injection case

According to Warner et al. (2006) "when only oil recovery and improvements in reservoir producing characteristics are considered, reservoir conditions for gas injection operations are usually more favorable when the reservoir is at or slightly below the oil bubble point pressure, unless the bubble point pressure is low compared with the initial reservoir pressure." This rule is applicable to conventional reservoirs. In order to estimate the best time to start the gas injection, simulations are done with three different starting times: (1) after five years of primary production, which is the case discussed above, (2) at the beginning of production, and (3) after 17 months of primary production. This last time is selected because at approximately 17 months the average

reservoir pressure is close to the oil bubble point pressure. **Figure 4-11** presents the results. The higher recoveries are obtained when injection starts at the beginning of production. The aforementioned rule of thumb for conventional reservoirs does not apply in this case. Maybe the bubble point pressure is too low compared to the initial reservoir pressure, or most likely the rule is not valid in fractured shale reservoirs due to the different mechanisms active when oil is displaced by gas in these types of reservoirs.

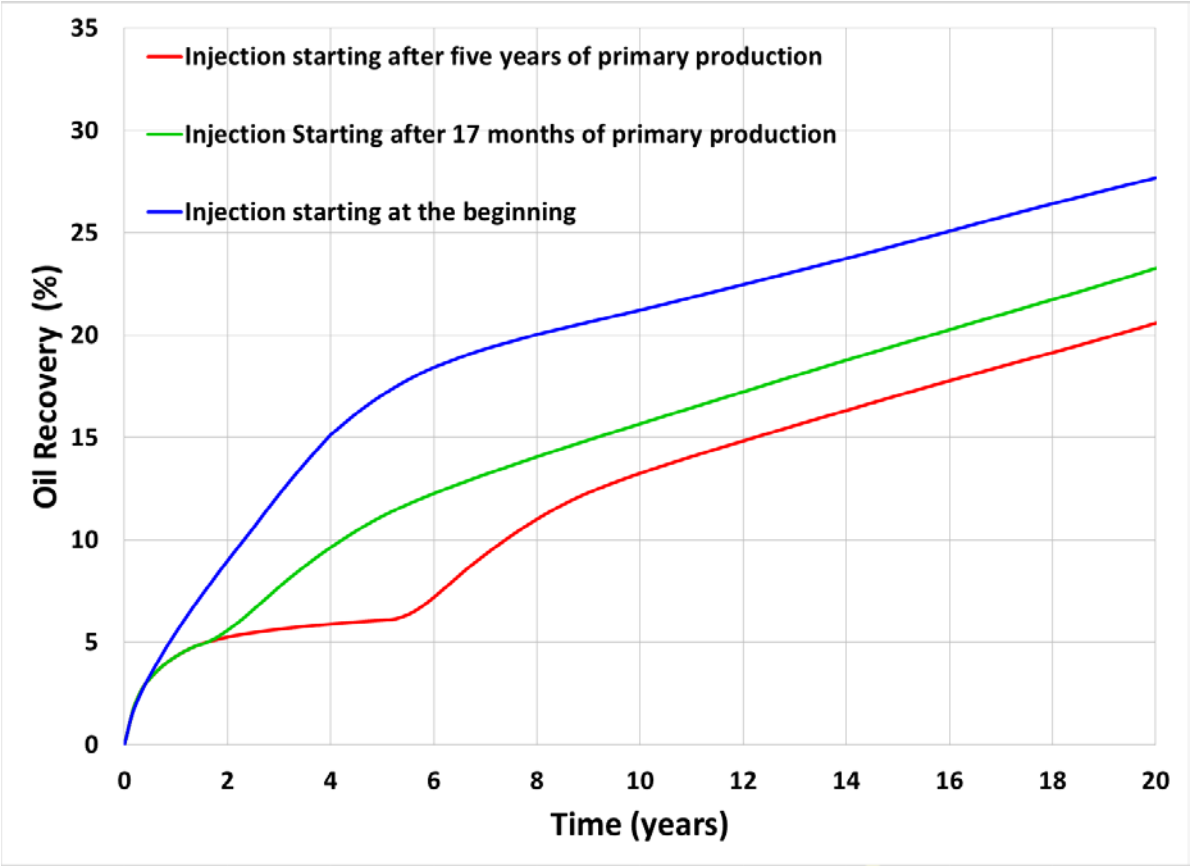

Figure 4-11. Different starting times for continuous gas injection in the oil container

As previously discussed during the description of the simulation model, the presence of molecular diffusion as a transport mechanism is considered throughout this study. In order to investigate the

effect of this phenomenon, further simulations are run where molecular diffusion is ignored. **Figure 4-12** confirms what was concluded in chapter three: molecular diffusion plays a fundamental role in the performance of a continuous dry gas injection project. In this case, without the "help" of molecular diffusion, the continuous gas injection would be a complete fiasco. The injected gas flows directly from the injection well to the production well through the hydraulic and natural fractures without penetrating the matrix. The result is a smaller recovery by continuous gas injection as compared to primary recovery.

As the higher the temperature, the more intense the mass transference due to molecular diffusion, continuous injection may benefit from an increase in the reservoir temperature. This can be done, for instance, by using electrical downhole heaters.

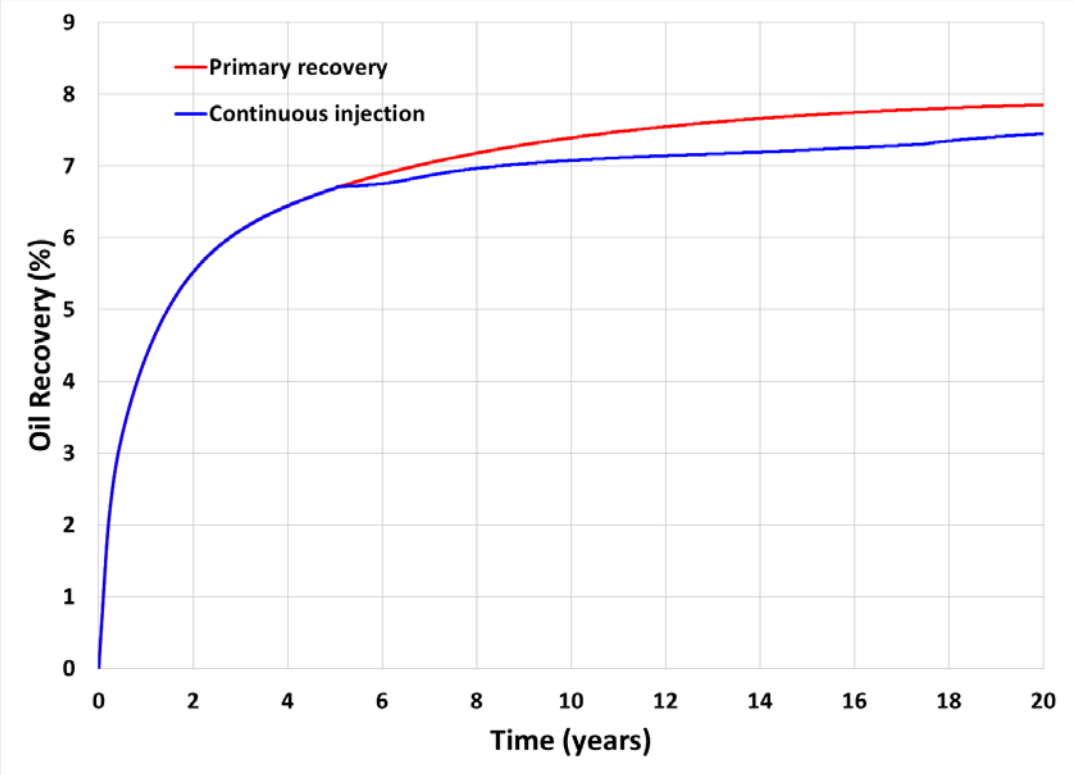

Figure 4-12. Oil recovery factor in the oil container by continuous gas injection when molecular diffusion is neglected

4.4.2 Condensate Container

During the last few years, there have been significant efforts to produce liquids from shale reservoirs due to more favourable economic considerations. However, oil recoveries have remained very low since the unique exploitation strategy has been drilling a large number of horizontal wells, which have been hydraulically fractured in multiple stages.

The approach developed in this thesis using the conceptual model presented in **Figure 4-1** leads to significant improvements in liquids recoveries from Eagle Ford shale reservoir containers. The vertical containment of the 'upside-down' oil, condensate and gas has been demonstrated by Ramirez and Aguilera (2016).

This thesis simulation results show that, in the presence of molecular diffusion, recoveries in the condensate container can be increased from 6.1% by primary production to 14.7% by gas injection (**Figure 4-13**). After 15 years of continuous gas injection, 1.3 pore volumes of gas at reservoir conditions are injected (**Figure 4-14**).

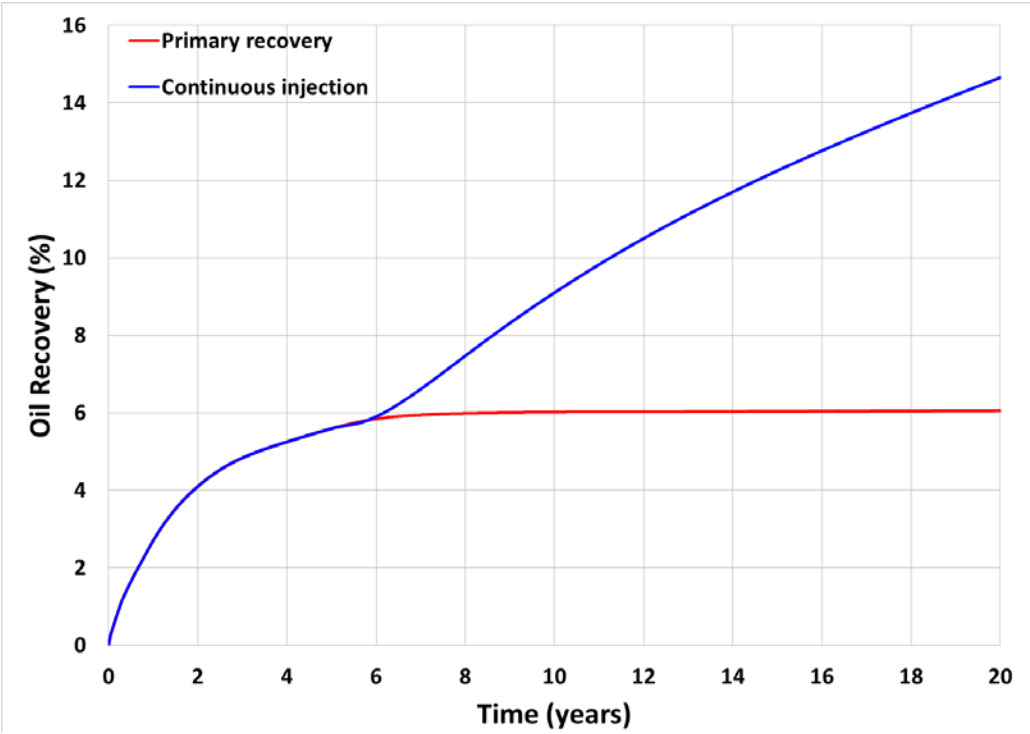

Figure 4-13. Oil recovery factor in the condensate container by continuous gas injection starting after five years of production

Figure 4-15 illustrates how the oil rate and the average reservoir pressure increase by implementing a continuous gas injection project in the condensate container. The initial rise in the oil rate once the gas injection starts is not as abrupt as in the oil container. Gas injection rate is very high during the first months of continuous injection in the condensate container. Then, it drop drastically and stabilizes at approximately 5.5 MMscf/day.

The time when the injection should start is also analyzed in the condensate container. The starting times are the same used for the oil container. Again, results show that the highest recoveries are obtained from the condensate container when injection starts at the beginning of production, as shown in **Figure 4-16**.

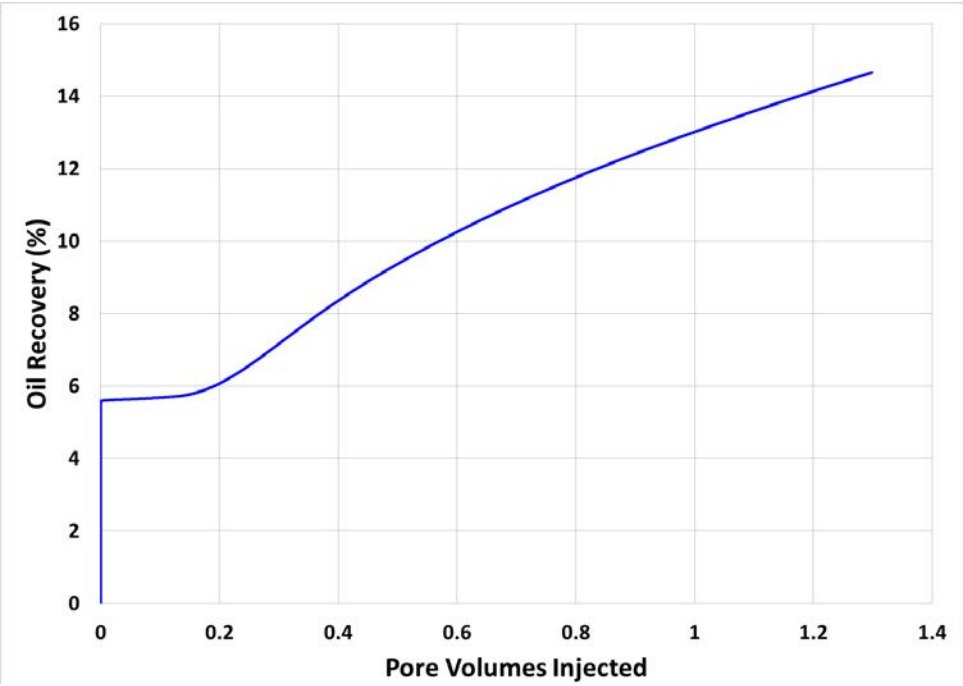

Figure 4-14. Oil recovery factor in the condensate container by continuous gas injection vs pore volumes injected

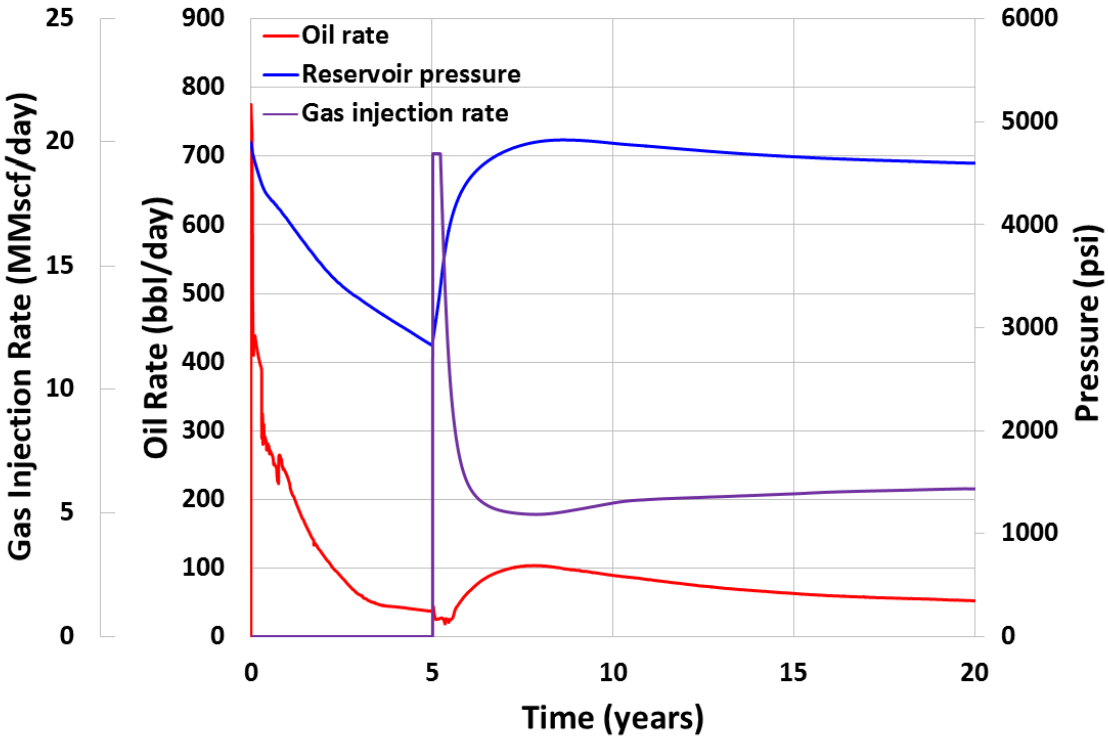

Figure 4-15. Oil production rate, gas injection rate and average reservoir pressure in the condensate container for the continuous gas injection case

The effect of molecular diffusion in the performance of a continuous dry gas injection project is displayed in **Figure 4-17.** As in the oil container, diffusion seems to be fundamental when using continuous dry gas injection to increase liquid recoveries from the condensate container. In this case, gas injection "kills" the liquid production from the reservoir and actually the recovery by gas injection is smaller than the primary recovery.

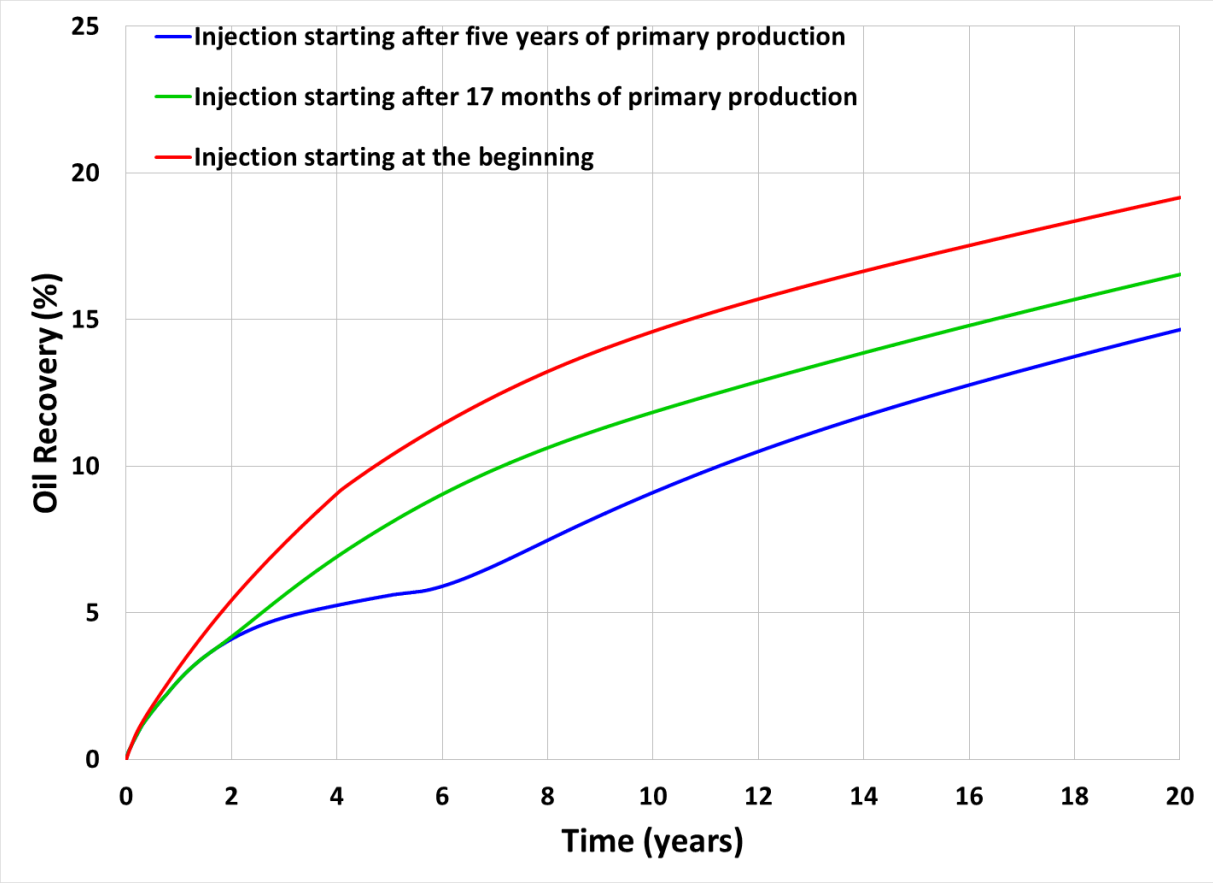

Figure 4-16. Different starting times for continuous gas injection in the condensate container

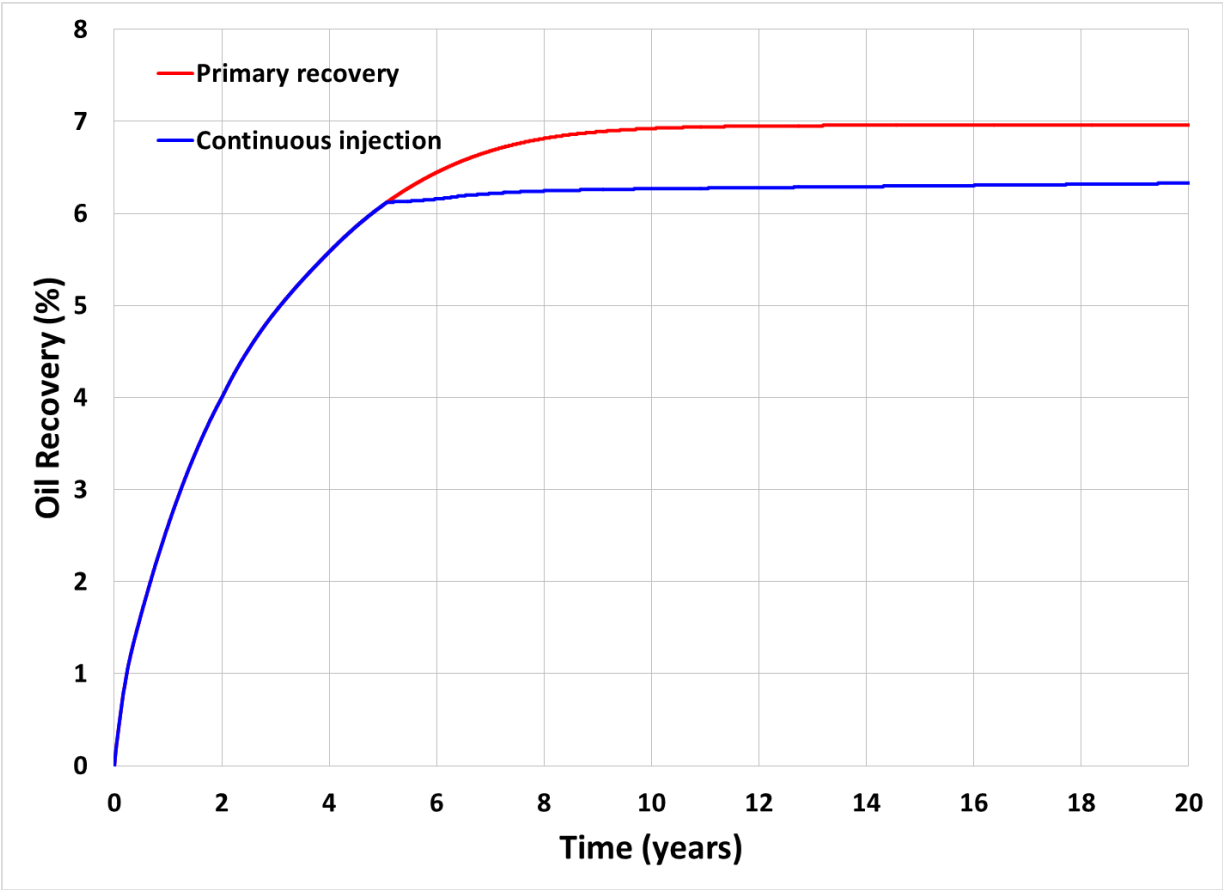

Figure 4-17. Oil recovery factor in the condensate container by continuous gas injection when molecular diffusion is neglected

4.5 Huff and Puff Gas Injection

To simulate the huff and puff gas injection scheme, the model used for the continuous gas injection case is modified. In the oil and condensate containers, the production wells are located in the center of the reservoir grid. As GEM does not allow to switch a well from producer to injector, injection wells are defined, located and perforated in the same place that the producers. Then, during the huff periods, the producers are shut in and the injectors are opened, and during the puff periods, the producers are opened and the injectors are shut in.

4.5.1 Oil Container

Oil recoveries in the oil container can be also increased by means of huff and puff dry gas injection. The results are much better than those obtained by continuous gas injection. Oil recovery after 20 years is 28.9%, which is four times the primary recovery (**Figure 4-18**). The best performance of the huff and puff gas injection can be explained by considering the gas flow from the injection to the production wells through the natural fractures. In the huff and puff, as the injection and production operations are done in the same well, the gas can penetrate the matrix more efficiently. In the continuous injection, the gas moves through fractures without allowing enough time for soaking and penetrating the matrix. **Figure 4-19** presents oil recoveries vs. pore volumes injected at reservoir conditions. After 15 years of gas injection, one pore volume of gas at reservoir conditions has been injected.

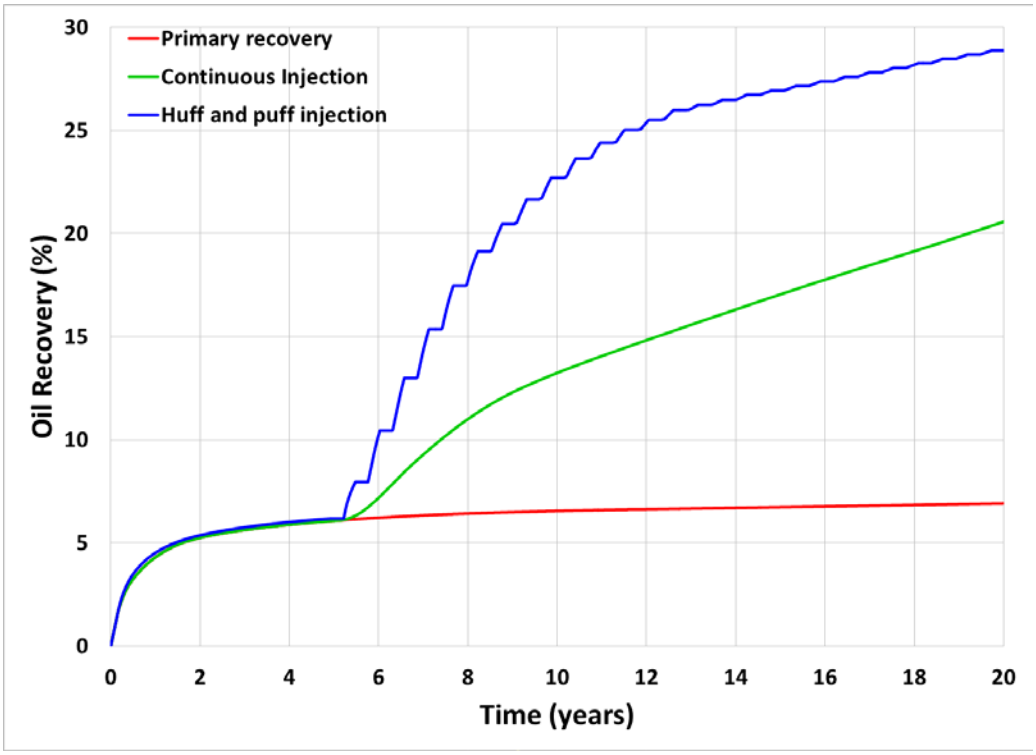

Figure 4-18. Oil recovery factor in the oil container by huff and puff gas injection starting after five years of production.

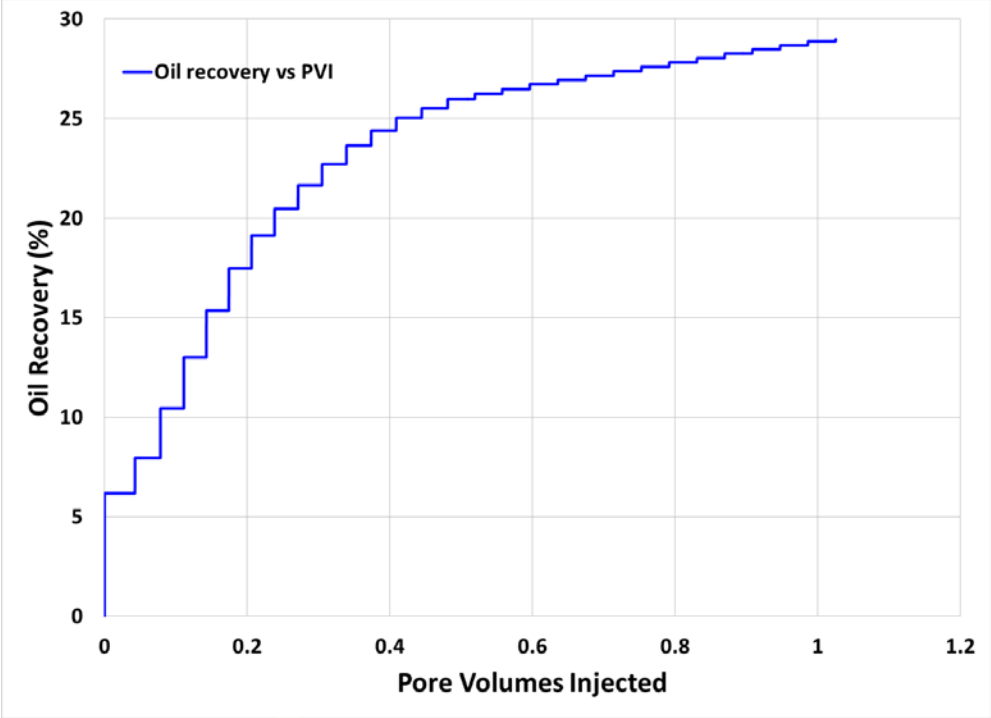

Figure 4-19. Oil recovery factor in the oil container by huff and puff gas injection vs pore volumes injected

The effect of huff and puff gas injection/production cycles on the oil rate and reservoir pressure is displayed very effectively in **Figure 4-20.** During the first cycles**,** the oil rate is restored to its initial value. Then, the oil rate gradually declines as the cycles go on, until stabilizing at about 80 bbl/day.

Thus the incremental in oil recovery by huff and puff becomes smaller as subsequent cycles go on. This may be improved by using longer cycles over time or by increasing the injection pressure and/or by increasing the injection rate once the huff and puff effectiveness starts to decrease (in this case it would be after five cycles). By implementing these improvements, the injected gas can travel further into the reservoir, thus contacting new oil during the late life of the process. These

ideas have not been tested in this thesis. It is recommended to test them in the future by running additional simulations.

Relative permeability hysteresis has not been included in this study. This phenomenon is more pronounced in the non-wetting phase (gas in this case), therefore the variation in the drainage-imbibition (injection-production) gas relative permeability curves may be significant. Relative permeability to gas would be larger during the injection than during production. On the other hand, the variation in the wetting phase (oil in this case) is in general small. Further studies must be carried out in order to determine the impact of relative permeability hysteresis on huff and puff gas injection in shale reservoirs.

In this simulation, gas injection rates during the huff periods, is always equal to 5.2 MMscf/day. During the puff periods the injection rate is, of course, equal to zero (**Figure 4-21**).

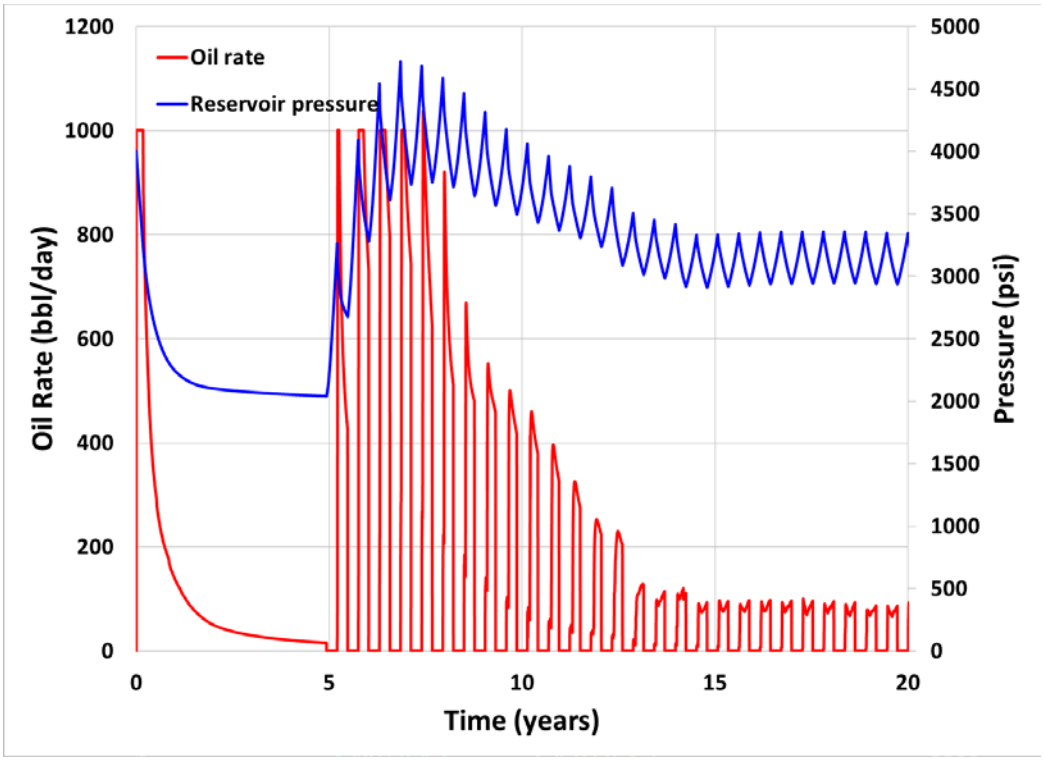

Figure 4-20. Oil production rate and average reservoir pressure in the oil container for the huff and puff gas injection case.

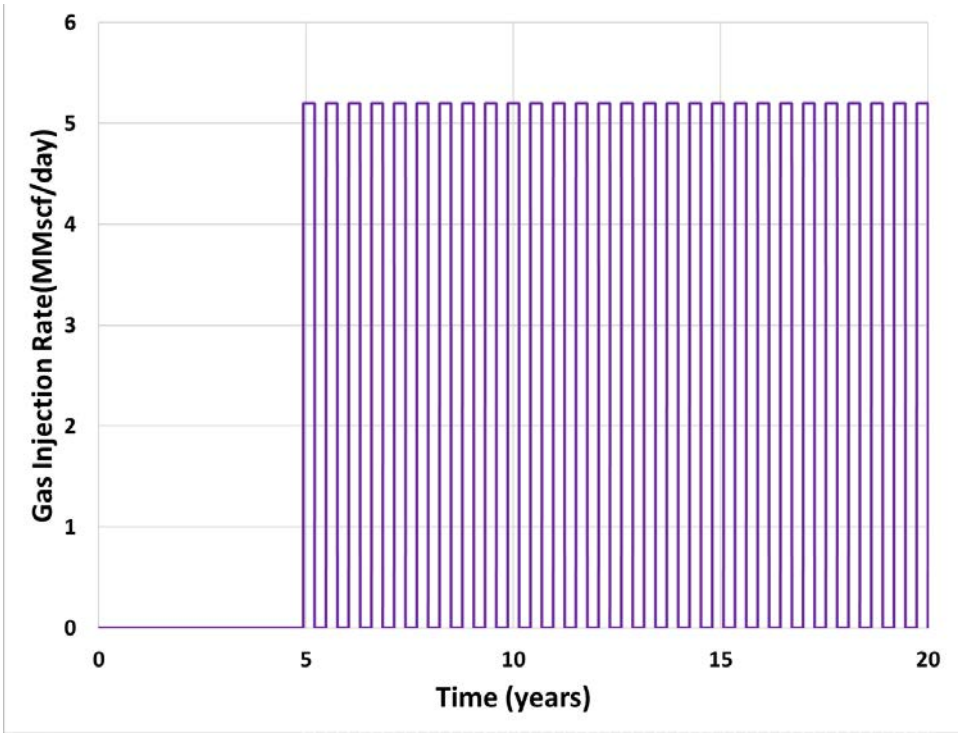

Figure 4-21. Gas injection rate in the oil container for the huff and puff gas injection case

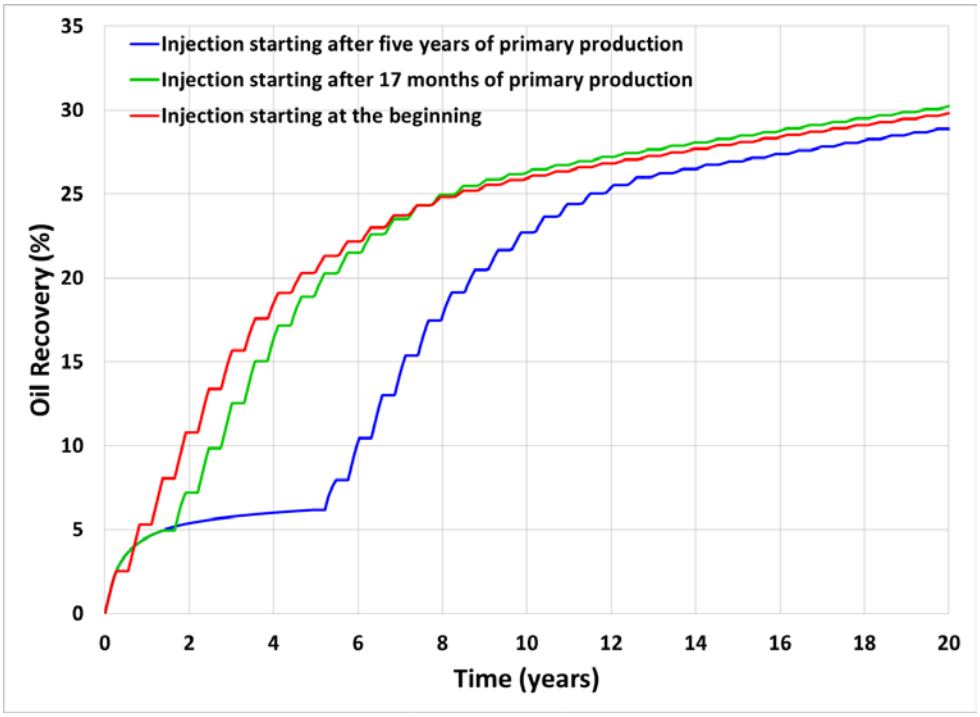

Figure 4-22. Different starting times for huff and puff gas injection in the oil container

The highest recovery (after 20 years of production) by huff and puff injection in the oil container is obtained when injection starts after 17 months of primary production. Starting huff and puff gas injection at this time also produces high early recoveries (**Figure 4-22**).

Previously, it has been demonstrated that the mass transfer by molecular diffusion is crucial when continuous gas injection is used to increase liquid recoveries in shale oil and condensate reservoirs. Conversely, the performance of a huff and puff injection is barely affected by the absence of molecular diffusion as shown in **Figure 4-23.** As only one well is used for injection and production, the gas remains in the reservoir at high pressure during the injection part of the cycle, instead of flowing from one well to another through the natural fractures. Therefore, even if there is not molecular diffusion, the gas is given enough time to penetrate the matrix.

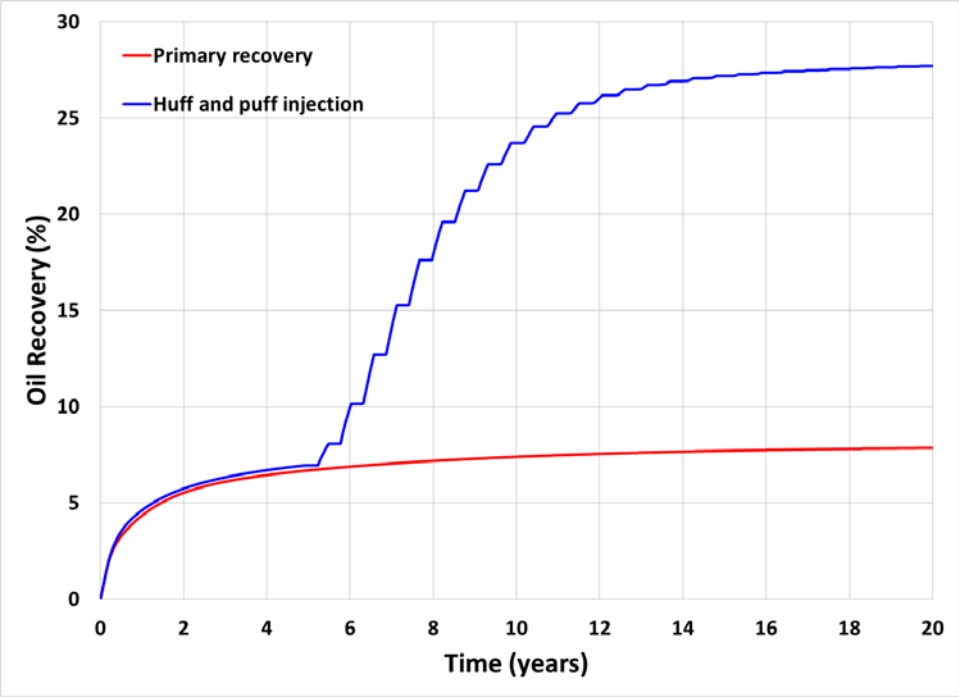

Figure 4-23. Oil recovery factor in the oil container by huff and puff gas injection when molecular diffusion is neglected

4.5.2 Condensate Container

Figure 4-24 compares oil recoveries from the condensate container by primary recovery, continuous, and huff and puff gas injection. The graph shows that the increment in oil recovery obtained by huff and puff gas injection is higher than that obtained by continuous injection. The oil recoveries by huff and puff vs the pore volumes of gas injected are shown in **Figure 4-25.** Oil rates and average reservoir pressures are presented in **Figure 4-26**.

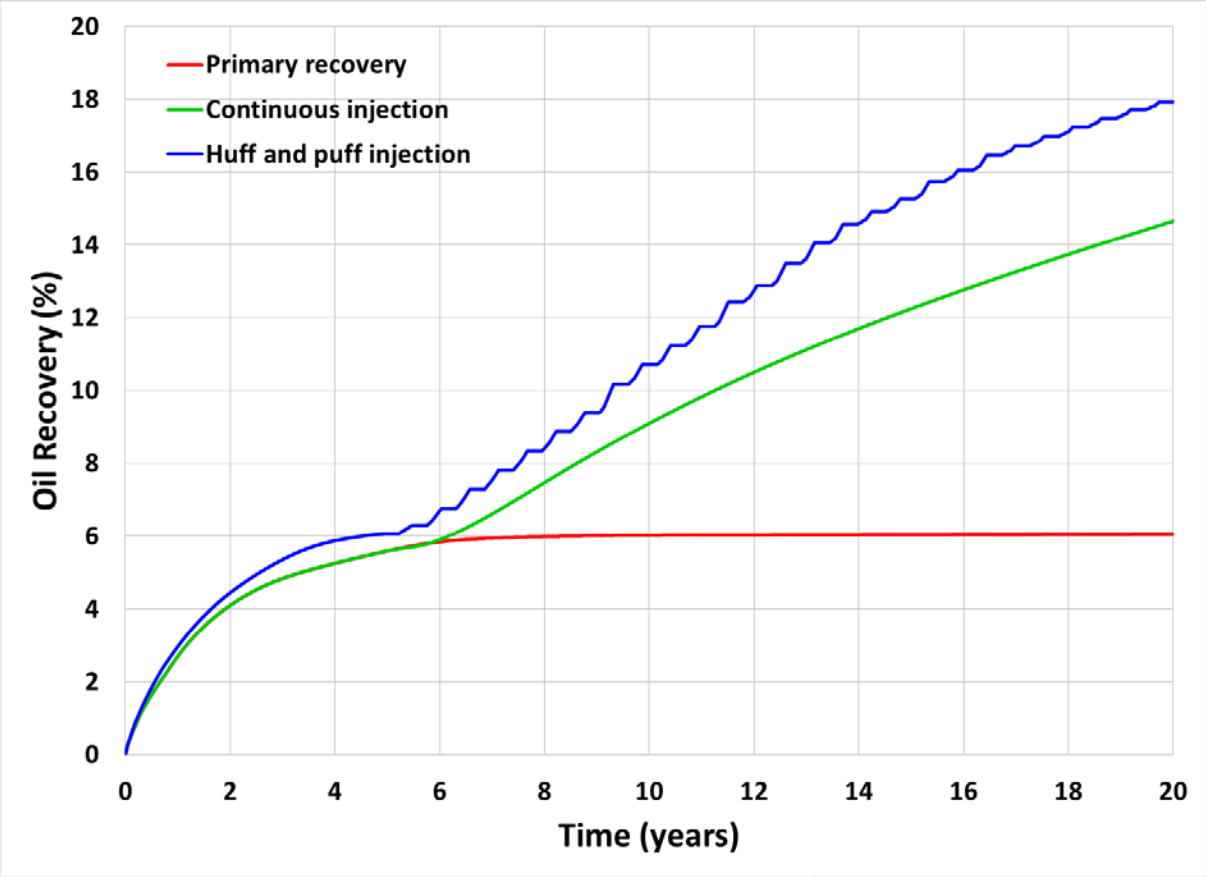

Figure 4-24. Oil recovery factor in the condensate container by huff and puff gas injection starting after five years of production

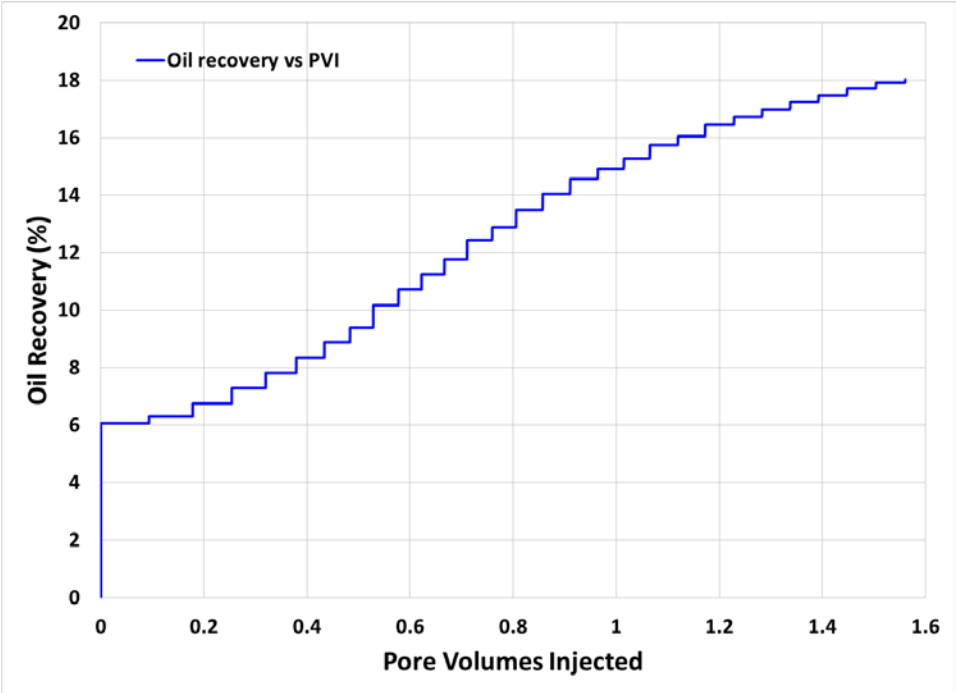

Figure 4-25. Oil recovery factor in the condensate container by huff and puff gas injection vs pore volumes injected

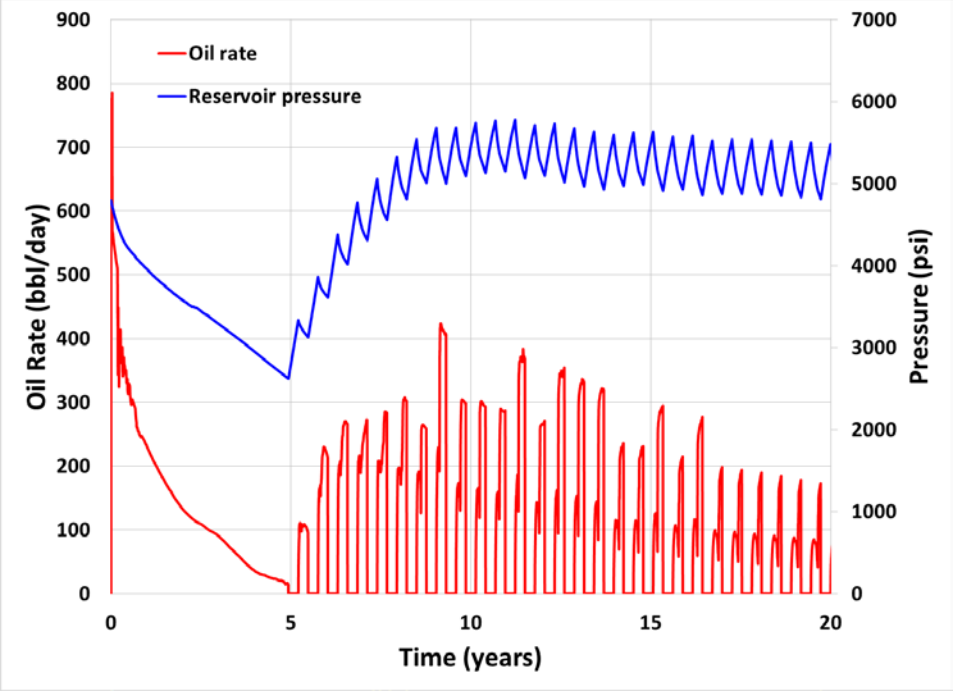

Figure 4-26. Oil production rate and average reservoir pressure in the condensate container for the huff and puff gas injection case

Gas injection rates are high in the condensate container for the huff and puff injection. During the first two cycles, it remains constant at 19.5 MMscf/day. In subsequent cycles, the initial gas injection rate is 19.5 MMscf/day, but then starts dropping (**Figure 4-27**)

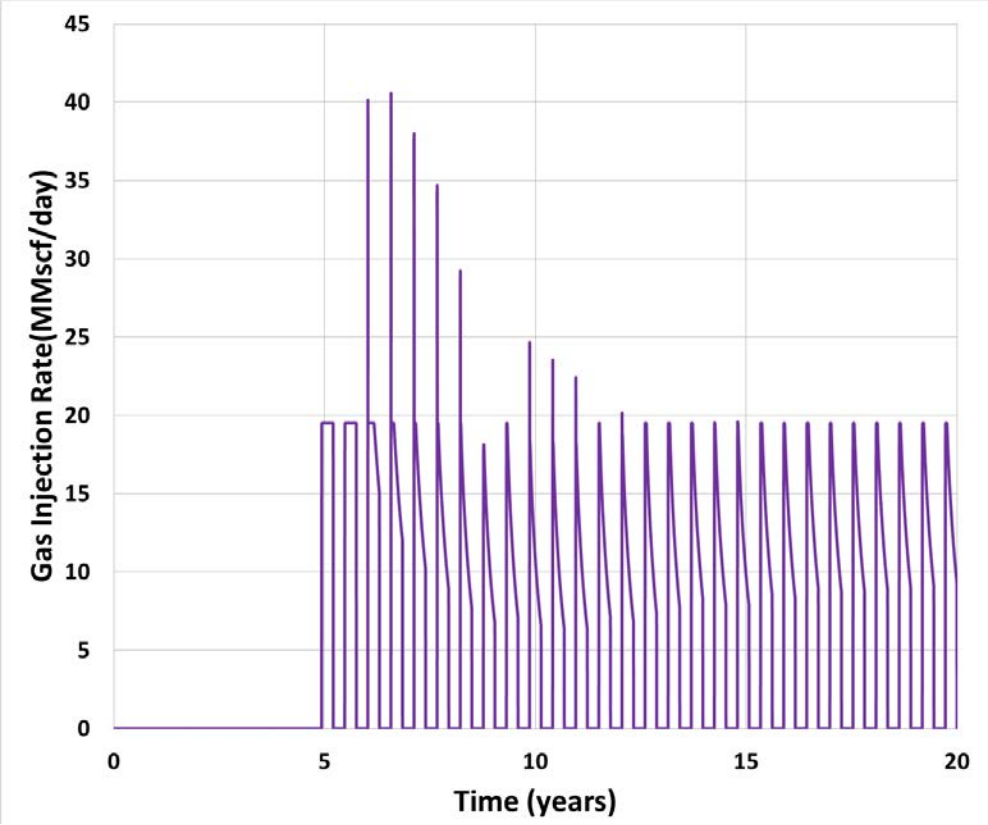

Figure 4-27. Oil production rate and average reservoir pressure in the condensate container for the huff and puff gas injection case

As in the oil container, the best time (among the times considered here) to start the huff and puff injection in the condensate container, is after 17 months of primary production (**Figure 4-28**).

In contrast to the continuous gas injection, the huff and puff gas injection performance is not affected by the absence of molecular diffusion, as shown in **Figure 4-29**. The oil recovery after 20 years of production is almost the same when molecular diffusion is considered and when it is ignored.

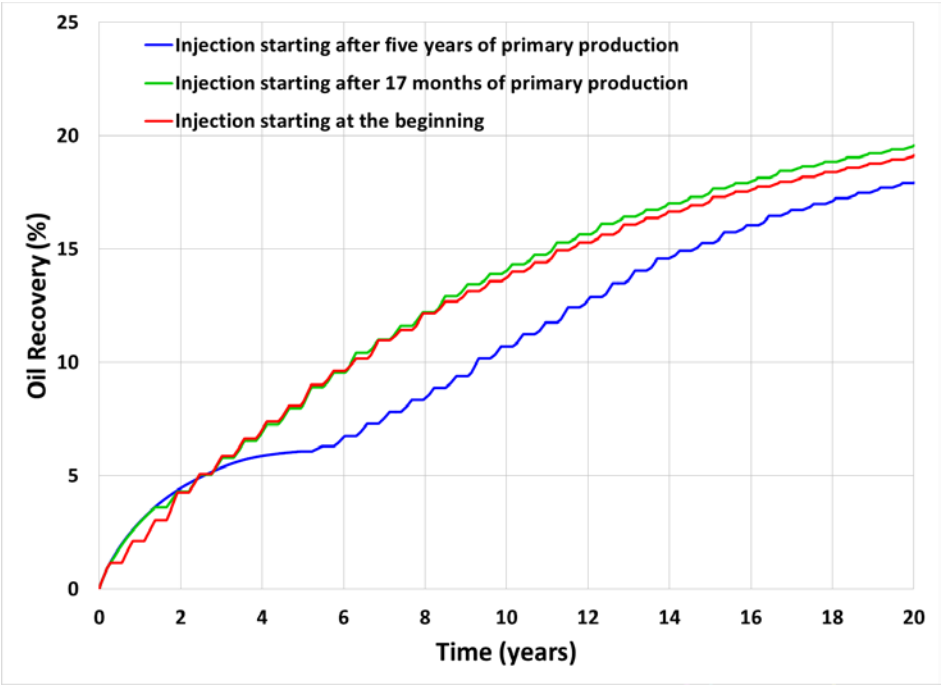

Figure 4-28. Different starting times for huff and puff gas injection in the condensate container

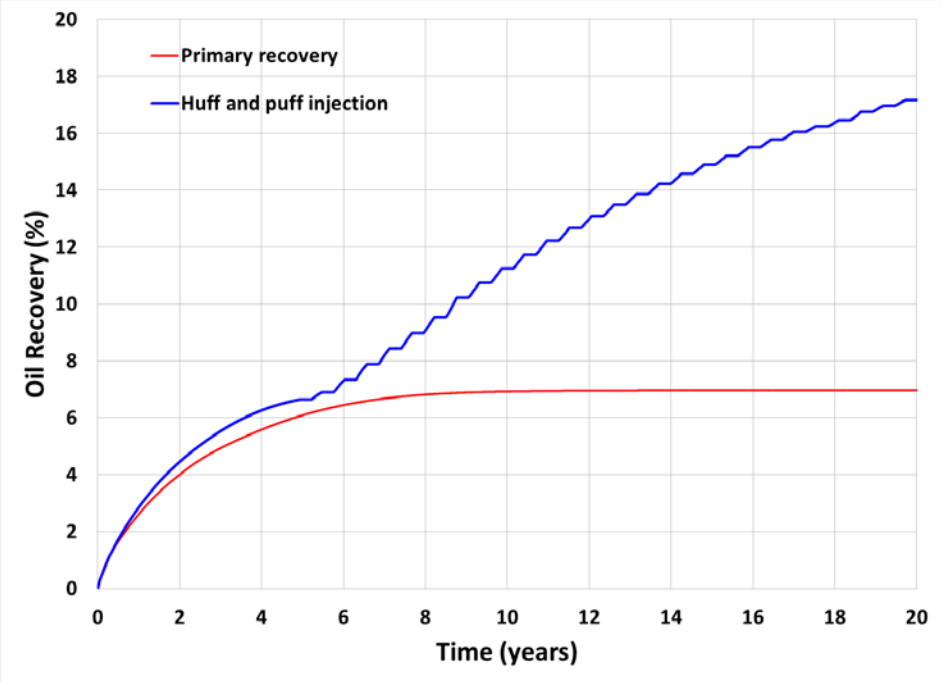

Figure 4-29. Oil recovery factor in the condensate container by huff and puff gas injection when molecular diffusion is neglected

4.6 Economic Analysis

So far, the evaluation of gas injection in shale reservoirs has been done in terms of oil production. In order to estimate the economic feasibility of gas injection, a simple economic analysis is carried out. The economic indicator used to analyze the different possibilities is the Net Present Value (NPV), which is defined as:

$$NPV = -A_0 + \sum_{i=1}^{n} \frac{C_i}{(1+r)^i} \qquad \textbf{Eq. 4-2}$$

Where A_0 is the total initial investment costs, C_i is the net cash flow during the period i, r is the discount rate and n the number of periods.

The cost of drilling and completing a well of 3250ft horizontal length is approximately USD 2.8 million. In addition, 13 hydraulic fracturing stages cost USD 1.4 million, for a total cost of USD 5.2 million. As the analysis is done separately for the oil and condensate containers, a half of the gas producer well cost is "charged" to each container.

The cost of compressors and additional gathering pipelines needed for gas injection is assumed to be USD 1 million per container. According to this, the initial investment per container is the total cost of drilling, completing and hydraulic fracturing the producer well, which is USD 5.2 million. After five years, a new inversion related to the cost of drilling the gas producer and the cost of compressors and additional gathering pipelines is done. The new inversion is equal to USD 3.6 million per container.

For the continuous gas injection, this cost assumes that the injector wells are pre-existent producer wells that have been converted. In the case where a new well must be drilled to inject gas, the new inversion after 5 years per container would be USD 8.8 million. Oil price is assumed to be 50

USD/barrel. The other input parameters needed to perform NPV calculations are taken from Wan et al. (2015). **Table 4-5** summarizes the parameters used for NPV calculations.

Table 4-5. Input parameters for NPV calculations

Economic Parameters	***Unit***	***Value***
Discount rate	fraction/yr	0.10
Working interest	fraction/yr	1.00
Royalty rate	fraction/yr	0.20
Net revenue interest	fraction/yr	0.80
Severance tax	fraction	0.05
Ad valorem tax	fraction	0.03
CAPEX (initial), $	$MM	5.2
OPEX, $	$/boe	4
Compressor and gathering pipelines	$MM	1
Oil price, $	$/barrel	50

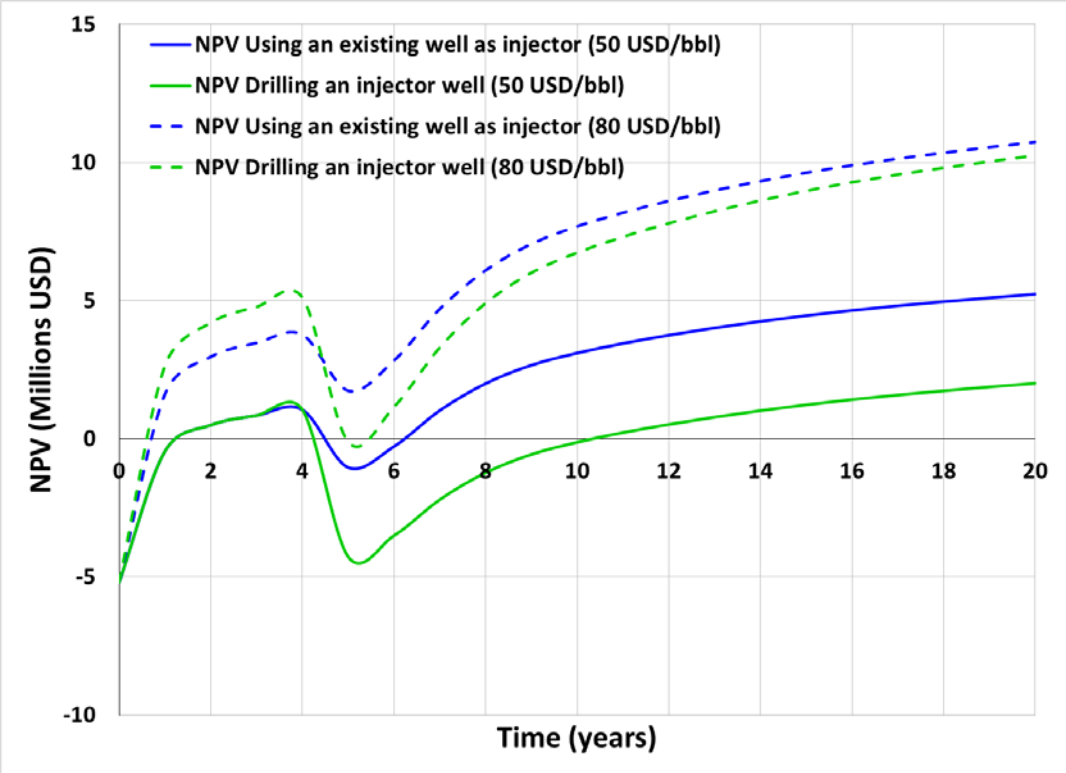

Figure 4-30. NPV calculations for continuous gas injection in the oil container

Figure 4-30, presents the NPV calculations for continuous gas injection the oil container. It shows that if a pre-existed well is used as the gas injector, the economic results of the continuous injection are satisfactory for an oil price of 50 USD/barrel. On the other hand, if drilling a new injector well is needed, in spite of the increment in oil recovery showed in **Figure 4-8**, the economic results of the continuous injection are deficient, continuing with primary production may be a better option. A higher oil price would be needed in this case, as it is shown in the plot. NPV results for continuous gas injection in the condensate container are shown in **Figure 4-31.** The conclusions are the same made for the oil container. Using a pre-existing well is the only way to make continuous gas injection profitable for an oil price of 50 USD/barrel.

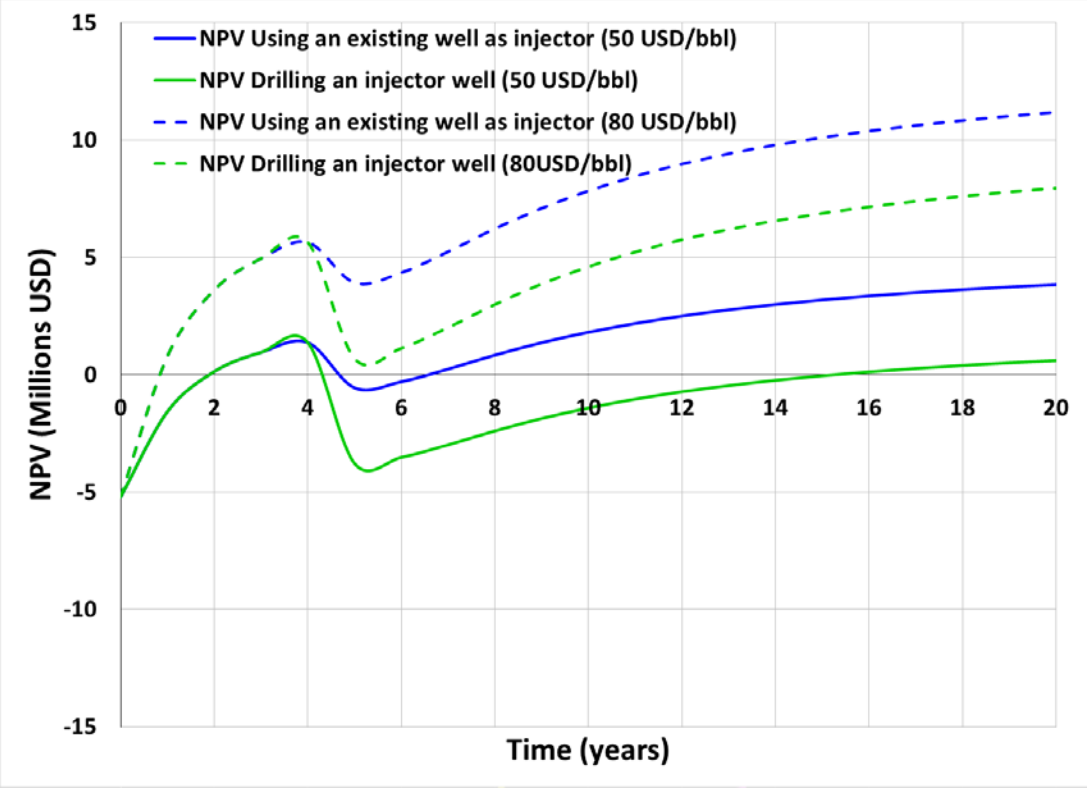

Figure 4-31. NPV calculations for continuous gas injection in the condensate container

The huff and puff injection only requires one well. This is one key advantage over the continuous injection in addition to the higher oil recoveries that can be obtained, especially in the oil container. **Figure 4-32**, shows the outstanding economic results that can be obtained by means of huff and puff gas injection in the oil container. After 20 years, the NPV is almost USD 11 million when considering an oil price of 50 USD/bbl. This is approximately the same NPV obtained by continuous gas injection at an oil price of 80 USD/bbl. Even for an oil price of 35 USD/bbl, the huff and puff injection in the oil container can be economic.

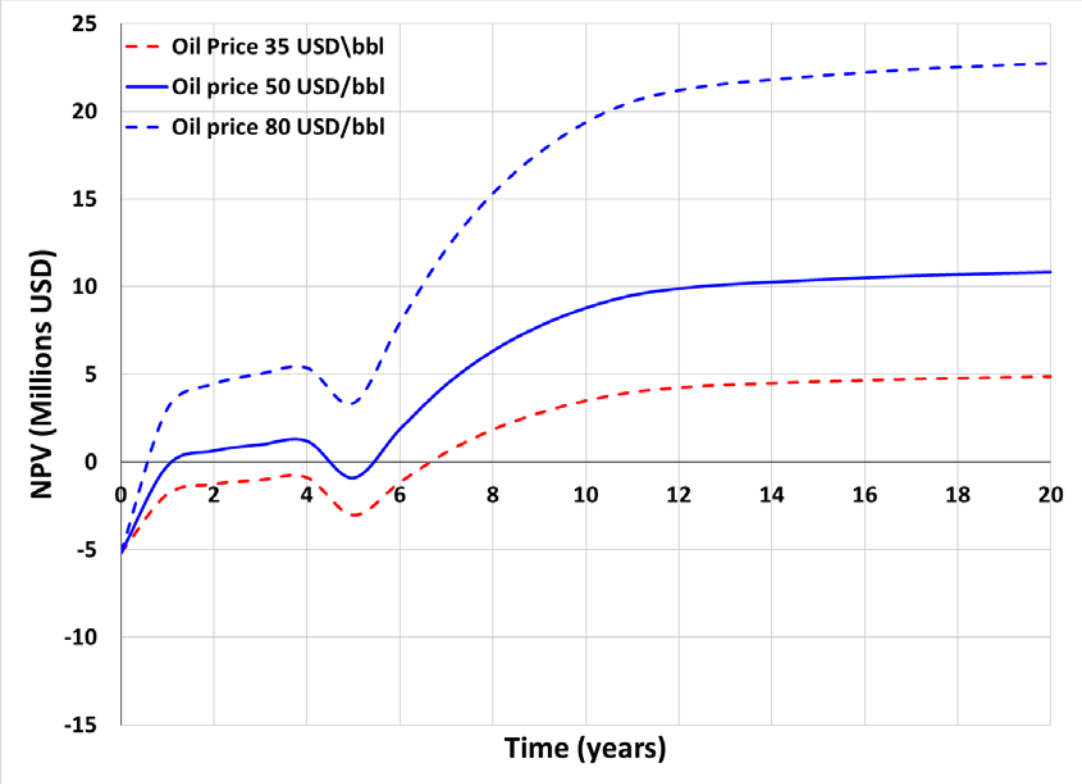

Figure 4-32. NPV calculations for huff and puff gas injection in the oil container

Results of NPV calculations for huff and puff injection in the condensate container are presented in **Figure 4-33**. The plot allows to conclude that economic results are better for huff and puff

injection as compared with continuous gas injection in the condensate container. However, the difference is not as significant as in the oil container.

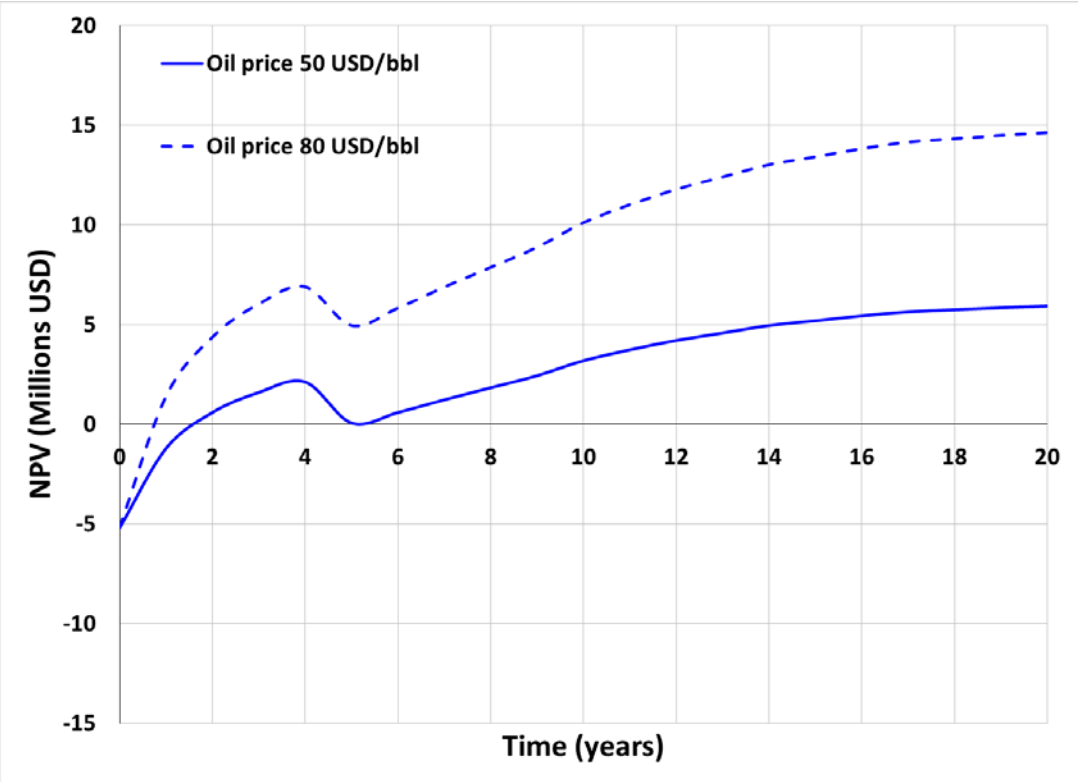

Figure 4-33. NPV calculations for huff and puff gas injection in the condensate container

Chapter Five: **Integrated Production Modelling**

A common practice in reservoir simulation is to model the different systems in the production chain separately without considering the effect of each other. Here is the problem: (1) Reservoir simulations generally do not take into account neither well-configurations nor the back pressures generated by the surface facilities, and (2) production facilities modelling does not consider the physics of fluid flow through porous media in the reservoir. A more accurate approach developed in this chapter is to integrate these models in order to have a holistic representation of the fluid flow process.

In the previous chapter, a model of a shale reservoir with three containers was built in a numerical simulator to investigate the use of gas injection to increase recoveries from shale oil and shale condensate containers. In order to include the effects of wells and surface processes, a model is developed in FORGAS (Schlumberger) and coupled with the shale reservoir model. The coupling is done at the bottom of the well. GEM and FORGAS share information at each time step to obtain results based on the following procedure:

"GEM provides the sandface inflow performance data and fluid composition at each time step for each well. GEM provides the fluid characterization for each component (e.g. critical pressure, critical temperature, etc.). FORGAS uses that information to calculate the pressure losses in the pipelines and wellbores and to determine the well flow rate. Either maximum deliverability and/or peak demand conditions will be computed. FORGAS will use the delivery target and the calculated peak demand conditions to determine the flow rates required for actual production. FORGAS will pass the actual production flow rate for each well zone to GEM so that GEM can calculate the new reservoir pressure and sandface inflow performance for the next time step" (Schlumberger, 2015).

The surface process is based on a methodology proposed by Bartolomeu et al. (2014) and is presented in **Figure 5-1.** The fluids produced from both, the oil and the condensate containers are first separated into oil and gas. After the separation, the gas goes through two processing stages. In the first stage, the CO_2 is removed from the gas stream. In the second stage, NGL are extracted from the stream and the remaining dry gas is reinjected in to the condensate container (and if needed, part of the dry gas could be reinjected into the oil container).

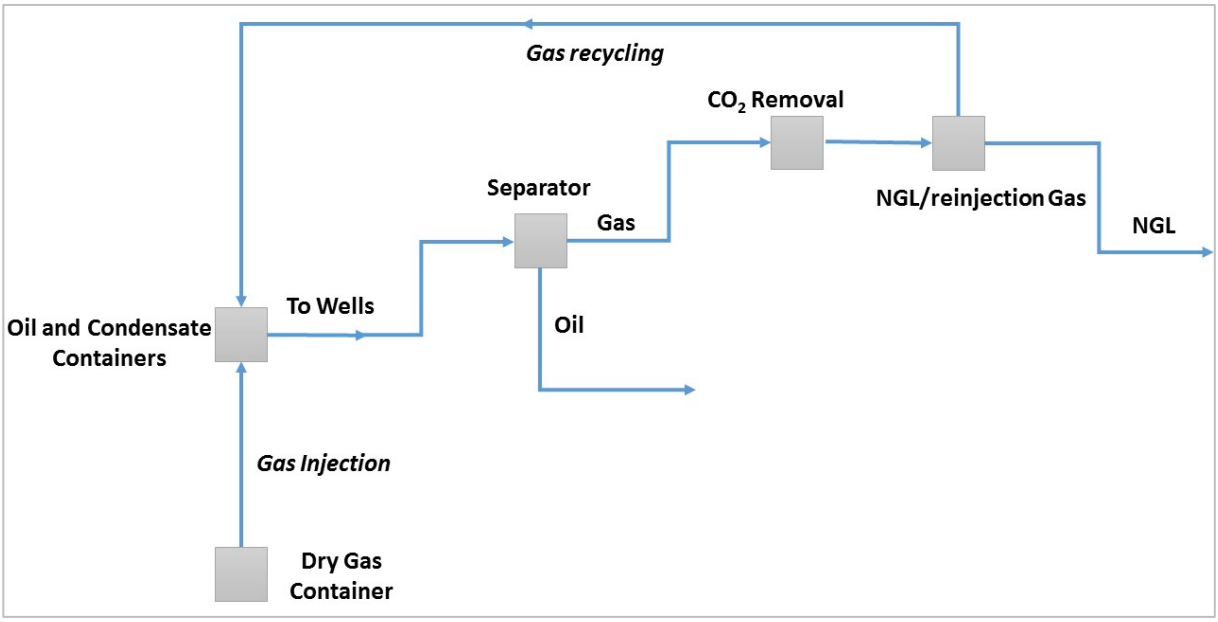

Figure 5-1. Surface process flow diagram (modified from Bartolomeu et. al, 2014)

5.1 Continuous injection

The first run made with the integrated production model, considers continuous injection and reinjection of dry gas. In this chapter, injection is started after four years of primary production.

5.1.1 Oil container

Figure 5-2 presents oil recoveries for the case of continuous gas injection in the oil container. Recovery goes from 3.3% by primary recovery to 22.5% by continuous gas injection. The incremental recovery is 19%, which is higher than the one obtained when the reservoir was

simulated in GEM (chapter four) without considering the integrated production modelling (13.7%). This can be explained by analyzing the BHPs in both models (**Figure 5-3**). In the GEM model the BHP is constant throughout the whole simulation (except for the first three months). This value is equal to the minimum BHP set as constraint in GEM. In the coupled model (GEM + FORGAS), the BHP is affected by the production system and is always higher than the minimum BHP constraint. In addition, during continuous gas injection, the BHP increases significantly which allows to reach bigger reservoir pressures.

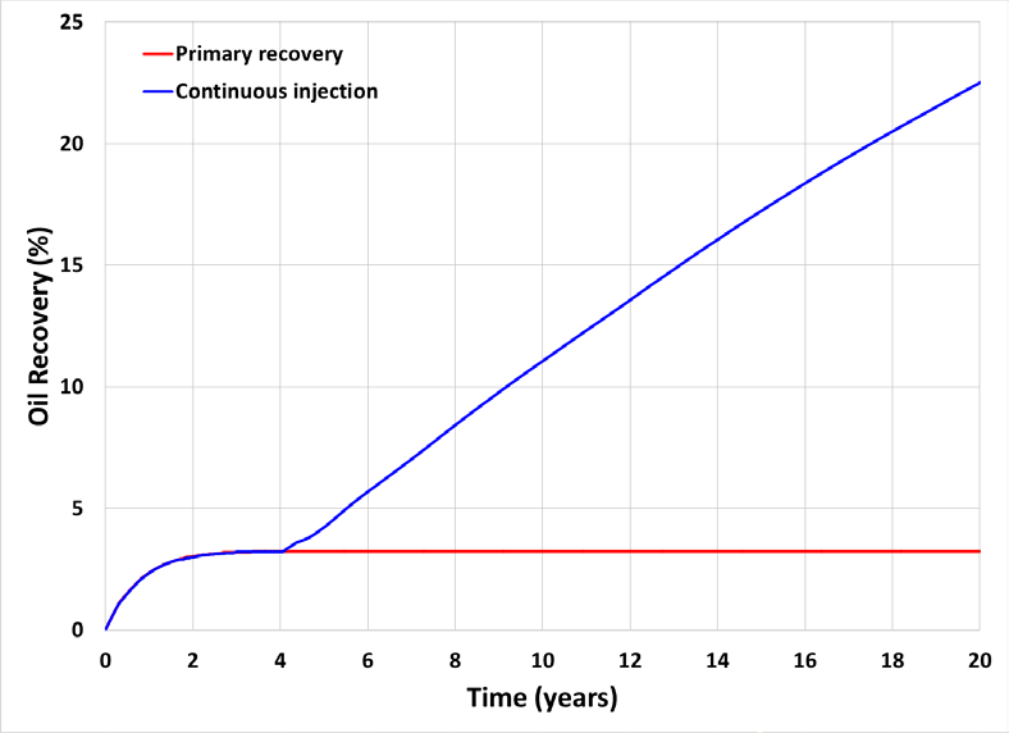

Figure 5-2. Oil recovery factor in the oil container by continuous gas injection

Chapter four explained that during the continuous injection, the injected gas flows through fractures without allowing enough time for penetrating the matrix. In the integrated model, this is mitigated by the higher BHP, which constraints to some extent the gas production. As a result, a

larger amount of gas penetrates the matrix, leading to higher recoveries compared to the GEM model where the BHP is lower and constant.

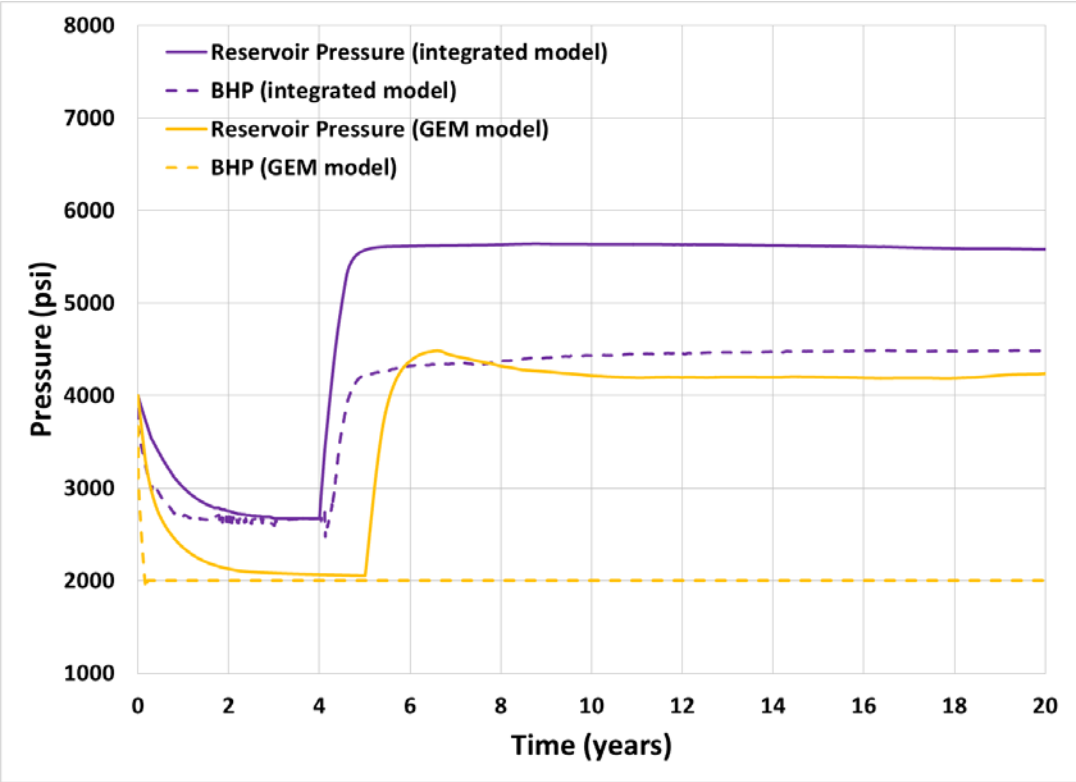

Figure 5-3. BHP and reservoir pressure in the oil container for the GEM and the integrated models

5.1.2 Condensate Container

Oil recoveries in the condensate container by continuous gas injection are shown in **Figure 5-4**. The situation is similar to that observed in the oil container. Although the incremental oil recovery after 20 years of simulated production is somewhat larger for the GEM model compared to the integrated model, it can be seen from the plots that in the GEM model alone (**Figure 4-13**), the curve is concave downwards, while in the integrated model (**Figure 5-4**), the curve is almost a straight line.

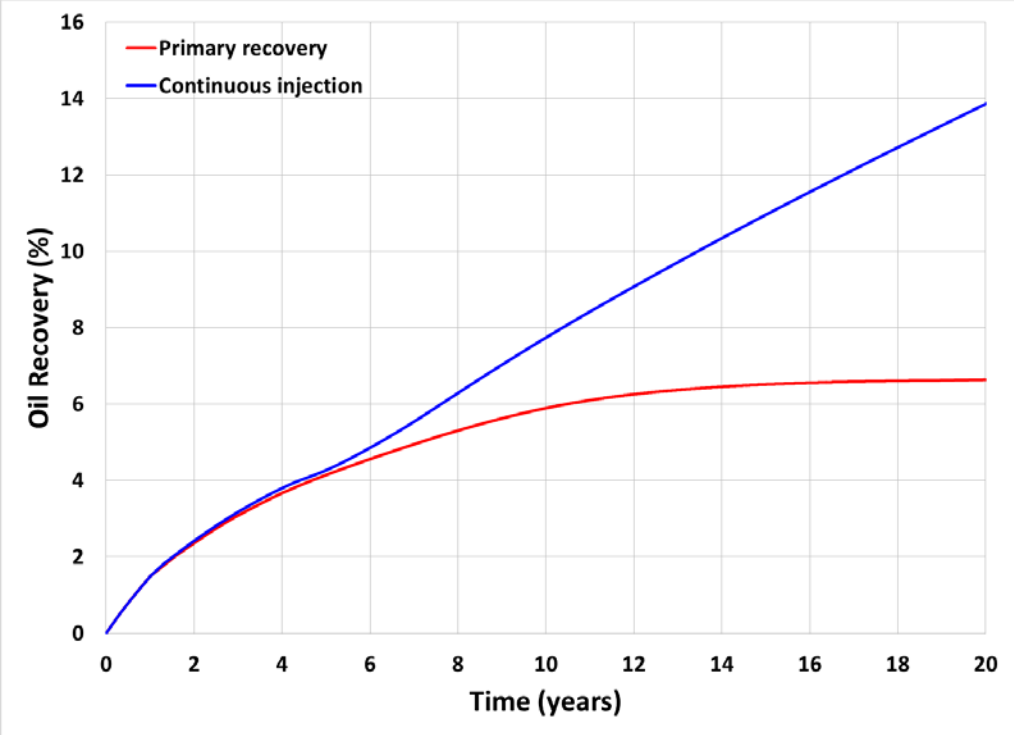

Figure 5-4. Oil recovery factor in the condensate container by continuous gas injection.

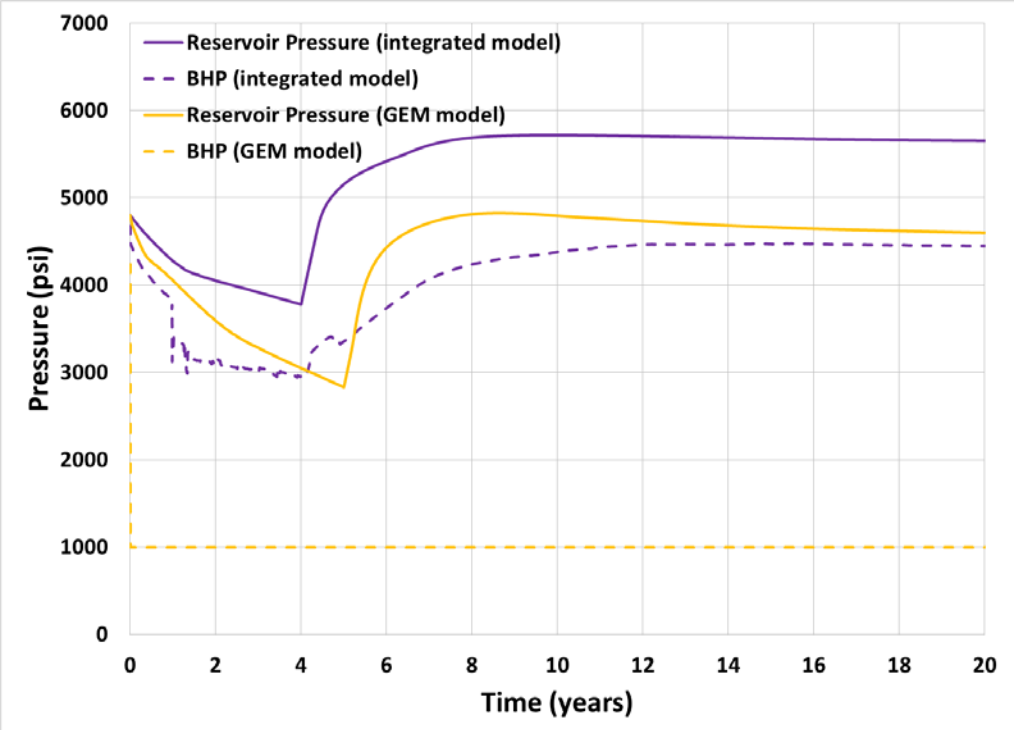

Figure 5-5. BHP and reservoir pressure in the condensate container for the GEM and the integrated models.

This means that in future years, the recovery increment would be higher in the integrated model. The BHP explanation presented above for the oil container (**Figure 5-3**) also applies for BHPs in the condensate container (see **Figure 5-5**).

5.2 Huff and Puff Injection

This section analyzes the effect of wells and surface facilities on huff and puff gas injection performance.

5.2.1 Oil container

Figure 5-6 presents oil recoveries in the oil container by huff and puff gas injection. The high BHPs caused by backpressures from the surface facilities affects negatively the gas huff and puff

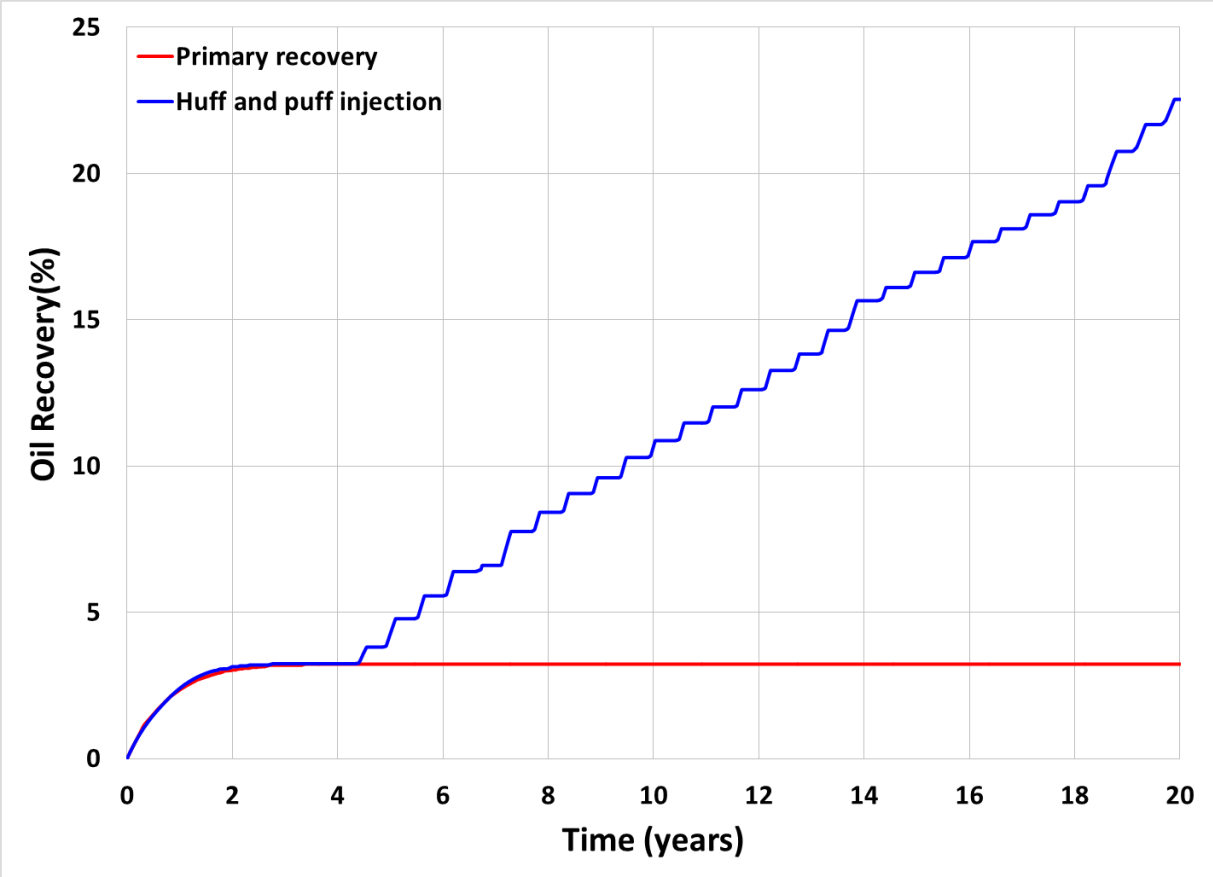

Figure 5-6. Oil recovery factor in the oil container by huff and puff gas injection.

gas injection during the first years. This is concluded by making a comparison with recoveries form the GEM model in chapter four. However, the increase in recoveries is more “stable” in the integrated model (recovery increases very slowly in the GEM model after six years of injection), which may deliver better results in the long term.

5.2.2 Condensate container

The facilities back pressures have a strong negative effect on the huff and puff gas injection performance in the condensate container (**Figure 5-7**). In chapter four, a significant improvement in oil recovery was obtained by huff and puff gas injection in the condensate container (**Figure 4-24)** using the GEM model, where the BHP declined freely during the puff periods to the minimum value defined as a constraint.

In the integrated model, the BHP also declines during the puff periods, but their values are larger than the constraint defined in GEM. As in the huff and puff the well is only producing half of the time, high production rates are mandatory in order to obtain good recovery results. Unlike in the oil container, these high rates cannot be obtained at high BHPs in the condensate container. Lower gas injection rates are also found to be associated with the backpressures.

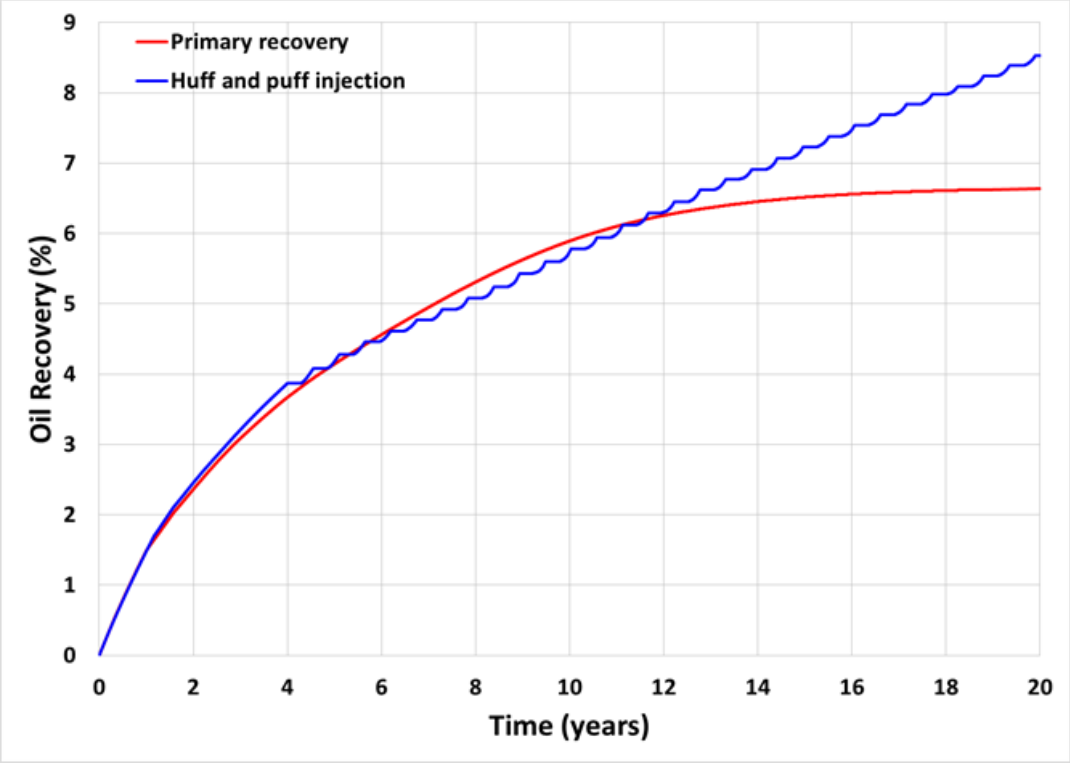

Figure 5-7. Oil recovery factor in the condensate container by huff and puff gas injection.

To avoid this problem, the surface facilities for the condensate container must be designed in such a way that the backpressure does not generate high BHPs. For example, a compressor installed close to the wellhead in the condensate container can reduce the wellhead pressure needed for the surface facilities system and therefore reduce the BHP. But will this compressor affect recovery from the oil container? This case is analyzed next.

Installation of a compressor close to the wellhead in the condensate container does barely affect oil recoveries from the oil container as shown in **Figure 5-8**. This is significant from a practical point of view.

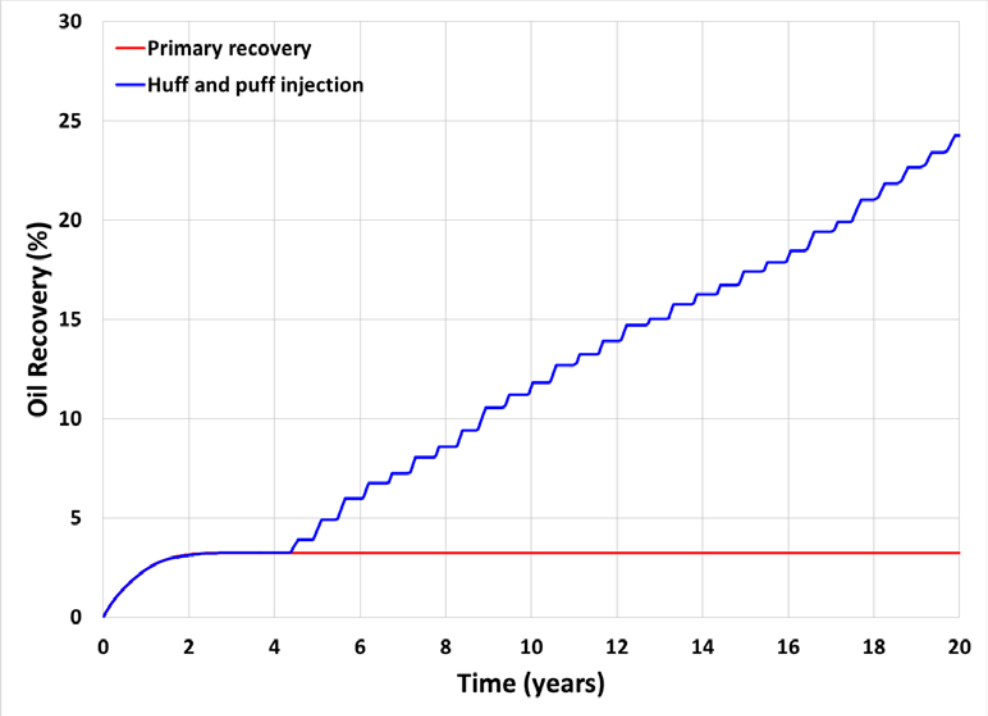

Figure 5-8. Oil recovery factor from the oil container by huff and puff gas injection for the case where a compressor is installed close to the wellhead in the condensate container

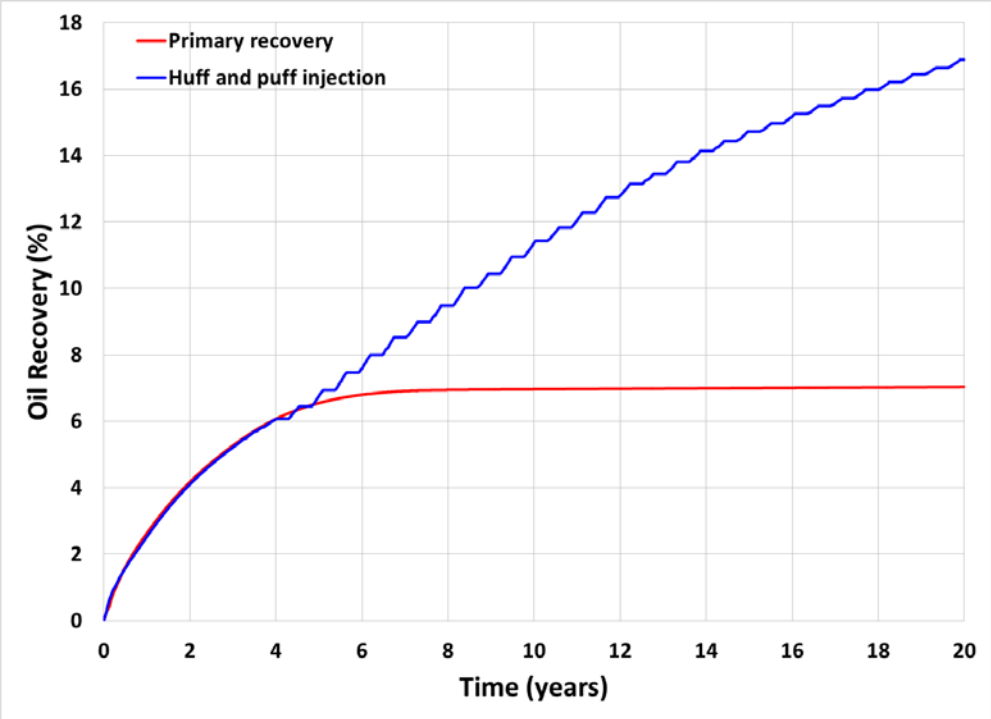

Figure 5-9. Oil recovery factor in the condensate container by huff and puff gas injection for the case where a compressor is installed close to the wellhead in the condensate container.

On the other hand**, Figure 5-9** shows that the inclusion of a compressor near the well producing from the condensate container helps to increase liquids recoveries by huff and puff gas injection. The BHPs are lower in this case, allowing thus to produce at higher rates during the puff periods. Another situation of practical importance is the case where a subsurface pump generates low BHPs in the producing well of the oil container. In this case, the subsurface pump helps to increase the recoveries obtained during the first years of the project, which in practice is desirable.

Results are presented in **Figure 5-10**. Notice that in just 12 years of production the recovery (25%+) is already larger than the recovery of about 23% obtained during 20 years without the subsurface pump (**Figure 5-6**). For comparison, note that the recovery after 12 years of production without the subsurface pump is only 12.5% as compared with 25%+ with the subsurface pump. The conclusion is reached that liquids recoveries from shales can be improved dramatically with the use of integrated production modelling that takes into account the reservoir, the wellbore and the surface installations.

A pump that generates low BHPs may also be used to solve the problem originated by the backpressures in the condensate container (in a real case, this pump must have the capacity to handle high GORs). Results are similar to those by installing a compressor close to the wellhead, as seen in **Figure 5-11.**

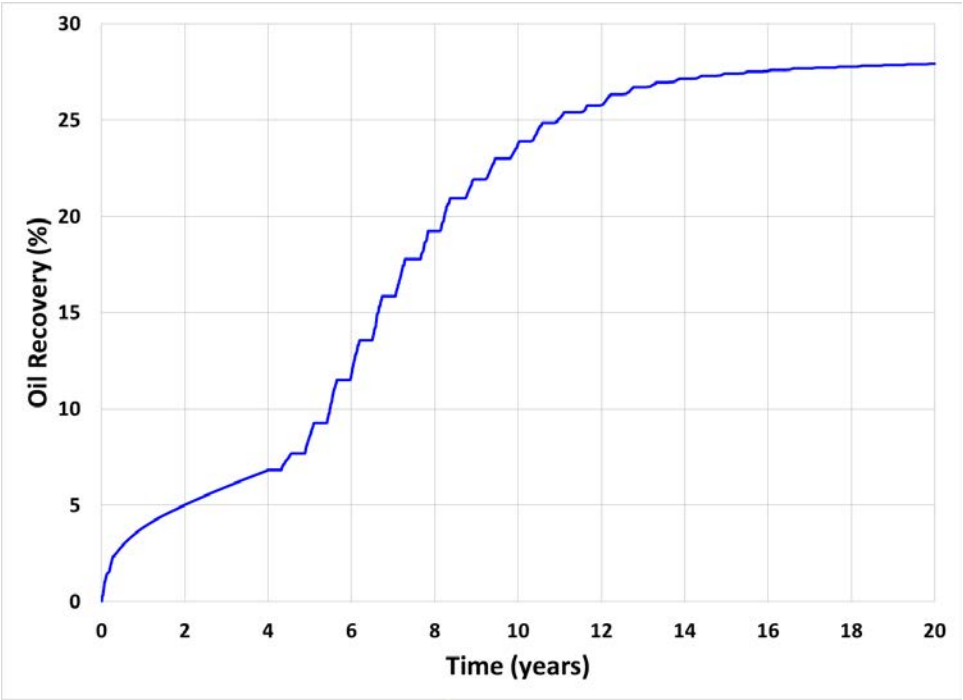

Figure 5-10. Oil recovery factor in the oil container by huff and puff gas injection for the subsurface pump that generates low BHPs case.

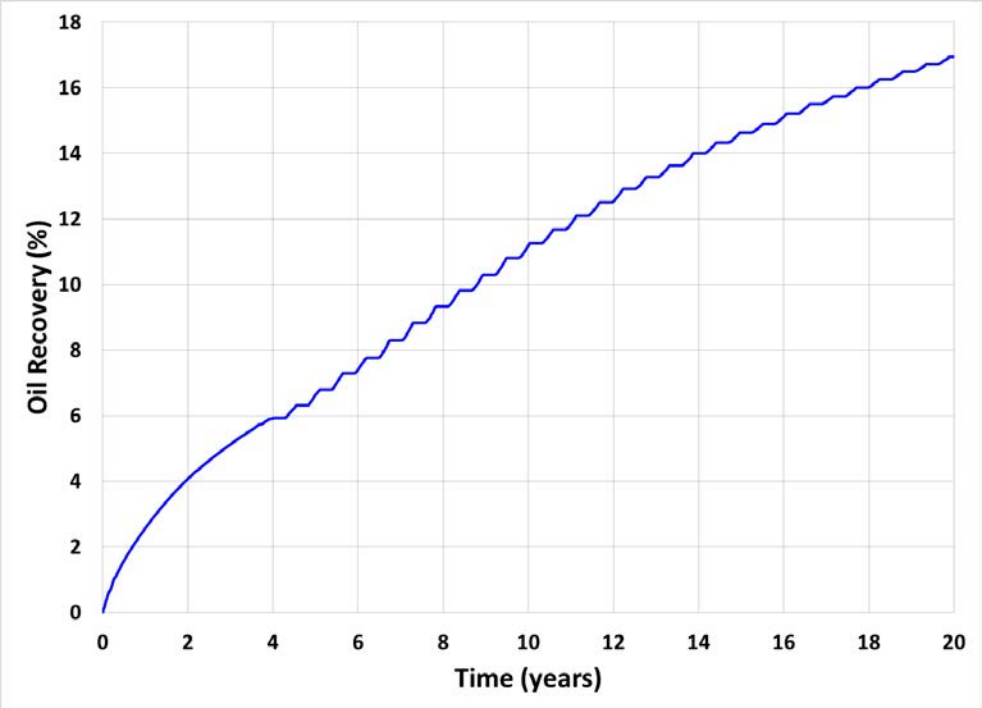

Figure 5-11. Oil recovery factor in the condensate container by huff and puff gas injection for the subsurface pump that generates low BHPs case.

Chapter Six: **Refracturing vs Infill Drilling**

As indicated previously, the percentage of the huge amounts of hydrocarbons stored in shale reservoirs that is being recovered with current production practices is very small. The wells start producing at medium to high rates and then, following the initial hydraulic fracturing job, production declines very fast. Oil companies and several researchers are contemplating different techniques to solve the small recovery problem. One of these techniques, the use of gas injection to increase liquid recoveries, has been investigated in this thesis. Another technique currently being considered by the industry is refracturing of existing wells (Urban et al., 2016). Some cases of successful refracturing jobs have been reported in the literature (Oruganti et al., 2015; Walser et al. 2016, and Hunter et al., 2015); two of those are shown in **Figure 6-1** and **Figure 6-2.**

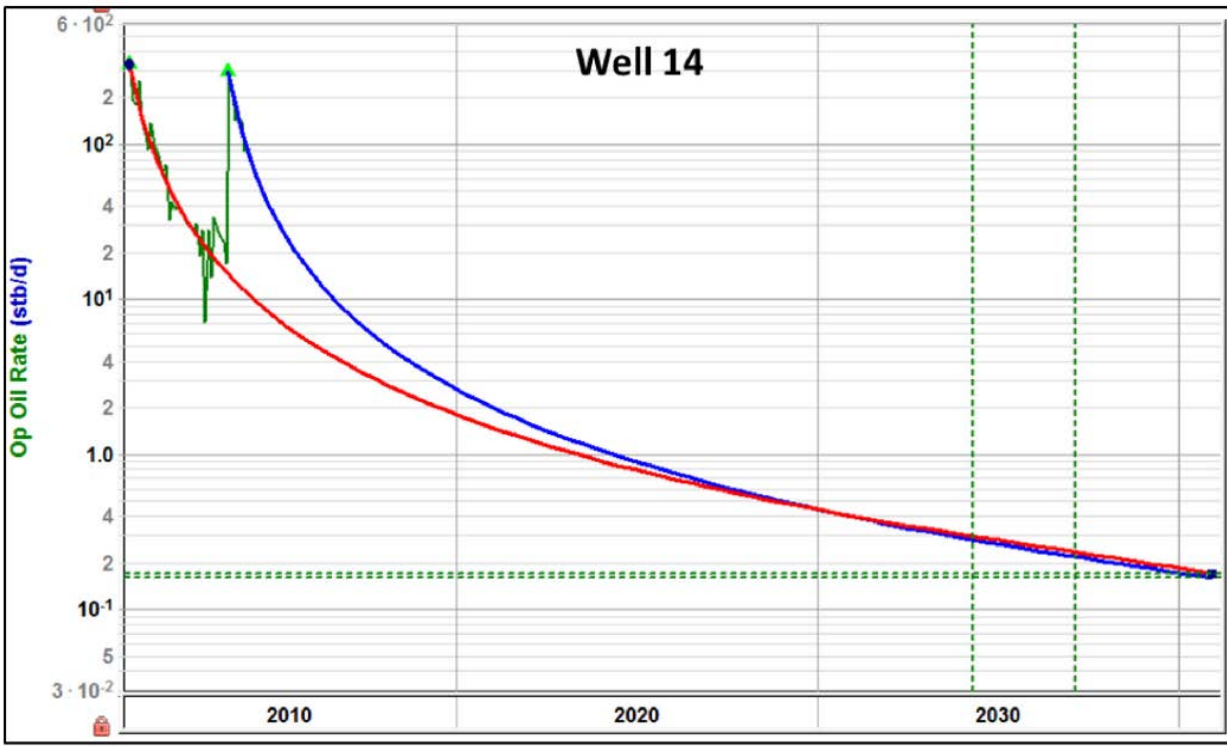

Figure 6-1. A Refractured oil well in the Eagle Ford (Oruganti et al., 2015).

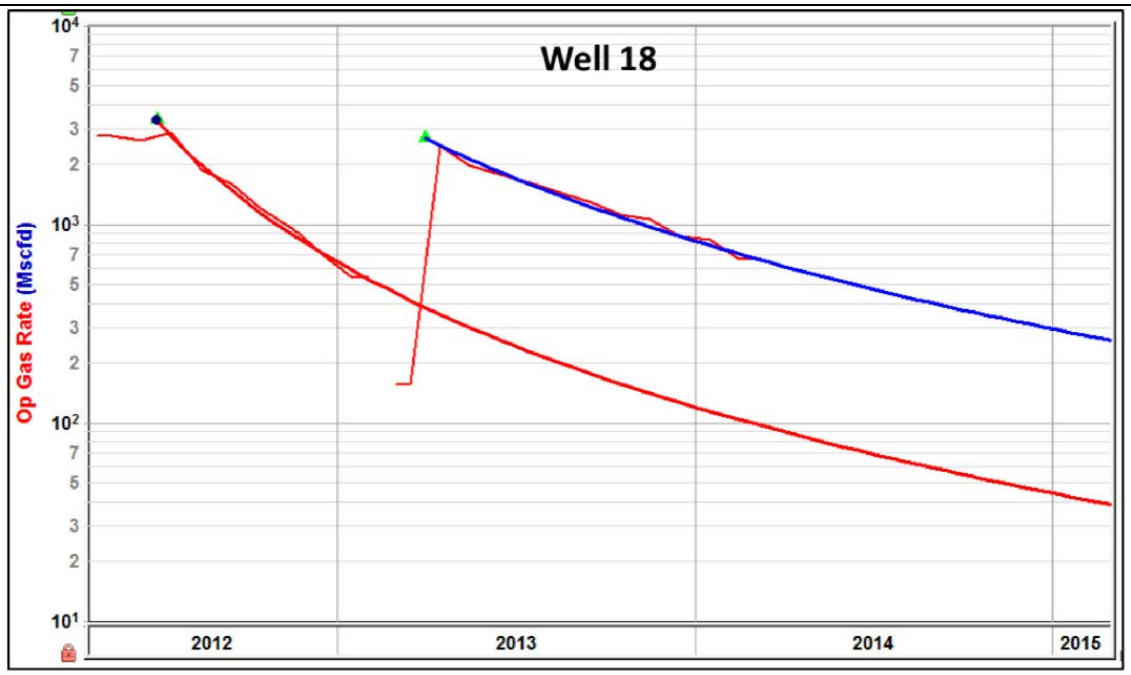

Figure 6-2. A Refractured gas condensate well in the Eagle Ford (Oruganti et al., 2015).

"Current technology in refracturing mainly entails the use of some form of diverter that is pumped into the wellbore before the refracturing operation. These diverters block the existing open perforations and enable pumping fluid into new perforations, thereby creating new hydraulic fractures" (Oruganti et al., 2015). Another option is refracturing through existing perforations.

As part of the investigation presented in this thesis, reservoir simulation is used to compare the performance of refracturing when the original fractures are reopened vs. the case where new fractures are created during the refracturing job. Finally, the benefits of refracturing are compared against the benefit of drilling infill wells.

6.1 Simulation Model

A compositional model is used in this study to simulate a shale reservoir with properties similar to those of the Eagle Ford. The model is built and run using GEM. A dual permeability approach is

used to represent the natural fracture network. Gas composition is 94.68% C1, 5,27 %C2 and 0.05 % C3. Multicomponent adsorption is included using the extended Langmuir isotherm (**Eq. 4-1).**

Two definitions used in this chapter are in order:

Refracturing refers to the reopening of old hydraulic fractures created in a horizontal well during the original hydraulic fracturing job.

Refracturing (New Fracture) refers to the creation of new hydraulic fractures in the same wellbore referred to in the previous definition.

In practice, after a hydraulic fracturing job is performed, hydraulic fractures start closing as the well goes on production and reservoir pressure is depleted. This increases the net stresses, particularly on hydraulic and natural fractures. This fact is incorporated in the present model using Piedrahita et al., (2016) correlation for tight petroleum reservoirs:

$$\frac{\phi}{\phi_i} = \left(\frac{K}{K_i}\right)^{1/3} = \frac{(logP_k)^{\alpha} - (logD)^{\alpha}}{(logE)^{\alpha} - (logD)^{\alpha}} \qquad \textbf{Eq. 6-1}$$

Where:

$$E(P_{ki}) = P_{ki} \qquad \textbf{Eq. 6-2}$$

$$D(P_{ki}) = a_1 - a_2 \cdot ln(P_{ki}) \qquad \textbf{Eq. 6-3}$$

$$a(P_{ki}) = b_1 \cdot {P_{ki}}^{b2} \qquad \textbf{Eq. 6-4}$$

Table 6-1 presents the values of sub-parameters estimated from data of the Nikanassin tight gas formation.

Table 6-1. Sub-parameter values a_1, a_2, b_1 and b_2 (Piedrahita et al., 2016)

Parameter	Factor	Sample Type		
		Horizontal	Vertical	Horizontal + Vertical
D	a_1	35911	18985	25866
	a_2	3030	1341	2031
α	b_1	1.5220	1.7245	1.6133
	b_2	0.1572	0.1552	0.1570

Table 6-2 shows the ratio of fracture porosity to initial fracture porosity and the ratio of fracture permeability to initial fracture permeability for different net stresses. Parameter for both horizontal and vertical core samples (Horizontal + Vertical in **Table 6-1**) are used in the calculations.

Table 6-2. Stress dependant properties

Pressure (psi)	Net Stress (psi)	ϕ_2/ϕ_{2i}	k_2/k_{2i}
6000	2000	1	1
5700	2300	0.944868	0.843555
5400	2600	0.892831	0.711717
5100	2900	0.843435	0.600005
4800	3200	0.796329	0.504984
4500	3500	0.751234	0.42396
4200	3800	0.707923	0.354779
3900	4100	0.666211	0.295689
3600	4400	0.625941	0.245245
3300	4700	0.586982	0.202244
3000	5000	0.549221	0.165669
2700	5300	0.512561	0.134659
2400	5600	0.476916	0.108474
2100	5900	0.442213	0.086476
1800	6200	0.408386	0.06811
1500	6500	0.375375	0.052893
1200	6800	0.34313	0.0404
900	7100	0.311603	0.030256
600	7400	0.280752	0.022129
300	7700	0.250538	0.015726

A horizontal well with multistage hydraulic fractures (13 stages) is drilled in the center of the reservoir. After 2.83 years, a refracturing job is performed. The simulation job assumes that the refracturing job is successful in all stages. Additional properties of the simulation model are shown in **Table 6-3**.

Two cases are considered. In the first case the refracturing job does not create new hydraulic fractures; it simply reopens the hydraulic fractures created in the original fracturing job, which have been closing continuously through the production life of the well. In the second case, new hydraulic fractures (they did not exist previously) are created by the refracturing job.

Figure 6-3 presents gas production rates for the two refracturing cases, considering different values of fracture capacity (product of fracture permeability times fracture aperture). A curve for the base case (without refracturing) is also included. The graph shows that gas production can be improved by refracturing in both cases, either by reopening the original fractures or by creating new fractures. When the refracturing treatment reopens the original fracture increasing the fracture capacity to its initial value (10 md-ft), the gas rate after refracturing is almost equal to the initial gas rate. Higher rates are obtained when the fracture capacity of the original fractures is increased beyond their initial value. Higher production rates are also obtained when new fractures are created (assuming that the new fractures have the same or better fracture capacity than the original fractures).

Figure 6-4 shows cumulative gas production for the same scenarios presented in **Figure 6-3**. The graph shows that, in general, better results are achieved when the refracturing job is able to create new fractures compared to those when the original fractures are reopened. The graph also shows that creating new fractures with 14 md-ft of flow capacity delivers higher cumulative production than increasing original fractures capacity to 22md-ft.

Table 6-3. Reservoir and wellbore parameters for the simulation model

Parameter	Symbol	Value	Units
Initial reservoir pressure	P_i	6,000	psi
Reservoir temperature	T	158	°F
Initial water saturation in matrix	S_{wm}	0.25	Fraction
Initial water saturation in fractures	S_{wf}	0.10	Fraction
Water compressibility	C_w	3.00E-06	1/psia
Matrix compressibility	C_m	1.00E-6	1/psia
Natural fracture compressibility	C_f	1.00E-5	1/psia
Formation Top	D_R	8,000	ft
Initial total stress on fractures	σ_t	8,000	psia
Langmuir volume CH4	V_L	34	SCF/TON
Langmuir volume C2H6	V_L	51	SCF/TON
Langmuir volume C3H8	V_L	95	SCF/TON
Langmuir pressure CH4	P_L	1562	Psi
Langmuir pressure C2H6	P_L	811	Psi
Langmuir pressure C3H8	P_L	844	psi
Matrix porosity	ϕ_m	0.060	Fraction
Natural fractures Porosity	ϕ_2	0.00055	Fraction
Matrix Permeability	k_m	0.0001	md
Natural Fracture Permeability	k_2	0.02	md
Natural Fracture Spacing		10	ft
Total Organic Carbon	TOC	2	% weight
Reservoir thickness	h	200	ft
Well drainage area	A	507.3	Acres
Hydraulic fracture half-length	x_{hf}	400	ft
Hydraulic Fracture Spacing		500	ft
Refracturing Spacing (New Fractures Cases)		250	ft
Length of the horizontal well	L	6,500	ft
Skin factor	S	0	-
Initial flow capacity of hydraulic fractures	$k_{hf}*w_{hf}$	10	md-ft
Bottomhole flowing pressure	P_{wf}	1,000	psi

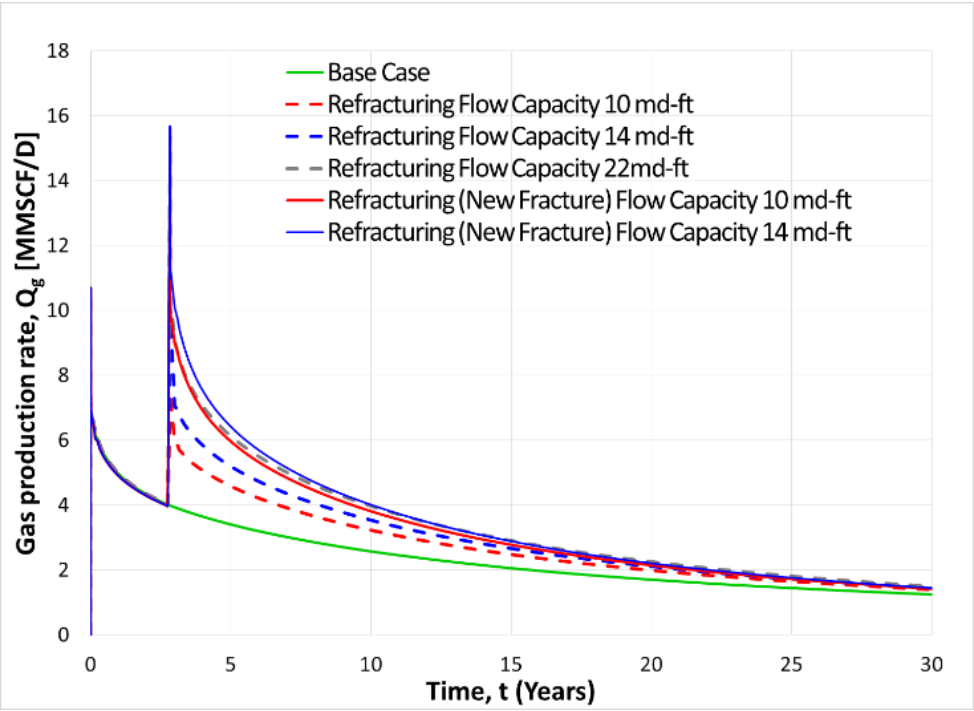

Figure 6-3. Gas production rates obtained from the simulation model. Refracturing refers to the cases where the original fractures are reopened. Refracturing (New Fractures) refers to the cases when new fractures are created.

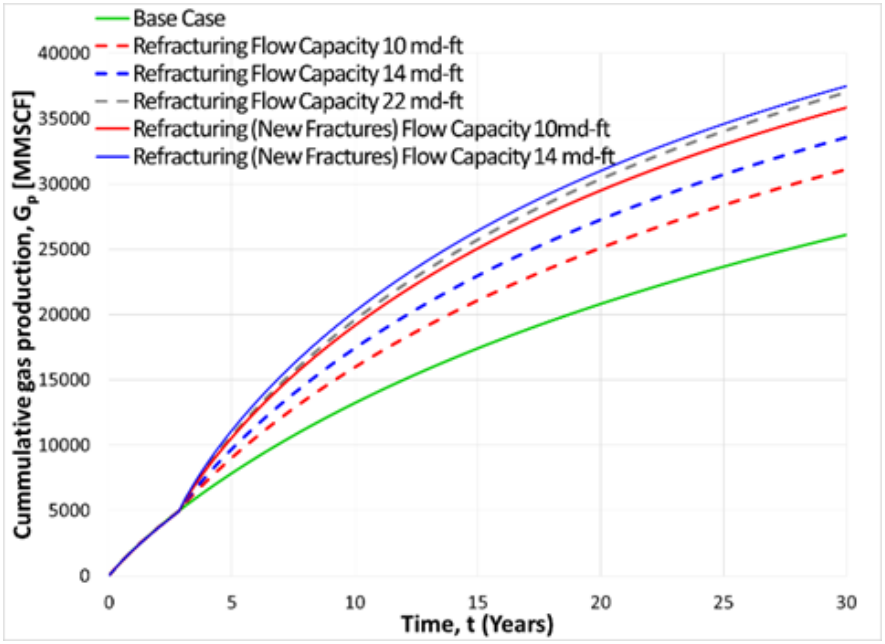

Figure 6-4. Cumulative gas production obtained from the simulation model. Refracturing refers to the cases when the original fractures are reopened. Refracturing (New Fractures) refers to the cases when new fractures are created.

6.2 Infill Drilling

A reservoir simulation case is run where instead of performing a refracturing job, an identical additional horizontal well with multistage hydraulic fractures is drilled after 2.83 years of production in order to compare the performance of refracturing vs infill drilling. Results are presented in **Figure 6-5**. The plot shows that a refracturing job that increases fracture capacity to 22 md-ft can deliver the same cumulative gas production as an infill well after 30 years. The same cumulative is achieved after 30 years of production when the refracturing job creates new fractures with capacity equal to only 13 md-ft.

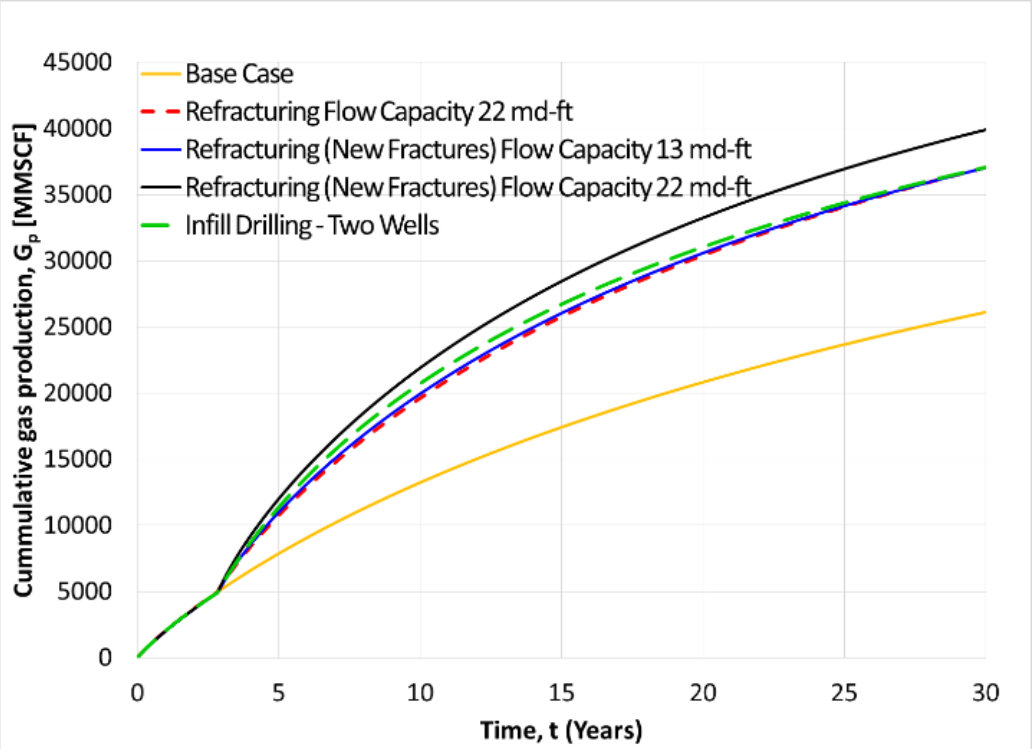

Figure 6-5. Comparison of refracturing vs. infill drilling in terms of ultimate recovery after 30 years based on simulation results.

6.3 Cost Effective Approach to Enhancing Recovery

It is found that, in general, refracturing is more cost effective than infill drilling. Rather than going into a detailed economic analysis, a comparison is made on the basis of the following practical information: Length of horizontal well: 6,500 ft (used in this chapter); hydraulic fracturing stages: 13 (used in this chapter); drilling cost: US$ 1.4 million; standard completion cost: $ 1.4 million; 13 HF stages cost: US$ 1.4 million; total cost: US$ 5.2 million. Thus, drilling an infill well, completing it and refracturing it would require a capital investment of US$ 5. 2 million. On the other hand, refracturing the well considered in this chapter after 2.83 years of production would require only an investment of approximately US$ 1.4+ million dollars.

This is significant as from the point of view of cumulative recovery, refracturing is also better. In fact, by considering the same reservoir properties and exactly the same hydrocarbons in place, the refracturing cumulative production is larger at any point on time during the 30 years simulated in this study as shown in **Figure 6-5**.

Chapter Seven: **Conclusions and Recommendations**

The use of dry gas injection to increase liquids recoveries from shale oil and shale condensate naturally fractured reservoir containers and the effect of refracturing horizontal wells have been investigated using primarily dual permeability reservoir simulation models. Results have led to the following conclusions and recommendations:

7.1 Conclusions

1. Liquid recovery from shale gas condensate and shale oil reservoir containers can be improved by means of dry gas injection. The availability of dry gas in the deepest container of the Eagle Ford shale (US) and the possibility of gas recycling operations in the condensate container make this reservoir a good candidate to implement the methodology developed in this thesis. The Duvernay shale in Canada is also a good candidate.
2. Huff and puff immiscible gas injection produces, in general, better liquids recoveries results that continuous gas injection. In huff and puff gas injection, the same well is used as injector and producer and as a result, the volume of gas needed is in most cases smaller due to the shut in periods.
3. Huff and puff gas injection delivers better economic results than continuous gas injection based on simulation results. If drilling an injection well is required, current (2016) oil prices (around US$ 50/bbl) make the continuous gas injection project unfeasible. In order to make it economic, a pre-existent production well must be converted to injector.
4. Integrating reservoir, wells and surface facilities models is very important when evaluating gas injection projects in shale reservoirs. Integrated production models provide a better understanding of the whole process and allow to find potential problems that otherwise may be overlooked.

5. Huff and puff gas injection in the condensate container is strongly affected by backpressures from surface installations. Facilities must be properly designed with a view to permit low BHP's during the puff periods. For example, adding a compressor near the well producing from the condensate container can increase liquid recovery from 8.5 to 17%
6. The downhole design is also very important in the oil container during huff and puff gas injection. For example, in just 12 years of huff and puff operations, the oil recovery of 25%+ with a subsurface pump is already larger than the recovery of about 24% obtained during 20 years of huff and puff without the subsurface pump.
7. Molecular diffusion plays a fundamental role in the performance of a continuous gas injection project in a naturally fractured shale oil reservoir container. It may determine if the gas injection is successful or fails. Therefore, understanding of diffusion through experimental work and modelling is very important in shale oil reservoirs.
8. In contrast to the continuous gas injection, huff and puff injection in oil and condensate shale reservoir containers is barely affected by the absence of molecular diffusion.
9. Injected fluids that achieve some degree of miscibility with reservoir oil produce better results than lean gas. Availability and price may be limiting factors in the use of these fluids.
10. In shale containers without natural fractures, evaluated in this thesis with a single porosity model, the performance of a gas injection project is strongly affected by matrix permeability. For each single porosity shale project, the permeability values that permit gas injection must be carefully pre-determined.

11. Numerical simulation shows that refracturing can increase gas production when new fractures are created and when the original fractures are reopened. Creating new fractures delivers, in general, better production results.

7.2 Recommendations

1. Build simulation cases that combine refracturing and gas injection.
2. Include stress dependant properties in the simulation model for gas injection.
3. Perform a sensitivity analysis to the relative permeabilities curves used in the simulation model.
4. Run additional cases where longer cycles are used in the huff and puff injection once its efficiency to improve the oil recovery decreases.
5. Carry out laboratory experiments of immiscible CH4 injection in cores saturated with oil to corroborate the conclusions presented in this simulation study.
6. Develop pilot gas injection programs in the field to corroborate the gas injection and refracturing findings presented in this study.

References

Addison, V. 2016. EOG Shifts Drilling Strategy, Pushes EOR. http://www.epmag.com/eog-shifts-drilling-strategy-pushes-eor-847741 (accessed 16 May 2016).

Agboada, D. K.and Ahmadi, M. 2013. Production Decline and Numerical Simulation Model Analysis of the Eagle Ford Shale Play. Presented at the SPE Western Regional & AAPG Pacific Section Meeting, Monterey, California, USA, 19-25 April. SPE 165315.

Ahmed, T. 2001. *Reservoir Engineering Handbook*, second edition. Houston, Texas: Gulf Professional Publishing.

Akinluyi, O. and Hazlett, R. 2016. EOR Potential for Lean Gas Reinjection in Zipper Fracs in Liquid-Rich Basins. DOIhttp://dx.doi.org/10.2118/179577. SPE-179577. SPE Improved Oil Recovery Conference, 11-13 April, Tulsa, Oklahoma, USA.

Arri, L. E., Yee, D., Morgan, W. D., & Jeansonne, M. W. 1992. Modeling Coalbed Methane Production with Binary Gas Sorption. Presented at the SPE Rocky Mountain Regional Meeting, Casper, Wyoming, USA, 18-21 May. SPE 24363.

Bartolomeu, M. J. and Abdrakhmanov, A. B. 2014. Integrated Production Modelling of Gas Condensate Field. Presented at the SPE Asia Pacific Oil & Gas Conference and Exhibition, Adelaide, Australia, 14-16 October. SPE 171453.

Buckley, S. E. and Leverett, M. C. 1942. Mechanism of Fluid Displacement in Sands. Transactions of the AIME. Volume 146, No 01, 107 – 116, December 1942. http://dx.doi.org/10.2118/942107-G.

Cao, Y., Yan, B., Alfi, M. and Killough, J. 2015. A Novel Compositional Model of Simulating Fluid Flow in Shale Reservoirs – Some Preliminary Test and Results. Presented at the SPE Reservoir Characterization and Simulation Conference and Exhibition, Abu Dhabi, UAE, 14-16 September. SPE 175589.

Daigle, H., Ezidiegwu, S. and Turner, R. 2015. Determining Relative Permeability in Shales by Including the Effects of Pore Structure on Unsaturated Diffusion and Advection. Presented at the SPE Annual Technical Conference and Exhibition, Houston, Texas, USA, 28-30 September. SPE 175019.

Fan, L., Martin, R.B., and Thompson, J.W. 2011. An Integrated Approach for Understanding Oil and Gas Reserves Potential in Eagle Ford Shale Formation. Presented at the Canadian Unconventional Resources Conference, Calgary, Alberta, Canada, 15-17 November. SPE 148751.

Fragoso, A., Wang, Y., Jing, G. and Aguilera, R. 2015. Improving Recovery of Liquids from Shales through Gas Recycling and Dry Gas Injection. SPE presented at the 177278 SPE Latin

American and Caribbean Petroleum Engineering Conference held in Quito, Ecuador, 18–20 November 2015.

Gilleland, K. 2011. Hydraulic Fracturing. Game-Changing Advances in Stimulation and Production Technology are Improving Well Economics. Schlumberger, 24 January 2011, https://www.slb.com/~/media/Files/stimulation/industry_articles/201101_ep_improving_well_economics.pdf (accessed 25 August 2016).

Green, D. and Willhite, P. 1998. *Enhanced Oil Recovery*. Richardson, Texas: SPE Textbook Series.

Hartmann, D. J. and Beaumont, E. A. 1999. Predicting Reservoir System Quality and Performance, in Exploring for Oil and Gas Traps, AAPG Treatise of Petroleum Geology, Handbook of Petroleum Geology, edited by Edward A. Beaumont and Norman H. Foster (1999) p. 9-1 to 9-154.

Hoffman B. T. and Evans, J. G. 2016. Improved Oil Recovery IOR Pilot Projects in the Bakken Formation. DOIhttp://dx.doi.org/10.2118/180270-MS. SPE-180270-MS. SPE Low Perm Symposium, 5-6 May, Denver, Colorado, USA.

Honarpour, M., Nagarajan, N., Orangi, A., Arasteh, F., Yao, Z. 2012. Characterization of Critical Fluid, Rock and Rock Fluid Properties-Impact on Reservoir Performance of Liquid-rich Shales. Presented at the SPE Annual Technical Conference and Exhibition, San Antonio, Texas, USA, 8-10 October. SPE 158042.

Hunter, W., Turner, M., Villalobos, J., Peña, A., & Baihly, J. 2015. Systematic Candidate Selection Improves Haynesville Refracturing Economics. World Oil Magazine, December 2015.

Jacobs, T. 2016. EOR-For-Shale Ideas to Boost Output Gain Traction, Journal of Petroleum Technology, June 2016.

Kovscek, A., Tang, G. and Vega, B. 2008. Experimental Investigation of Oil Recovery from Siliceous Shale by CO_2. Presented at the 2008 SPE Annual Technical Conference, Denver, Colorado, USA, 21-24 September. SPE 115679.

Maini, B., Class Notes, University of Calgary, 2015

Martin, R., Baihly, J., Malpani, R., Lindsay, G., Atwood, K. 2011. Understanding Production from Eagle Ford-Austin Chalk System. Presented at the SPE Annual Technical Conference and Exhibition, Denver, Colorado, 30 October-2 November. SPE 145117.

Oruganti, Y., Mittal, R., McBurney, C., & Rodriguez, A. 2015. Re-Fracturing in Eagle Ford and Bakken to Increase Reserves and Generate Incremental NPV – Field Study. Presented at the SPE Hydraulic Fracturing Technology Conference, The Woodlands, Texas, USA, 3-5 February. SPE 173340.

Pathak, M., Deo, M., Craig, J., Levey, R. 2014. Geologic Controls on Production of Shale Play Resources: Case of the Eagle Ford, Bakken and Niobrara. Presented at the Unconventional Resources Technology Conference, Denver, Colorado, 25-27 August. URTeC 1922781.

Piedrahita, J., Lopez, B., and Aguilera, R., 2016. A Generalized Methodology for Estimating Stress-Dependent Properties in Tight Petroleum Reservoirs and its Application to Drill Cuttings Data. Presented at the Unconventional Resources Technology Conference, San Antonio, Texas, USA, 1-3 August. URTeC 2461443

Railroad Commission of Texas. 2016. Eagle Ford Information. http://www.rrc.state.tx.us/oil-gas/major-oil-gas-formations/eagle-ford-shale/ (accessed 25 May 2016)

Ramirez, J. and Aguilera, R. 2016. Factors Controlling Fluid Migration and Distribution in the Eagle Ford Shale. SPE Formation Evaluation and Engineering. SPE 171626-PA (in press; posted June 2016). http://dx.doi.org/10.2118/171626-PA

Schlumberger. 2015. FORGAS User Manual, 22nd edition. Schlumberger. 2016. EOR. Oilfield Glossary, http://www.glossary.oilfield.slb.com/Terms/e/eor.aspx (accessed 16 May 2016).

Schlumberger. 2016. Shale. Oilfield Glossary, http://www.glossary.oilfield.slb.com/Terms/s/shale.aspx (accessed 10 May 2016).

Suhrer, M., Toelke, J., Diaz, E., Grader, A., Walls, J., Restrepo D., Cantisano, M., Cespedes,S. 2013. Computed Two-Phase Relative Permeability Using Digital Rock Physics in a Shale Formation. Presented at the International Symposium of the Society of Core Analysts, Napa Valley, California, USA, 16-19 September. http://www.jgmaas.com/SCA/2013/SCA2013-037.pdf.

Shuler, P., Lu, Z., Ma, Q., and Tang, Y. 2016. Surfactant Huff-n-Puff Application Potentials for Unconventional Reservoirs. http://dx.doi.org/10.2118/179667. SPE-179667-MS. Improved Oil Recovery Conference, 11-13 April, Tulsa, Oklahoma.

Sigmund, P.M. 1976. Prediction of Molecular Diffusion at Reservoir Conditions. Part II – Estimating the Effects of Molecular Diffusion and Convective Mixing in Multicomponent Systems. Journal of Canadian Petroleum Technology. Volume 15, No 03, 53-62, July 1976.

Urban, E., Orozco, D., Fragoso, A., Selvan, K. and Aguilera, R., 2016. Refracturing vs. Infill Drilling – A Cost Effective Approach to Enhancing Recovery in Shale Reservoirs. SPE paper 2461604 presented at the Unconventional Resources Technology Conference held in San Antonio, Texas, USA, 1-3 August 2016.

Walser, D. 2016. Leveraging Subsurface Insight, Screening, and Diversion Technology in Refracturing. Journal of Petroleum Technology. Volume 68, No. 01, January 2016.

Wan, T., Sheng, J. and Soliman, M., 2013 (a). Evaluation of the EOR potential in shale oil reservoirs by cyclic gas injection. Presented at the SPWLA 54th Annual Logging Symposium, New Orleans, Louisiana, USA, 22-26 June. Paper SPWLA-d-12-00119

Wan, T., Sheng, J. and Soliman, M., 2013 (b). Evaluation of the EOR potential in fractured shale oil reservoirs by cyclic gas injection. Presented at the Unconventional Resources Technology Conference, Denver, Colorado, USA, 12–14 August. Paper SPE 168880 or URTeC 1611383

Wan, T. and Sheng, J., 2015. Compositional Modelling of the Diffusion Effect on EOR Process in Fractured Shale-Oil Reservoirs by Gasflooding. Journal of Canadian Petroleum Technology. Volume 54, No. 02, 107 – 115, March 2015. http://dx.doi.org/10.2118/2014-1891403-PA

Wang, J., and Liu, Y. 2011. Well Performance Modeling of Eagle Ford Shale Oil Reservoirs. Presented at the North American Unconventional Gas Conference and Exhibition, The Woodlands, Texas, 14-16 June. SPE 144427.

Wang, D., Zhang, J., Butler, R., Olatunji, K. 2016 (a). Scaling Laboratory-Data Surfactant-Imbibition Rates to the Field in Fractured Shale Formations. SPE Reservoir Evaluation & Engineering. SPE 178489-PA (in press; posted February 2016). http://dx.doi.org/10.2118/178489-PA

Wang, D., Dawson, M., Butler, R., Li, H., Zhang, J., and Olatunji, K. 2016 (b). Optimizing Water Chemistry to Improve Oil Recovery from the Middle Bakken Formation. http://dx.doi.org/10.2118/179541. SPE-179541. SPE Improved Oil Recovery Conference, 11-13 April, Tulsa, Oklahoma, USA

Warner, H. and Holstein, E. 2006. Immiscible Gas Injection in Oil Reservoirs. In *Petroleum Engineering Handbook*, Ed. E. Holstein, Vol 5, Chap. 12, 1103-1132. Richardson, Texas: Society of Petroleum Engineers.